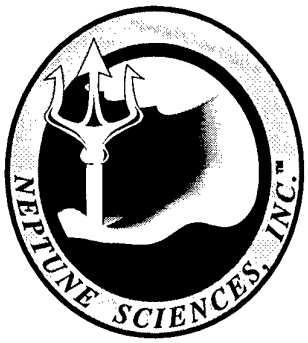

NEPTUNE SCIENCES, INC.

Final Report

Research and Development of Automated Battery Chargers/Analyzers

CONTRACT. NO. N00164-96-C-0048

Copy No. 006

Distributed to: DTIC

W.P. No.

Revision	Description	Date	Prep	Check	Approved
0	Release	1/31/00	BLM	RTM	CJD

1. CONTENTS

2. LIST OF FIGURES

3. LIST OF TABLES

4. BACKGROUND

The contract for Research and Development of Automated Battery Chargers/Analyzers was awarded to Neptune Sciences, Inc. to develop advanced battery charging and non-invasive real-time battery diagnostic/analysis techniques. To complete this project Neptune Sciences, Inc. used its considerable in-house expertise in hardware and software development as well as in data collection and analysis. Where additional expertise was required, consultants from industry and academia were retained. Throughout this project, special effort was made to use commercial off-the-shelf (COTS) hardware whenever possible.

The goal was to find a better way to determine the state of charge of various types of batteries and create a database for each type and capacity of battery tested. This database could be integrated into a smart charger/analyzer that could determine the remaining life of primary batteries and test secondary batteries and charge them using the most efficient means possible.

It was hoped that through the use of complex waveforms, a more efficient means of charging secondary batteries could be developed, but research in this area yielded little or no positive results. Therefore, the focus of this project shifted to finding the state of charge, and the charging methods were limited to constant voltage (CV) and constant current (CC), which are the two most common methods used in industry today.

Research to determine the state of charge for various types of batteries yielded good results. Neptune Sciences, Inc. developed techniques to take reliable data from primary and secondary batteries and use that data to determine the state of charge for a given battery using statistical analysis and neural networks. Efforts were made to analyze the data using time domain analysis and frequency domain analysis techniques, but only the time domain analysis yielded good results. Therefore, this report focuses on the use of pulse testing to determine a battery's state of charge, and it outlines the testing methods, algorithms, hardware and software used for testing.

5. TECHNICAL APPROACH

For this report, pulse testing refers to the collection of the voltage response of a battery or cell in response to a series of low-level current pulses. Different chemistries required different pulse frequencies and amplitudes, but the basic treatise is always the same, look at the voltage response.

The amount of current applied, especially to the primary batteries, was very low and caused no significant discharge. The secondary batteries were also charged with the same current used for discharge. Therefore, the pulse testing used was essentially non-invasive, that is, it did not cause a significant change in the state of the batteries tested.

For each battery tested, a controlled current was applied, and the voltage response was measured. The voltage response curve was analyzed using different mathematical methods. From this analysis, a model of the voltage response was developed. The batteries were then fully discharged to determine the batteries actual state of charge. The hypothesis is that batteries and cells have a consistent voltage response to current stimuli depending on their state of charge.

There are several variables that affect the voltage response of a battery, such as state of charge, temperature, battery capacity, time since last charge/discharge, battery chemistry, etc. Because of time constraints, only state of charge vs. voltage response was modeled, and other variables were held constant throughout testing.

6. DATA COLLECTION PROCEDURE

The testing procedures for each of the different types of batteries were essentially the same. Only the values of the charge/discharge current changed between battery types. As previously mentioned, there are several factors that influence the voltage response of a battery during pulse testing. In order to model the state of charge vs. voltage response for a particular type of battery, the other variables had to be held constant. The procedures for testing a given group of batteries are outlined below:

1. Hold the temperature constant during testing by means of an environmental chamber.
2. Use only one capacity for each of the different battery chemistries (e.g. don't compare 2 Volt 12.5 AH Lead Acid Cell data to 2Volt 25 AH Lead Acid Cell data).
3. Place each of the cells/batteries at different depths of discharge using battery cyclers (charge/discharge for secondary, discharge for primary)
4. Rest the cells/batteries for approximately 24 hours.
5. Pulse test each of the cells/batteries. (pulse testing consists of 32 cycles of charge/discharge for secondary batteries and discharge/rest for primary batteries).
6. Fully discharge each of the cells/batteries to determine their actual state of charge.

These general procedures were followed in testing each of the groups of batteries. The next few pages give specific information about each of the types of cells/batteries tested and the procedures used to test them. A sample plot of the pulse test data is included for each of the battery types.

6.1 Lithium Sulfur Dioxide Primary Cell:

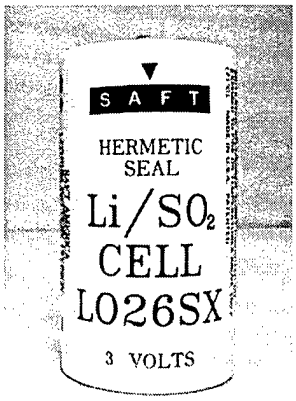

Chemistry: Lithium Sulfur Dioxide
Part Number: LO26SX
Manufacturer: SAFT
Capacity - 8 Amp Hours
Nominal Voltage: 2.8 Volts
Open Circuit Voltage: 3 Volts

1. Cells were placed at different states of charge using constant current discharge.
   Random discharge times between 0 and 5 hours were selected
   Constant discharge = C/5 or –1.6 amp
   Sampling frequency = 1 Hz.
   Minimum Voltage: 2 volts
   Maximum voltage limits = 4 volts for safeguard.
2. Cells were pulse tested after a period of rest of at least one day
   Sampling frequency = 50 KHz.
   Discharge Current (-C/100) = -0.08 A, Rest Current (0) = 0 A
   Period = 10 seconds, 50% duty cycle
   Number of periods = 32
3. Cells were fully discharged at –C/5 or –1.6 Amperes until the voltage dropped below 2 Volts

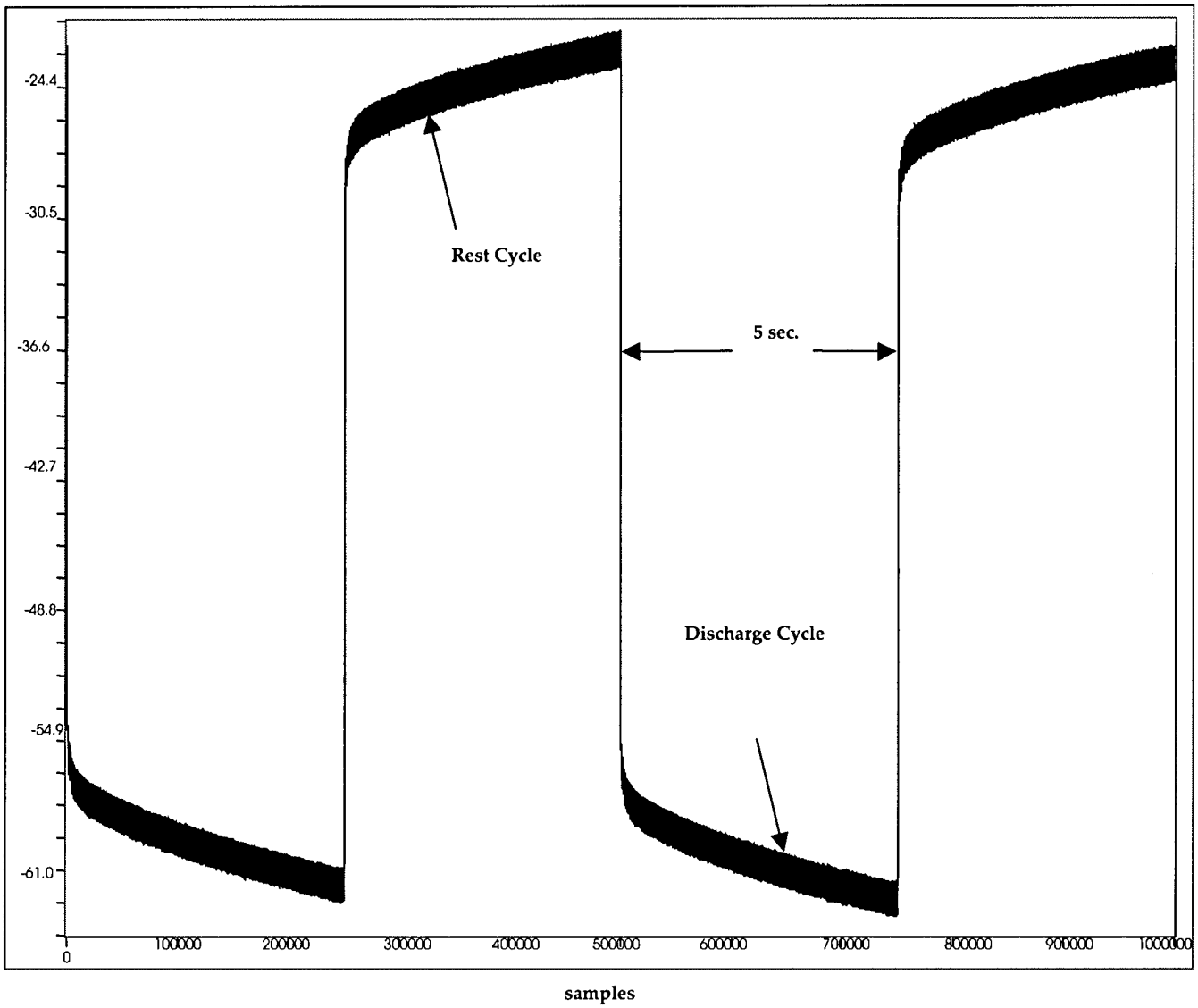

Figure 6-1 Pulse Test Curve for Two Cycles of Discharge and Rest for a Primary Lithium Cell

6.2 Lithium Sulfur Dioxide Primary Battery:

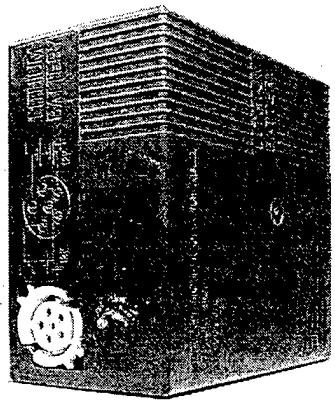

Chemistry: Lithium Sulfur Dioxide
Part Number: BA5590A
Manufacturer: Hawker - Ethernacell
Capacity - 14.4 Amp Hours in 12 volt parallel configuration
Nominal Voltage: 12 Volts
Open Circuit Voltage: 15 Volts (After passivation)

1. Batteries were placed at different states of charge using constant current discharge.
   Specific discharge time between 0 and 5 hours were selected
   Constant discharge = C/5 or –2.88 amps
   Sampling frequency = 1 Hz.
   Minimum Voltage = 10 volts
   Maximum voltage limits = 20 volts for safeguard.
2. Batteries were pulse tested after a period of rest of at least one day
   Sampling frequency = 50 KHz.
   Discharge Current (-C/100) = -0.144 A, Rest Current (-C/3600) = -0.004 A
   Period = 10 seconds, 50% duty cycle
   Number of periods = 32
   The BA5590 batteries have internal diodes that prevent charge currents from being induced into the batteries. The diodes act as an open circuit for positive currents. This open circuit behavior causes the internal feedback circuitry of the power supply to max out for currents that are positive or zero. For this reason, the rest current is also negative.
3. Batteries were fully discharged at –C/5 or –2.88 Amperes until the voltage dropped below 10 Volts.

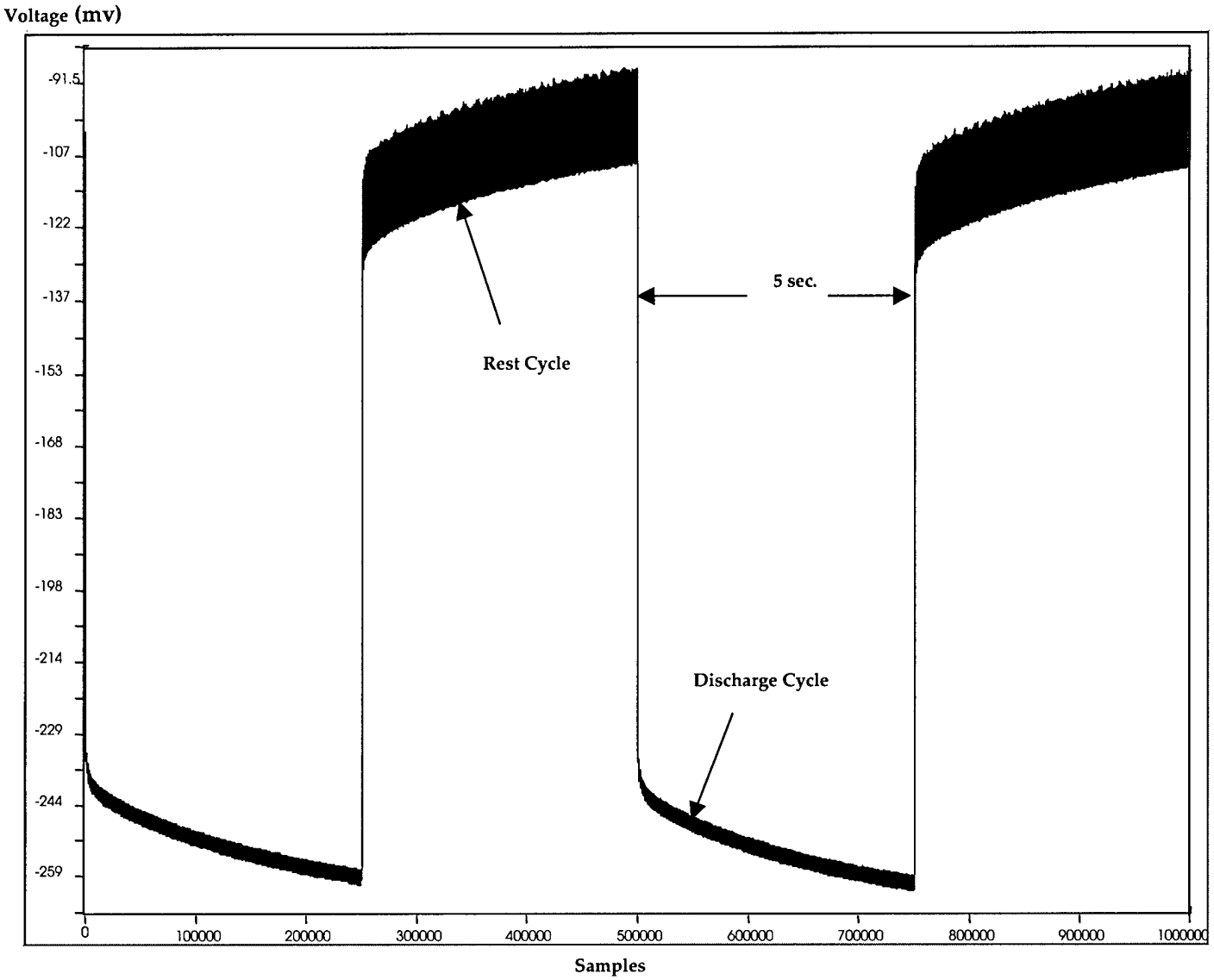

Figure 6-2 Pulse Test Curve for Two Cycles of discharge and Rest for a Primary Lithium Battery

6.3 Lead Acid Secondary Cells:

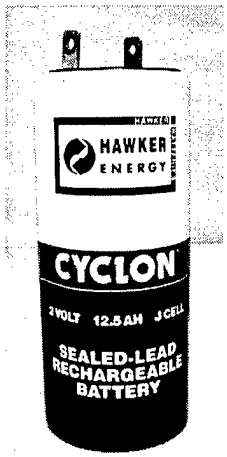

Chemistry: Lead Acid
Part Number: Hawker Cyclon 0840-0004
Manufacturer: Hawker Energy
Capacity - 12.5 Amp Hours
Nominal Voltage: 2 Volts
Open Circuit Voltage: 2.2 Volts

1. Cells were brought to full discharge voltage at C/5 or –2.5 Amperes until the voltage was 1.65 volts.
2. Cells were placed at different states of charge using constant voltage charging.
   Random charge times between 0 and 4 hours were selected
   Maximum Current = 12 amperes.
   Set voltage = 2.45 volts.
   Sampling frequency = 1 Hz.
   Minimum and maximum voltage limits = 1.5 and 3 volts for safeguards.
3. Cells were pulse tested after a period of rest of at least one day
   Sampling frequency = 50 KHz.
   Discharge Current (-C/40) = -0.3125 A, Charge Current (C/40) = +0.3125 A
   Period = 10 seconds, 50% duty cycle
   Number of periods = 32
4. Cell were fully discharged at –C/5 or –2.5 Amperes until the voltage dropped below 1.65 Volts

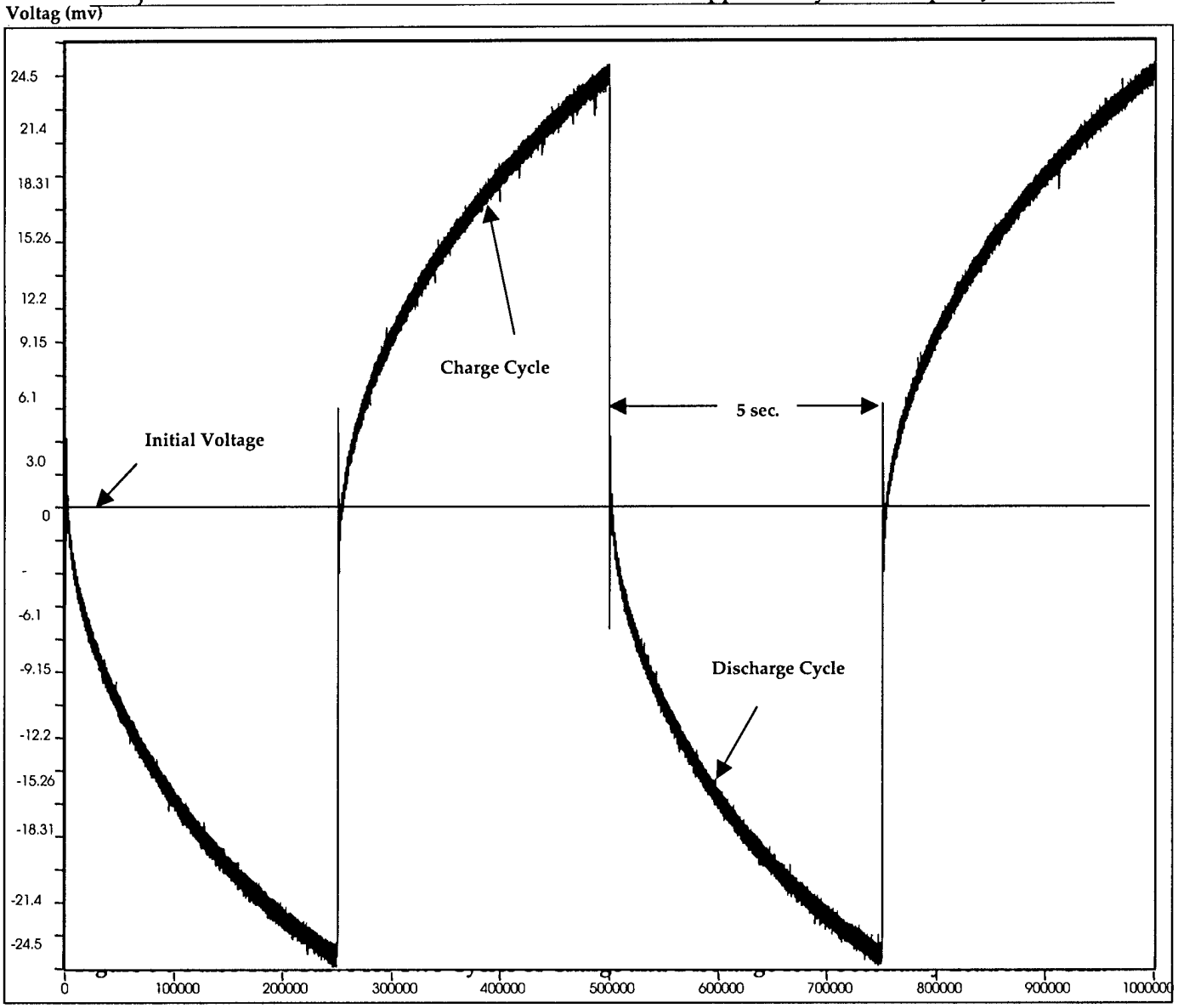

Figure 6-3 Pulse Test Curve for Two Cycles of Charge and Discharge for a Secondary Lead Acid Cell.

6.4 Lead Acid Secondary Batteries:

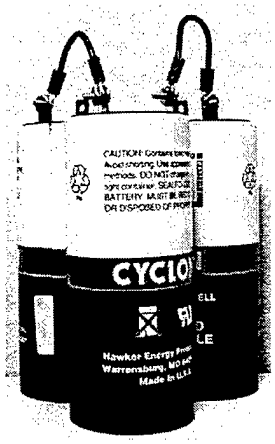

Chemistry: Lead Acid
Part Number: NPN - Assembly of 3 Hawker cells
Manufacturer: Hawker
Capacity - 12.5 Amp Hours
Nominal Voltage: 6 Volts
Open Circuit Voltage: 6.6 Volts

1. Batteries were brought to full discharge voltage at C/5 or –2.5 Amperes until the voltage read was 4.95 volts or 1.65 volts per cell.
2. Batteries were placed at different states of charge using constant voltage charging.
   Random charge times between 0 and 4 hours were selected
   Maximum Current = 12 amperes.
   Set voltage = 7.35 volts or 2.45 volts per cell.
   Sampling frequency = 1 Hz.
   Minimum and maximum voltage limits set at 4.5 and 9 volts for safeguards.
3. Batteries were pulse tested after a period of rest of at least one day
   Sampling frequency = 50 KHz.
   Discharge Current (C/40) = -0.3125 A, Charge Current (-C/40) = +0.3125 A
   Period = 10 seconds, 50% duty cycle
   Number of periods = 32
5. Batteries were fully discharged at –C/5 or –2.5 Amperes until the voltage dropped below 4.95 Volts.

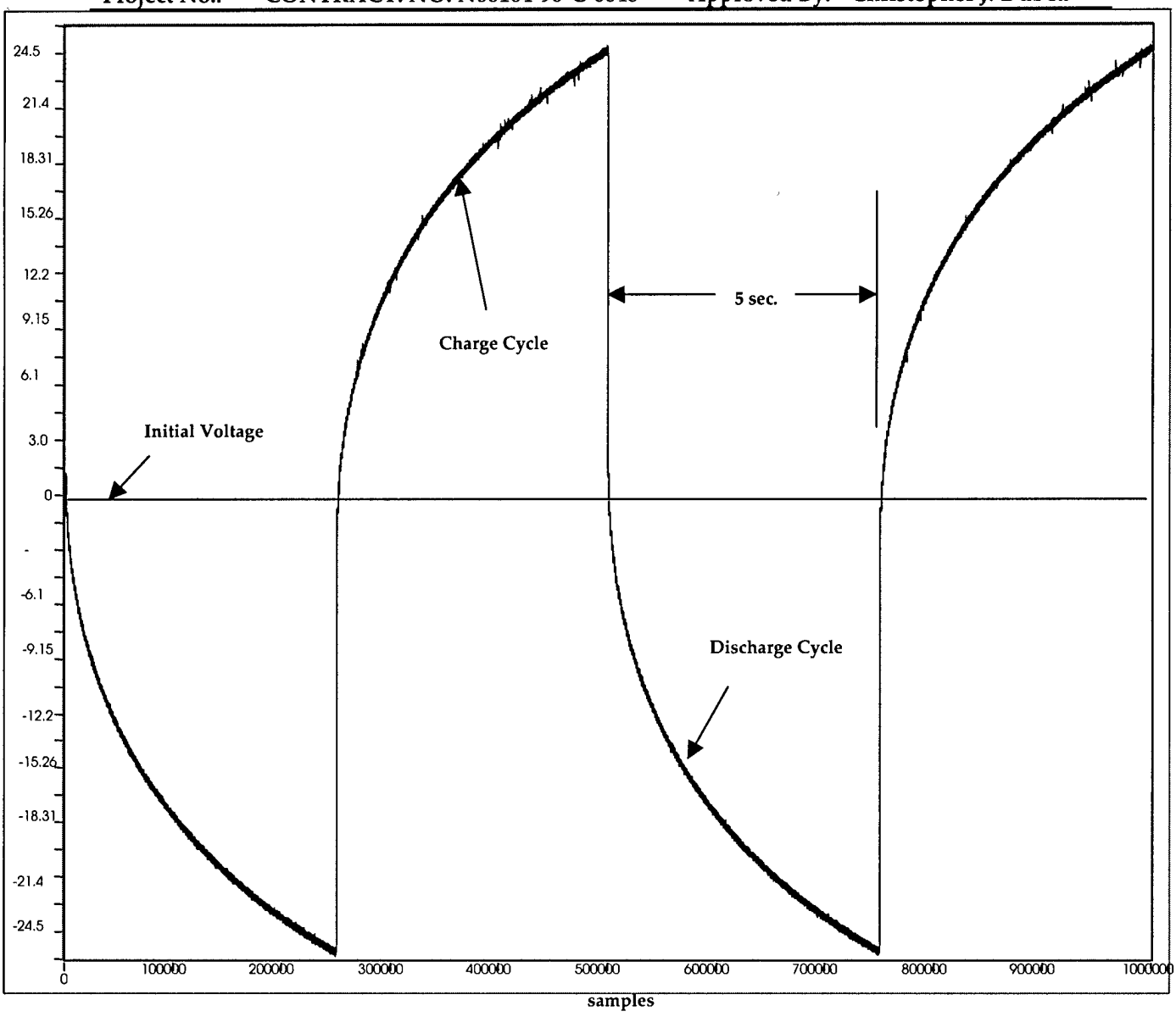

Figure 6-4 Pulse Test Curve for Two Cycles of Charge and Discharge for a Secondary Lead Acid Battery

6.5 Nickel Cadmium Secondary Batteries:

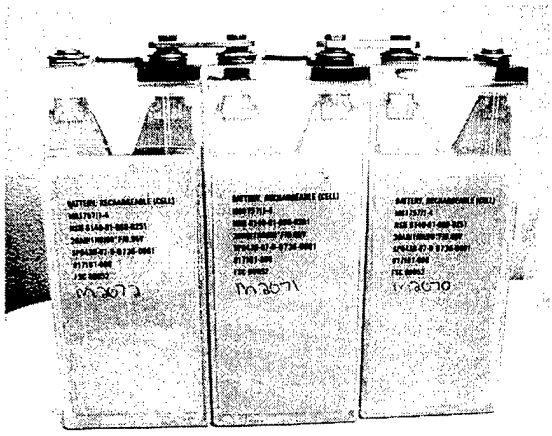

Chemistry: Nickel Cadmium
Part Number: NPN - Assembly of three M81757/1-4 cells
Manufacturer: unknown
Capacity - 20 Amp Hours
Nominal Voltage: 3.75 Volts
Open Circuit Voltage: 3.75 Volts

1. Cells were retrieved from storage fully discharged.
2. Cells were fully charged using constant voltage
3. Cells were charged until 4 hours had passed or the cell drew less than 1 amp
   Maximum Current = 60 amperes.
   Set Voltage = 1.5 volts per cell
   Sampling Frequency = 1 Hz
   Minimum and maximum voltage limits = 0.85 and 3 volts for safeguards.
4. Cells with similar characteristics were chosen to build batteries. Batteries were composed of three cells in series.
5. Batteries were brought to full discharge voltage at C/2 or –20 Amperes until the voltage was 2.55 volts or 0.85 volts per cell.
6. Batteries were placed at different states of charge using constant voltage charging.
   Random charge times between 0 and 4 hours were selected
   Maximum Current = 60 amperes.
   Set voltage = 4.5 volts or 1.5 volts per cell.
   Sampling frequency = 1 Hz.
   Minimum and maximum voltage limits = 1.5 and 9 volts for safeguards.
7. Batteries were pulse tested after a period of rest of at least one day
   Sampling frequency = 50 KHz.
   Discharge Current (-C/20) = -1 A, Charge Current (C/20) = +1 A
   Period = 10 seconds, 50% duty cycle
   Number of periods = 32
8. Batteries were fully discharged at –C/2 or –10 Amperes until the voltage dropped below 2.55 volts or .85 volts per cell.

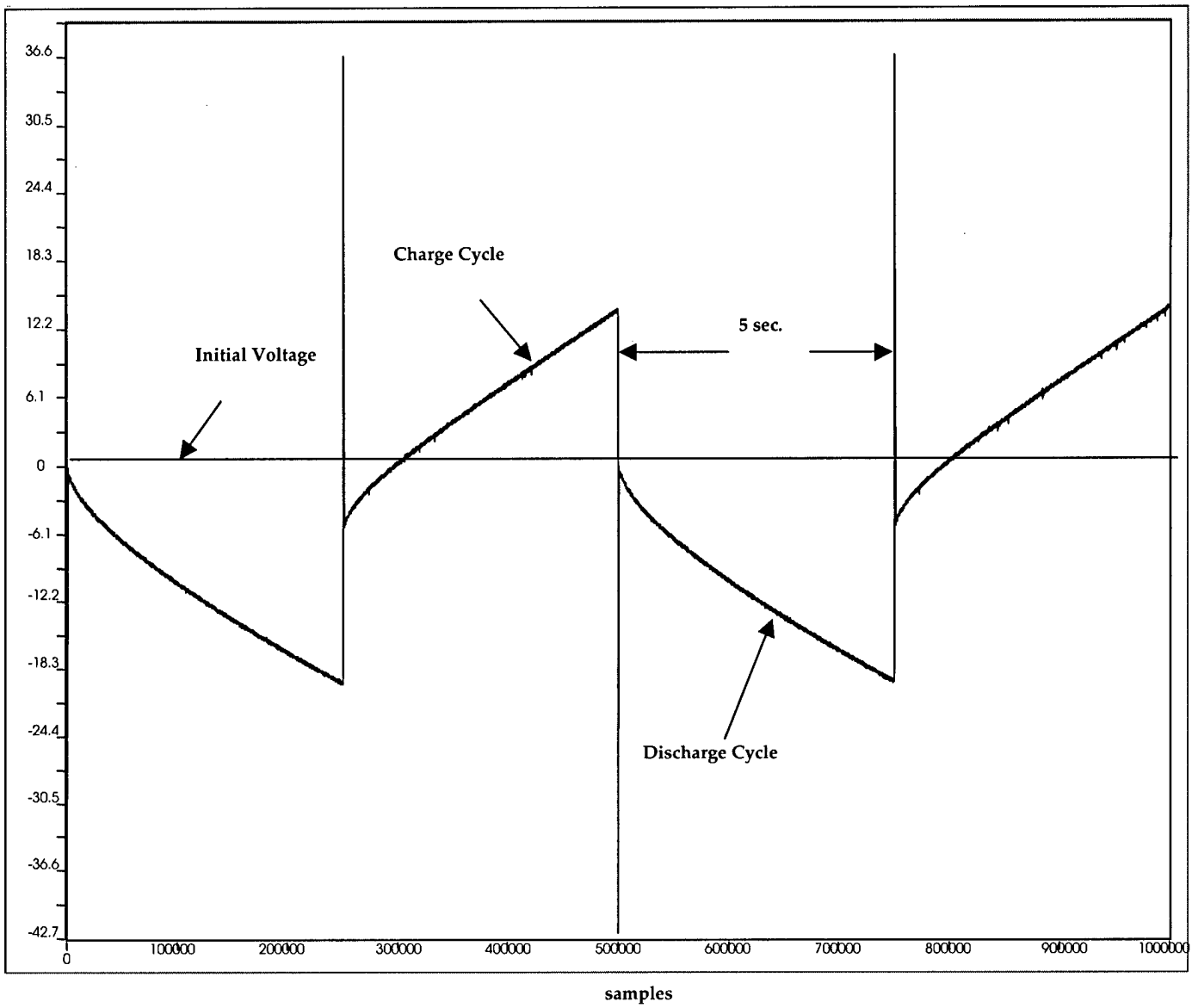

Figure 6-5 Pulse Test Curve for Two Cycles of Charge and Discharge for a Secondary Nickel Cadmium Battery

7. RESEARCH INSTRUMENTS/TOOLS

The equipment used to test and cycle batteries used the same basic design across different hardware configurations. Hardware able to charge and discharge with the required speed and accuracy was chosen. Analog signals from the data acquisition card were used to control the current. For constant current charging, the analog signal was set to drive the required amperage. For constant voltage charging, the current was controlled while the voltage was monitored. A software feedback loop was used to keep the voltage constant by controlling the current. For Pulse Testing the current was changed and the voltage was monitored at 50 KHz. The data acquisition system used a COTS 16-bit data acquisition card from National Instruments. The same hardware suite was used to implement a charger, discharger, and Current Pulse Tester. Figure 7.1 shows a block diagram of the hardware platform. Notice the offset placed at the sense point. This offset was used to increase the dynamic range of the Analog to Digital converter. The offset voltage was set to the open circuit voltage of the battery, which made the voltage at the sense point zero when the battery experienced a current of 0 amperes. Excitations of small currents produced very small changes on the battery voltage. A programmable gain amplifier was used to amplify the voltage response, which was impossible without the offset null.

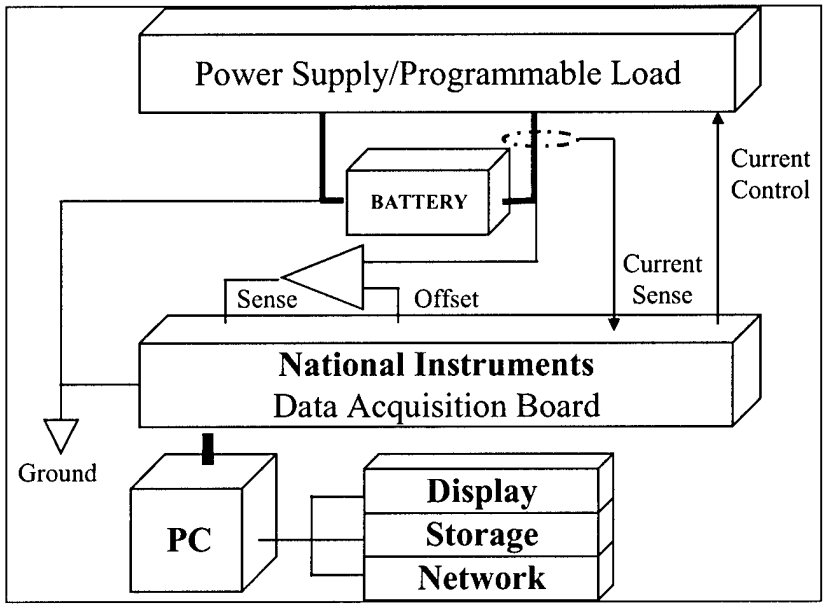

Figure 7-1 Basic Hardware Design.

The following pages depict the different configurations that were used for testing and conditioning of batteries:

7.1 400 Watt – Constant Voltage / Constant Current Cycler

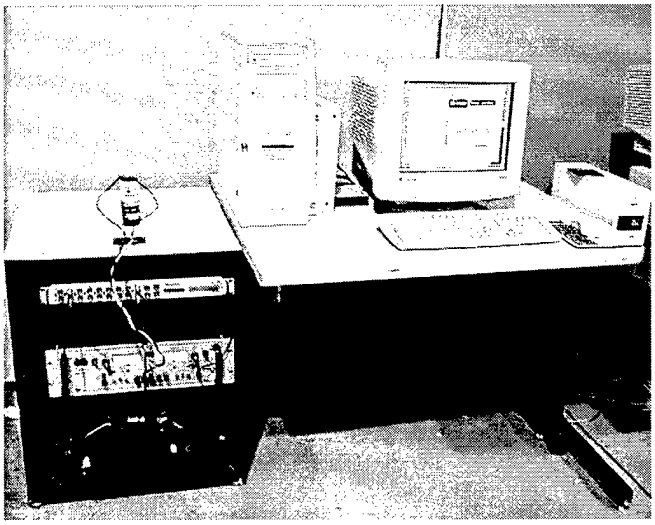

LABVIEW / PC Controlled
COTS KEPCO Power Supply 400 Watt Unit – 20 Volt/20 Amps and 36 Volt/12Amps
National Instruments Data Acquisition Card. 16-bit analog I/O
Non-Intrusive current measurement through Hall effect current sensors
Monitor and log up to eight battery voltages
Full configuration through LABVIEW (Windows) front panel
Configurable on constant current or constant voltage charge/discharge

7.2 Three Kilowatt – Constant Voltage / Constant Current Cycler

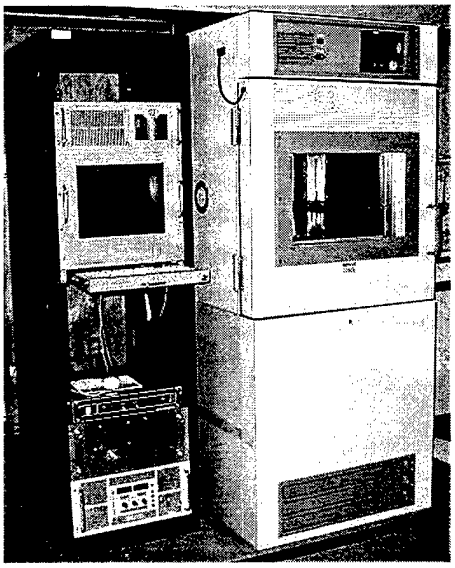

Rise Time: 50 microseconds 0 to 50 Amps
Fall Time: Less than 300 microseconds
Power Range: 0 to 60 Volts @ ±50 Amps
COTS programmable load and programmable power supply.

7.3 600 Watt – Two Quadrant Power Cycler

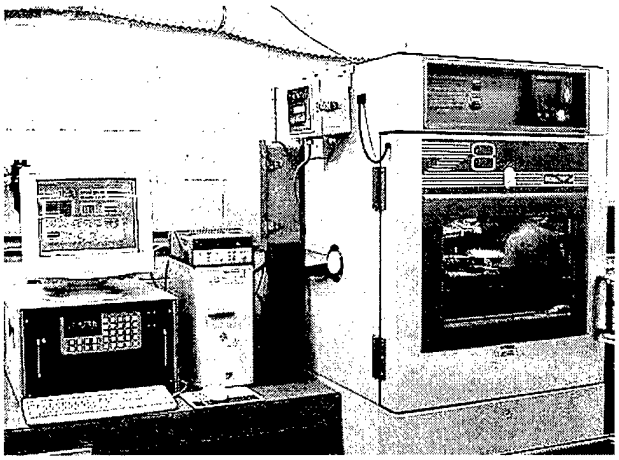

This unit was initially used to cycle batteries. It's use was discontinued because of maintainability issues of OEM designed equipment.
Microprocessor (Motorola Model-8) Controlled Stand-alone operation
Eight individual power transistor modules for a total of 24 Ampere, 30 Volt Capability
GPIB-488 Interface to HP34970A Data Acquisition / Switch Unit for multiple battery testing
GPIC-488 Interface to Thermal Chambers
Serial Interface to PC
LABVIEW Graphical User Interface
All boards OEM Designed

8. ANALYSIS

Analysis of the data collected represented a significant part of the total effort of this project. The goal was to use the data collected from the batteries to create a model of the state of charge vs. current pulse response for each of the types of batteries tested. It is important to note that only the discharge curves of the pulse test data were analyzed for both primary and secondary batteries/cells.

Dr. Elizabeth Podlaha of Louisiana State University was retained by Neptune Sciences, Inc. to verify the mathematical models created through chemical analysis. She verified that each of the processes contained in the model equations could be correlated to a particular chemical process.

Mr. David Fabre of Neptune Sciences initially created models from the pulse test data using multiple linear regression (MLR). Dr. Badiollah (Badie) R. Asrabadi of Nicholls State University verified his procedure and modeling strategy and prescribed stringent normality tests for the data. MLR modeling showed good results considering the limited number of batteries available for each set, which created a marginal sample size and limited the verification process.

Mr. Fabre also used an artificial neural network (ANN) for modeling certain battery types. Again, the limited sample size hampered the ability to train the ANN, but the ANN was still able to predict state of charge with good accuracy. ANN modeling was much easier to accomplish than MLR modeling and had similar results. However, the work done in normalizing the data for MLR was beneficial in ensuring the success of the ANN.

8.1 Chemical Analysis of Mathematical Models

Dr. Podlaha performed a thorough analysis of the battery processes for both secondary lead-acid and primary lithum cells. She compared the sum of exponentials model (SEM) used to fit pulsed battery test data to the actual electrochemical phenomena.

The first parameterization model developed by Neptune Science, Inc. was based on describing the measured response of the battery to a pulse test as a series of exponents. For a constant current discharge/charge cycle each of the two parts of the pulse can be described by

$$v(t) = a_o + \sum_i a_i e^{-t/b_i} \qquad [1]$$

This mathematical function described above identifies discrete time constants that can be compared to an electrochemical system for pulse testing on the order of a few seconds.

There are four fundamental electrical and electrochemical concepts that are to be considered to describe the measured potential:

1) ohmic resistance
2) capacitive double layer charging of the electrode-solution interface
3) reaction kinetic resistance
4) diffusion resistance

8.1.1 **Ohmic resistance (constant): DESCRIBES A_O**

The first constant in the statistical model, equation [1], describes the instantaneous voltage change measured when a cell is either discharged or charged. This constant represents ohmic drop in the cell. The ohmic resistance in the cell is due to the electrolyte conductivity, *k*, solid reactant and product conductivities, σ, separator conductivity, σ_s and all solid current collectors (i.e. poles, grids, etc.). The largest resistance is often attributed to the electrolyte. However, if passive oxide layers form over the solid metal surfaces, then the solid resistance may dominate the ohmic drop.

In porous electrodes (such as the lead-acid cell and nickel-cadmium cell) Ohm's law describes the current per cross-sectional area, *i* in the (1) solid, matrix phase and in the (2) solution phase when there are no concentration gradients[i].

$$i_1 = -\sigma \frac{\partial \phi_1}{\partial x}; \quad i_2 = -\kappa \frac{\partial \phi_2}{\partial x} \qquad [2]$$

The change of the solution and matrix potentials have been assumed to change as a function of only one direction for simplicity, but it can, of course, be generalized for all directions.

Notice that the potential drop can also have a distribution in the cell and is not necessarily constant throughout. Both the solid and solution conductivities, σ and κ, are effective quantities and depend on the porosity of the electrodes. Thus, batteries that have large internal distribution of reactants as a consequence of demanding discharges may exhibit regions (particularly near the separator) where the electrode porosity is greatly decreased or even blocked resulting in a large ohmic drop.

Summary: The initial potential drop, characterized by a_0, reflects the internal ohmic drop and may signify poorly distributed reactants and products, or the presence of passivated solids that would result in shortened cell lifetimes.

8.1.2 Capactive double layer charging (time dependent)

At the electrode-solution interface there is a region where electroneutrality does not occur (a space charge). This region is often modeled as a parallel plate capacitor with a very small separation distance of a few angstroms, resulting in a rather high capacitance. In order for electrochemical reactions to occur, charge must be provided to the double-layer region so that its potential can be raised to the value required for the reactions.

The discharge (or charge) of the double layer can be described as:

$$i_n = -C \frac{\partial(\phi_1 - \phi_2)}{\partial t} = \frac{\mathrm{I}}{\mathrm{a}} \qquad [3]$$

where i_n is the current per interfacial area. Inspection of this equation shows that for a constant current discharge, *I* in Amps, will lead to a *linear*, not exponential, decrease of the

potential with time. To compare directly to equation [3] a constant current discharge, *I*, equals $i_n a$, where *a* is the interfacial area per unit volume.

However, a linear decrease of potential with an applied current is not usually observable for a battery system due to the interaction of two important processes: in one limit the ohmic drop and in another limit the reaction kinetics.

Summary: An ideal capacitance response is linear, not exponential, and is indicative of the charging and discharging of the electrode-solution interface in the absence of ohmic effects, kinetic effects and concentration gradients.

8.1.3 Capactive double layer charging with ohmic drop: (very fast time constants)

At the moment of discharge (or charge) of a cell there may be a distribution of ohmic drop which will also cause a distribution of the capacitive double-layer effect so that equation [2] and [3] are related. For porous electrodes the current per interfacial area is

$$i_n a = \frac{\partial i_1}{\partial x} = -\frac{\partial i_2}{\partial x} \qquad [4]$$

thus, it is easy to see that derivative of equation [2] is directly proportional to equation [3].

$$-C\frac{\partial(\phi_1 - \phi_2)}{\partial t} = -\frac{\sigma}{a}\frac{\partial^2 \phi_1}{\partial x^2} = +\frac{\kappa}{a}\frac{\partial^2 \phi_2}{\partial x^2} \qquad [5]$$

The solution of this equation has recently been solved by Srinivasan *et al.*[ii] As expected, the solution of the potential drop from this second order differential equation is predicted to be an exponential change. Thus, the statistical model in equation [1] should be able to fit this type of behavior well.

The simultaneous influence of the ohmic and capactive feature presented in equation [5] neglects the electrochemical reactions and concentration influences. So, it is directly applicable to electrochemical capacitors or the start of discharge/charge of a cell. For a cell or battery, the behavior predicted by equation [5] would be manifested in the first few exponential terms before the influence of the electrochemical reactions take over.

Summary: The change between ohmic and capacitive effects during an applied current results in an exponential decrease of the voltage with time. This represents one of the fastest time constant in the Neptune statistical model, equation [1].

8.1.4 Capactive double layer charging with kinetic resistance: (medium-fast time constants)

At long enough times (ms scale), the ohmic effect becomes insignificant. Before the electrode-solution double layer is completely charged (or discharged), however, the current is divided between the current at the double layer (capacitive), I_C, and the current used for the electrochemical reactions, or faradaic, I_F, current. The capacitive current arises from the charging (or discharging) of the double-layer, and the faradaic current refers to the current that goes to the electrochemical reactions. Neglecting ohmic effects, initially, all the current that is applied is capacitive. As the potential changes, the electrochemical reactions begin, and the current progressively becomes more faradaic. Eventually, the capacitive current goes to zero, and all of the current is faradaic. The behavior is similar to a capacitor in parallel with a resistor:

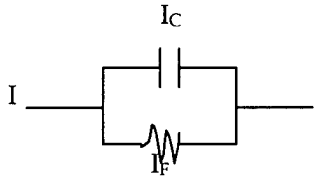

In order to analyze the time constants involved in the transition between capacitive and faradaic processes, the detailed reactions must be specified. Regardless of the system, a generalized approach can be taken assuming that the electrochemical reactions at steady state take the typical form described by a Tafel or Butler-Volmer exponential rate expression

$$\frac{\partial i_2}{\partial x} = a i_o \left\{ exp\left(\frac{\alpha_a F}{RT}(\phi_1 - \phi_2) \right) - exp\left(-\frac{\alpha_c F}{RT}(\phi_1 - \phi_2) \right) \right\} \qquad [6]$$

Note that these exponential terms are not time dependent. Since some of the current is diverted to charging (or discharging) the double layer, this equation is set equal to equation [3] by considering equation [4]

$$C\frac{\partial(\phi_1 - \phi_2)}{\partial t} = i_o \left\{ exp\left(\frac{\alpha_a F}{RT}(\phi_1 - \phi_2) \right) - exp\left(-\frac{\alpha_c F}{RT}(\phi_1 - \phi_2) \right) \right\} \qquad [7]$$

The solution of this nonlinear differential equation describes the change of the potential with time. The above equation has been solved assuming a constant capacitance, and the complex solution (not shown here) contains exponential terms. If

$$\frac{nF(\phi_1 - \phi_2)}{RT} << 1$$

then the solution can be greatly simplified and reduces to a simple exponential form:

$$potential\ drop\ (\phi_1 - \phi_2) = (\phi_1 - \phi_2)_\infty \{1 - exp(-t/\tau)\} \qquad [8]$$

where τ is a relaxation time : $(RT/nFi_o)\ C$

The exchange current density, i_o, characterizes the reaction. Of course there are multiple reactions occurring in a battery system, so in order to evaluate the relative importance of the kinetic contribution, the slowest step would be considered. In general, the faster the reaction, the smaller the relaxation time. For very sluggish reactions, the time constant is long. Depending on the system, this time constant could be on the order of 10-1000 ms.

Summary: The change between capacitive and electrochemical kinetic effects during an applied current results in an exponential decrease of the voltage with time. This represents time constants slower than the ohmic to capacitive change.

8.1.5 Electrokinetic effects only (flat potential vs time responses)

The transient effects of the electrochemical reactions are extremely fast and are usually characterized with impedance spectroscopy using modulated current or potential with frequencies in the 10^{-4} to 10^{-6} Hz (0.1-0.001 ms) range. These influences would not be easily detected with the pulsed square-wave testing mentioned here, and a steady state is reasonably assumed. Once the ohmic and capactive effects die out, if kinetics are dominating, a steady potential with respect to time would be observed, assuming that diffusional effects are negligible, and there are no physical changes in the battery. Physical changes in the battery will eventually occur during discharge and charge, which will then change the kinetic response.

At steady state the rate equations are a function of potential and would be sensitive to the test conditions (i.e. applied discharge or charge current).

Summary: Steady state electrochemical kinetic effects are described by a flat potential versus time response with constant current discharge (or charge) as long as there are no diffusional effects or physical changes in the battery.

8.1.6 Diffusion Effects

8.1.6.1 Diffusion only: (potential drop varies with the square root of time, long time constants)

Diffusional effects are characterized by the relaxation of species that participate in the electrochemical reaction. If capacitive, ohmic and kinetic effects are negligible, and the length of the pulse test is long, so that in each pulse a steady state concentration gradient is achieved, then the potential is controlled by the solution of Fick's second law. The potential response of a purely diffusion controlled reaction will vary as the square root of time. This applies to diffusion of ions to the electrode surface, which is important to aqueous porous battery systems such as the lead-acid battery and also applies to solid-state diffusion as in the lithium cells.

The time required for diffusion to reach a steady state depends on the boundary layer thickness, δ, and the diffusion coefficient of the species, D; $\tau = \delta^2/\pi D$.

For ionic species, the diffusion coefficient is typically $10^{-5}cm^2/s$, and the boundary layer thickness is on the order of 100 microns. The time constant for the diffusion process is expected to be on the order of a couple seconds for aqueous electrolytes (i.e. the lead-acid cell). For solid-state diffusion this time constant is much longer.

If, however, cycles of the pulse test are so short that the concentration changes have not reached a steady state before the current is changed, then the discharge response will be governed by an exponential function[iii].

8.1.6.2 Diffusion and kinetic control: (middle time constants, exponential variations)

One of the most challenging problems to describe is the mixed control between kinetic and diffusion. Many models can be found in the literature to describe this mixed control with time since it is also important in describing the total discharge curve of a battery. The fundamentals are outlined by Newman *et al.*[iv]

These time constants are difficult to assess because they are highly dependent on the system under study. A simple numerical model was presented to Crane at the last visit that included these processes as well as the ohmic effect.

Summary: Diffusion represents the longest time constant. The potential response of a diffusion controlled reaction with time to a constant current discharge (or charge) is not exponential, but it varies with the square root of time. If however, a steady state is not reached by the time the current is changed in a pulse test, then the response can be described well with an exponential function. Mixed kinetic and diffusion control is highly nonlinear and may be reasonably represented by the sum of exponents model.

8.1.7 Lead-acid (Hawker cell)

The statistical model correlates well with the discharge pulse experimental data for some regions of the pulse test. These are the curved regions of the pulse shown in the Figure 8-1 below.

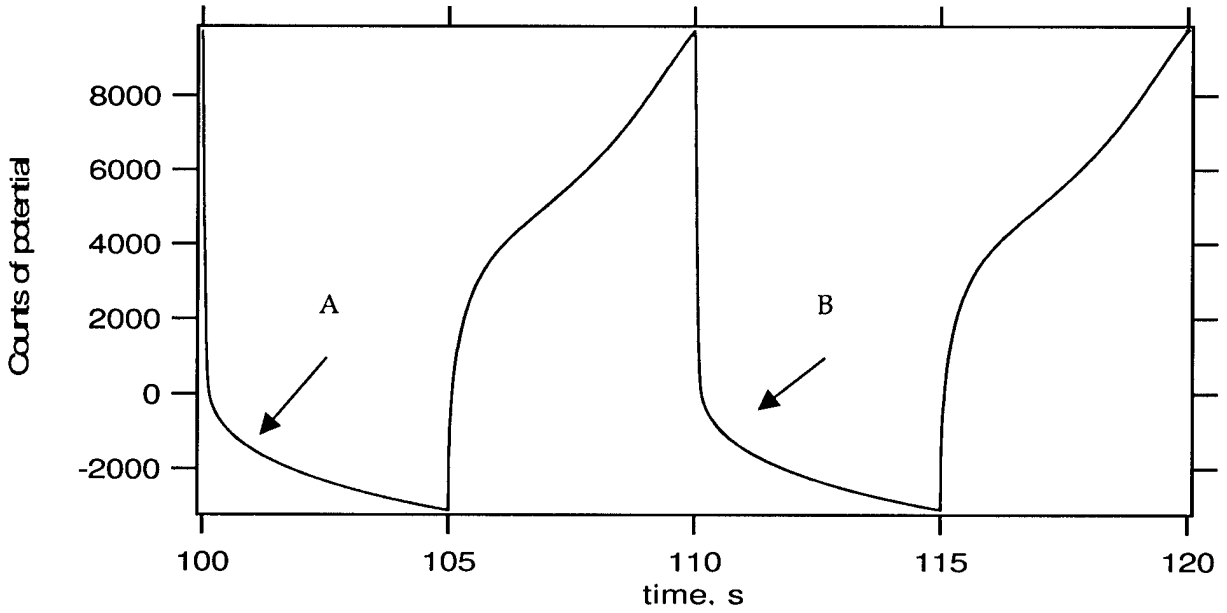

Figure 8-1 Typical pulse response of a lead-acid Hawker cell.

The most important processes in this indicated region is the transition from capacitive to kinetic control (point A above) and the influence of diffusion on kinetics (point B above), which can be reproduced by a sum of exponential functions. The initial potential decrease is well characterized by the a_0 constant in equation [1] and represents the ohmic drop.

A plot of the data with the square root of time is given in Figure 8-2.

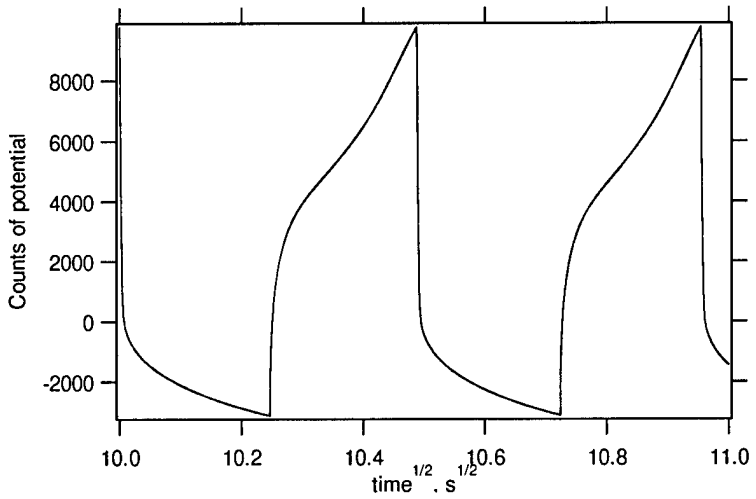

Figure 8-2 Time scale plotted as the square root

Near the end of the discharge pulse, this region is not well described by the sum of the exponent model, equation [1]. The deviation from the exponential model may signify more diffusion control. In this region, as depicted in Figure 8.2, the potential change is shown as a function of the square root of time. Since the potential variation seems somewhat linear on this figure, diffusion may be important in this region.

Another deviation from the exponential correlation was observed at short time scales. As shown in Figure 8-3, the potential recorded as counts (32000counts/0.2V) shows an almost linear potential-time response. This indicates that capacitive effects are dominant, and according to equation [3], should be linear. This clearly indicates a deviation from the sum of exponents' model.

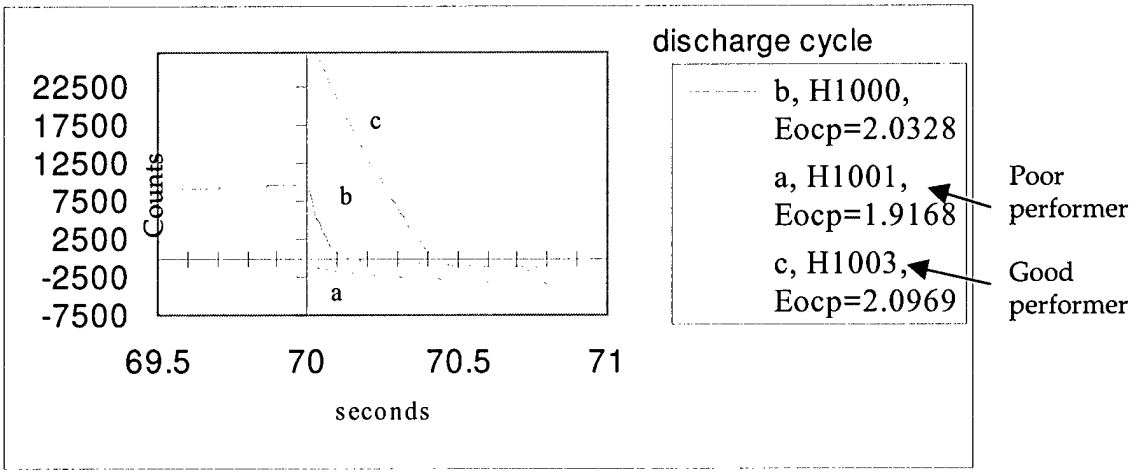

Figure 8-3 First second of discharge pulse.

8.1.8 Primary lithium cells

The potential change during pulse testing of the lithium cells included both an exponential region and a square root dependent time region. Figure 8-4 shows a typical pulse for two different discharge rates.

The pulsing time is greatly reduced since the reactions are more facile. The curved regions observed in Figure 8-4 can be modeled by the sum of exponents' model. However, the majority of the pulse appears linear with the square root of time. This signifies a diffusion-controlled process and a definite deviation from the sum of exponents' model.

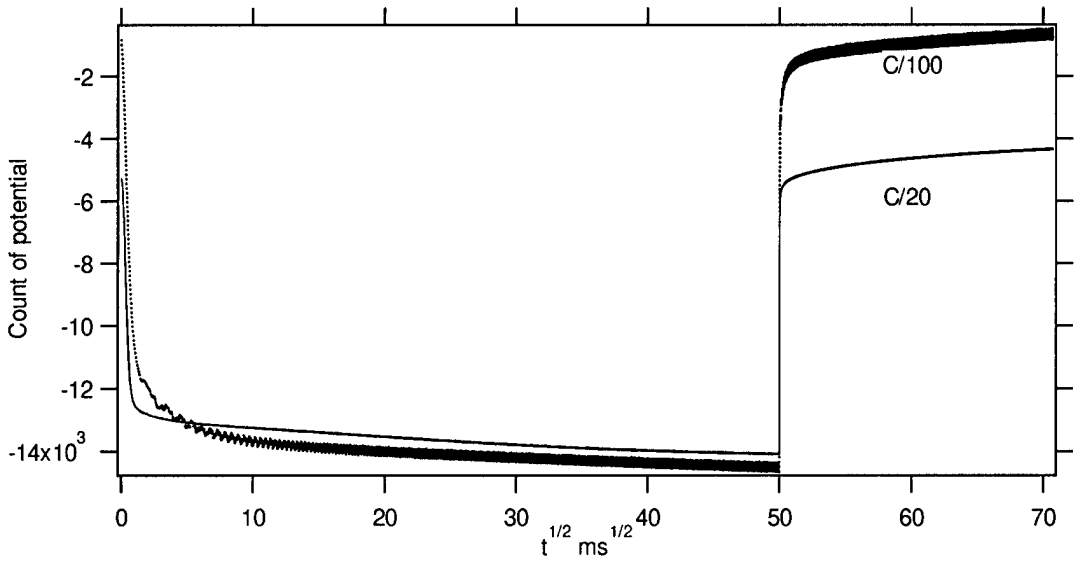

Figure 8-4 Lithium pulse plotted with the square root of time.

Figure 8-5 is another example of the pulse test or a discharge rate of C/100 (1/2 s cycles). This graph shows all 32 cycles of the test, and the diffusion control is also evident. Notice that the potential continues to drop with each pulse as the diffusion controlled reaction proceeds. The diffusion process can be either ionic diffusion in the solution or solid-state intercalation diffusion. Since the time scales are very short, the diffusion in this case must be those of the solid-state. According to Verbrugge *et al.*[v], the slope of these linear regions on a square root time plot can be directly correlated to the state of charge.

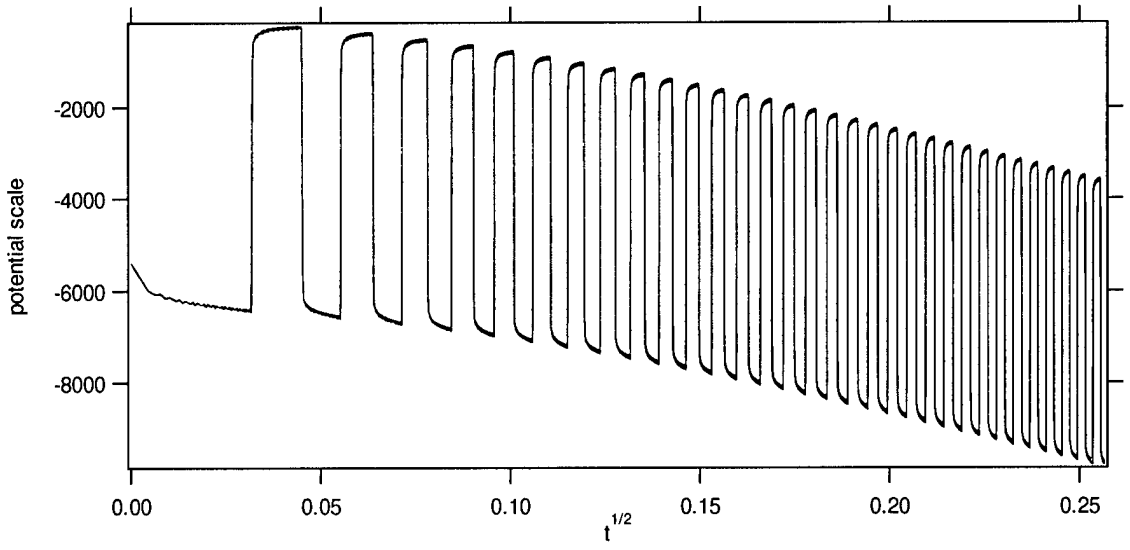

Figure 8-5 Lithium discharge pulse at C/100 with an open circuit relaxation time.

8.1.9 Conclusion

An attempt was made to generalize all possible processes and determine if a sum of exponentials is a reasonable fitting model to use in pulse battery testing. Theory does support that changes between processes result in exponential functions of potential with time. Deviations from exponential behavior can be accounted for as well. For example, diffusion processes can result in potential functions that are linear with the square root of time.

8.2 Multiple Linear Regression

The first attempt made to model a battery's state of charge vs. its voltage response to pulse testing was through multiple linear regression (MLR, for references see Draper & Smith and Kleinbaum, et.al.). Dr. Badie helped to verify the procedure and improve the modeling strategy. For each battery type, the MLR model was created using these steps:

1. Tests of normality were used to clean up the data
2. The equation of the discharge response was determined through curve fitting.
3. The parameters for the equation were solved for each battery tested.
4. MLR was performed using the equation parameters as predictors and the time of discharge (empirical) as the dependant variable.

8.2.1 Data Cleaning

The quality control consisted of first discarding any data for which the residuals calculated by the model were extremely large, and then computing the mean and the standard deviation of each parameter for each cell/battery. Any values that fell outside the mean ±3 standard deviations were discarded.

8.2.2 Curve Fitting

Initially, a significant amount of time was spent trying to fit the curve of the data from the first set of batteries (lead acid), and attempting to reduce high frequency noise in the data sets. It was later determined that commercial curve fitting and optimization software worked sufficiently well to describe these curves. Dr. Podlaha verified these equations to ensure their validity. The high frequency noise in the data was significantly reduced through hardware modifications. Also, it was later determined that this high frequency noise had no effect on the results derived from the data.

8.2.3 Software

The *mlrout* program was written in ANSI C (see Kernighan & Ritchie) to perform the curve fits on a single pulse test file. It is easily adjusted to add more equations. It uses the method of singular value decomposition to perform its task as outlined in Numerical Recipes in C (Press, et.al.). Figure 8-6 shows the top-down diagram of the *mlrout* program (see Dale and Orshalick for an overview of top-down methods). Note that starred (*'ed) modules can run as stand alone programs and were used to create the inputs for the TableCurve 3D software. The *getavg* program averages the results of *mlrout*.

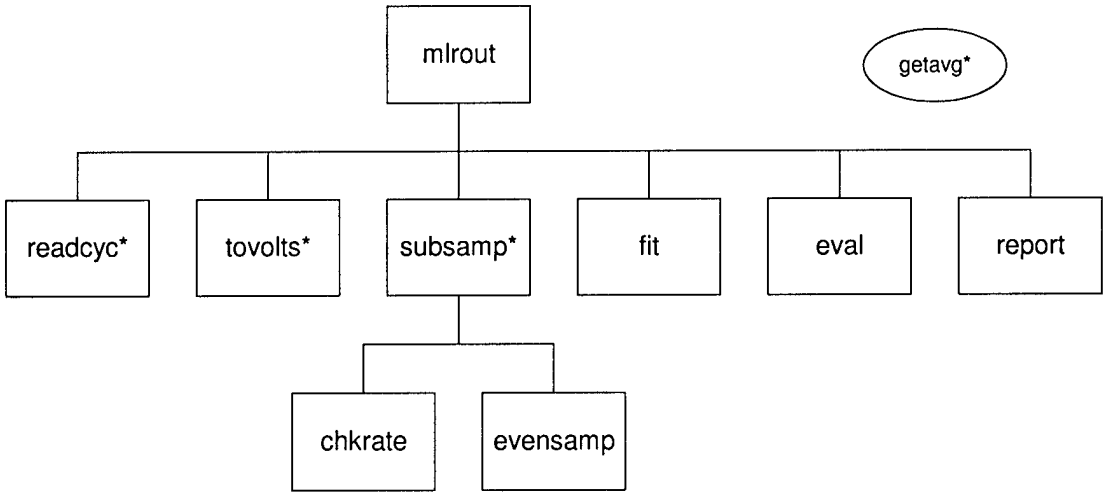

Figure 8-6 Top-down design diagram for the MLR output generating program.

Matlab™ was used to perform stepwise regression on the summarized *mlrout* output files and to test the normality (normplot.m) of the data.

GNU Octave is a high-level interactive language for numerical calculations, which is similar to matlab (see http://www.che.wisc.edu/octave/octave.html). Octave was used for plotting the data files and for MLR coefficient estimation.

Jandel Scientific's TableCurve 3D v1.0 is a curve fitting package that fits nearly 40,000 curves at a time and produces a list of the best fits. The input files from *mlrout* were input directly into TableCurve 3D.

8.3 Artificial Neural Networks

After the successful use of MLR to model state of charge vs pulse test voltage response, an artificial neural network (ANN) was employed for the same purpose. The ADAptive LINear Element (ADALINE) Network was chosen for this application because it is simple to implement and easy to understand.

The ADALINE network uses a pure linear transfer function described by,

$$\begin{aligned} a &= purelin(n) \\ &= purelin\ (wp + b) \end{aligned} \qquad [9]$$

where w is the matrix of weights, p is the input vector, and b is the bias vector. Since the ADALINE network prefers smooth data, the input files were decimated at 100Hz using the *subsamp* program before being input, and the voltage and time were scaled so that they both fell within the exclusive interval (0,1). Therefore, for these battery tests, the transfer function had the form,

$$a[32,1] = purelin(w[32,500]p[500,1] + b[32,1]) \qquad [10]$$

with the input vector p of length 500 corresponding to the number of datapoints in one discharge cycle (5 seconds of discharge data at 100 Hz), weight matrix of 32 rows and 500 columns corresponding to the 32 cycles and input vector length, and bias vector of length 32. Passing an input through the ADELINE is synonymous with performing a large dot product with a bias added.

It uses performance learning, and it applies the Least Mean Squared (LMS) learning law to adjust the weights and biases in a supervised notion until some criteria are met. LMS is also known as the Widrow learning law, the Widrow/Hoff learning law, and the delta rule. It can be stated as

$$w(k+1) = w(k) + 2\alpha ep \qquad [11]$$

where k represents the iteration number, and $e = t - a$, where t is the target value in the supervised training sense, and $0 < a < 1$ is the learning rate. The learning rate can be calculated analytically but is usually "tweaked".

Hecht-Neilsen describes the ADALINE's output as determining the hyperplane that is perpendicular to the weights that a particular input vector lies on. He also states that the ADALINE is sometimes called a linear combiner or affine combiner.

The training for the weight matrix and bias vector was accomplished using Octave. The source code (runem.m) is referenced in Appendix D.

9. RESULTS

9.1 Lead Acid Cells

9.1.1 Multiple Linear Regression - Lead Acid Cells

Dr. Podlaha verified through her electro-chemical analysis that the SEM worked well on the lead acid cells. The SEM in equation [1] was rewritten for the sampled data. It can be summarized as

$$V = a_0 + \sum_{i=1}^{5} a_i e^{-(ln2)C/b_i} \qquad [12]$$

where V is the digitized voltage in counts (a 16 bit short word in [-2^15, 2^15-1] corresponding to the voltage) and C is the count of the sample number (in the interval [1, 250000], which is 5 seconds of data at 50 kHz).

Figure 9-1 below shows a plot of a selection of the pulse curves for a Hawker cell with serial number H1030. Notice that beyond the first few cycles the curves seem almost identical.

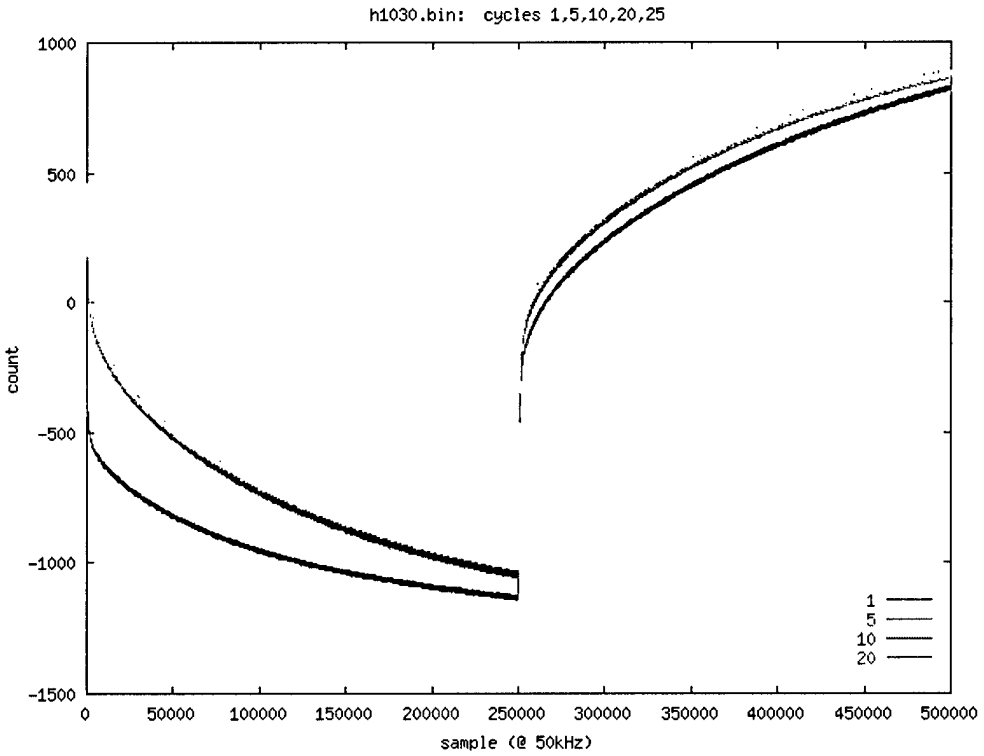

Figure 9-1 Over plot of the raw samples versus their A/D count.

The first cycles in each pulse test of the lead acid batteries were obviously outliers in the set, and for that reason, the first five cycles of each pulse test on the lead acid batteries were discarded. For each cell, the 27 remaining pulse curves were averaged using the *getavg* program, and then the parameters for equation [12] were solved for the averaged pulse curve using Octave. These data were then gathered into a set of 24 different cells. This cell set was then tested for normality (see Appendix B: Dr. Badie's Summary of Statistical Analysis of Secondary Data) and the following linear predictive model was produced:

$$T_d = F(v_0, a_0, a_1, b_1, a_2, b_2, a_3, b_3, a_4, b_4, a_5, b_5) \quad [13]$$

where v0 is the initial voltage at the beginning of the test. Table 9-1 shows the output of the SEM. There are 14 columns for each of the 25 rows. Each row represents the result of SEM curve fitting for one of the cells tested, including all the a_i, b_i, the initial voltage v_0, and the dependent variable T_d.

ID	v0	a0	a1	b1	a2	b2	a3	b3	a4	b4	a5	b5	Td
1002	2.10	-2001.93	1793.04	133774.75	553.85	16105.03	552.37	2715.44	246.25	539.94	23.65	31.14	9832.00
1003	2.11	-1825.51	1544.92	152942.27	469.65	17025.78	473.51	2614.28	279.37	531.66	27.64	24.56	10226.00
1005	2.12	-1279.51	957.16	121714.32	206.43	18018.09	113.83	3217.62	101.47	359.67	121.91	62.73	10104.00
1008	2.11	-1697.02	1547.83	183799.89	180.39	18505.03	250.03	3241.50	212.33	456.54	39.66	73.96	9248.00
1009	2.10	-1439.59	1310.63	107104.07	194.61	14256.03	181.22	2658.40	314.35	414.79	67.08	63.45	8012.00
1010	2.04	-908.11	542.50	136301.49	164.94	18951.43	91.20	3112.06	163.10	376.66	65.12	74.26	5443.00
1011	2.13	-1769.68	1741.27	165951.24	247.63	18733.63	304.81	3227.75	214.84	505.32	27.27	79.04	10704.00
1013	1.99	-979.32	603.99	107810.78	151.56	18125.73	92.25	3156.78	179.88	348.43	88.02	69.82	2055.00
1014	2.08	-1028.42	718.54	145884.96	187.58	17081.92	151.95	2774.32	224.35	424.73	47.09	64.80	7660.00
1016	2.10	-1647.28	1299.63	170912.85	344.00	17436.17	253.52	2921.89	206.95	465.46	33.35	55.22	8762.00
1017	2.12	-2001.31	1658.54	140629.44	524.33	16076.67	451.16	2788.30	234.08	523.27	30.89	30.98	9429.00
1018	2.12	-1854.64	1439.61	128787.71	265.19	19986.93	146.67	3286.37	179.55	354.80	169.61	59.41	10187.00
1020	2.11	-1901.30	1622.67	135521.60	510.07	15921.46	508.19	2674.22	245.47	533.07	32.45	33.59	8998.00
1021	2.11	-1931.00	1600.31	111318.30	384.32	14786.75	812.30	2260.63	257.20	541.72	35.60	35.28	9211.00
1023	2.09	-1866.57	1499.75	116790.07	449.47	16586.61	750.08	2422.09	273.10	555.50	33.78	34.62	8518.00
1024	2.12	-1972.23	1713.26	123643.88	600.74	15857.76	573.58	2702.36	233.80	545.49	27.57	28.30	9569.00
1028	2.00	-1144.02	878.76	106572.79	178.12	16361.52	118.21	2978.32	287.15	362.81	86.32	65.72	2474.00
1029	1.99	-1113.57	886.76	102472.84	185.99	16273.33	98.98	3164.41	176.19	334.71	96.35	78.28	2454.00
1030	2.00	-1201.00	966.45	101483.32	177.10	15131.20	141.54	2698.49	327.67	388.08	72.01	62.30	2826.00
1031	2.02	-1185.11	897.27	104682.81	213.99	16872.32	164.16	2608.34	313.32	425.91	52.16	54.92	4296.00
1032	2.01	-1191.11	858.76	110077.72	176.08	15459.64	155.39	2459.63	356.13	414.46	51.95	47.61	4508.00
1035	2.06	-1504.75	1044.29	121959.62	227.23	14653.38	375.90	2113.70	345.62	479.97	38.09	35.40	6795.00
1036	2.05	-1175.83	905.48	128296.30	194.58	15885.87	166.67	2557.48	296.75	419.06	51.06	52.47	6269.00
1037	2.07	-1414.38	1098.37	155765.14	288.22	17065.32	228.78	2791.03	238.75	452.97	45.46	60.08	7096.00

Table 9-1 SEM Data for Lead Acid Cells

The number of predictors was decreased from twelve to nine by using several automatic best-possible-regression methods, which eliminated parameters b_1, a_2, and a_3 from the MLR model.

The reduced model produced by the MLR is described by the following equation:

$$T_d = -81710.4971 + 53188.8252*v_0 + 3.6843*a_0 + 6.6078*a_1 + 0.7523*b_2 - 5.3176*b_3 - 11.0156*a_4 - 33.7442*b_4 - 28.9083*a_5 - 37.0279*b_5 \quad [14]$$

As with all prediction equations, this equation will only work on cells that have a state of charge within the range of charges of the cells used in the MLR. In other words, this equation will interpolate well, but it will not extrapolate.

Figure 9-2 is a classic residual plot of the fitted data. It shows a nice uniform banding about zero. The observation with the largest residual seems to be an outlier and could have been excluded, but the sample size was small, and it was left in the set.

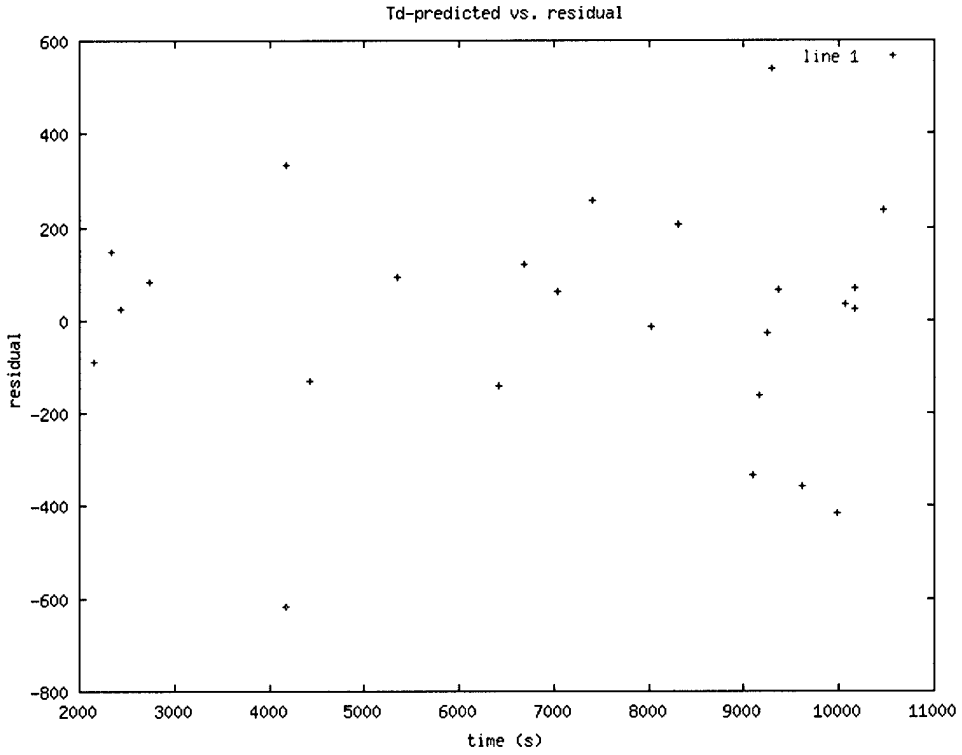

Figure 9-2 Residual plot of the MLR predicted values vs. their residuals for Lead Acid Cells.

The observation at about 4000 s may be an outlier. These data, overall, do not defeat any tests of normality.

The next figure shows the concurrent plot of the estimated time with its real time.

Note: In all plots with axes labeled "cell id", the axis is not continuous. The cells are simply ordered so that they flow naturally up and to the right.

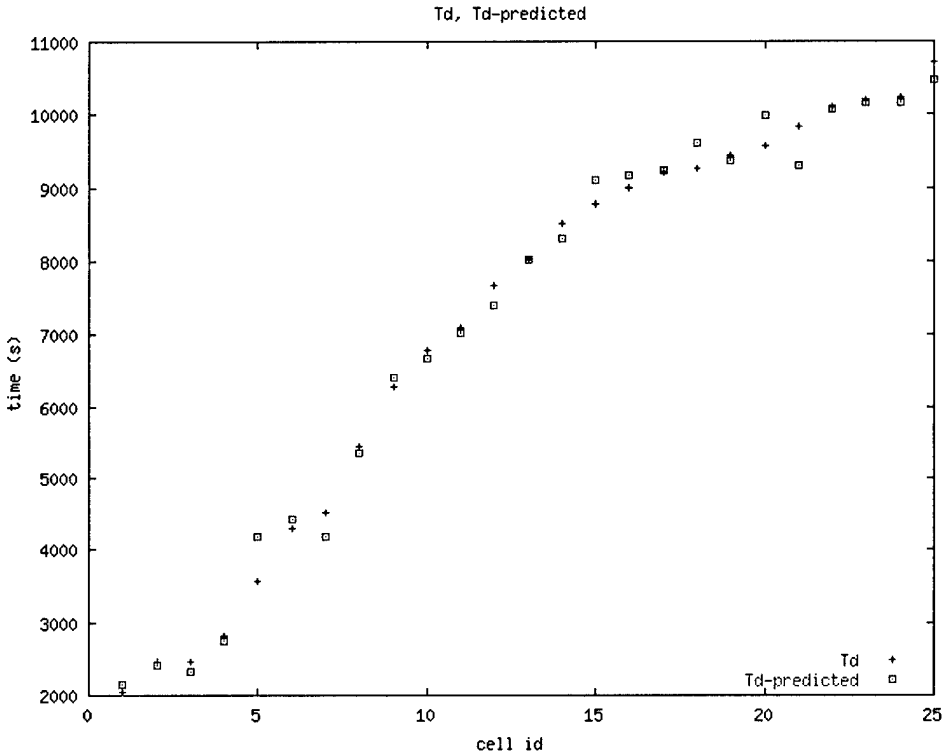

Figure 9-3 Over plot of the MLR predicted time to discharge and its true value for Lead Acid Cells.

Figure 9-4 shows a proportional error or relative error plot. The data seem banded about +/- 8% with the outlier at about 18%.

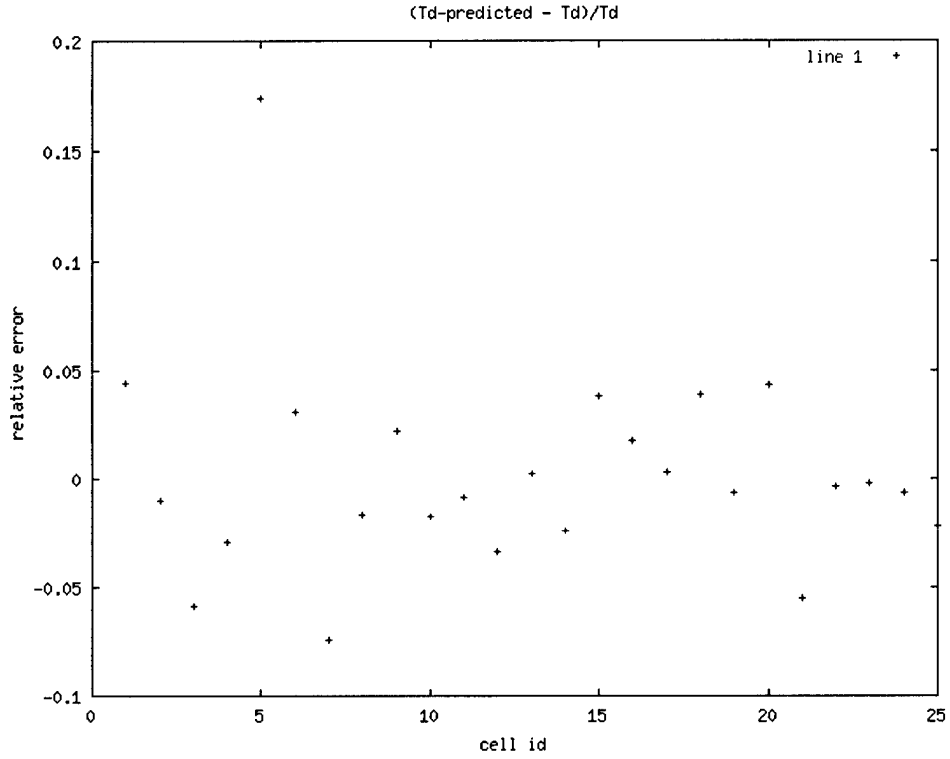

Figure 9-4 Proportional or relative error plot for Lead Acid Cells using MLR.

The cell with id 1 was overestimated by about 5%. Cell id 3 was underestimated by about 6%.

The Hawker cell manual indicates that the state of charge for a cell can be determined within +/- 25% by measuring the open circuit voltage. This was confirmed by condensing the linear predictive model in equation [13] to

$$T_d = F(v_0) \qquad [15]$$

which worked quite well for these data. Figure 9-5 shows the overplot of the predicted and real times (comparable to Figure 9-3). Notice how the model is more spread at the endpoints. The extra predictors help to clamp down on the ends. For these cells the v_0-only model was used as a pre-test/sanity-check when things didn't verify well or as a preliminary guess before discharging.

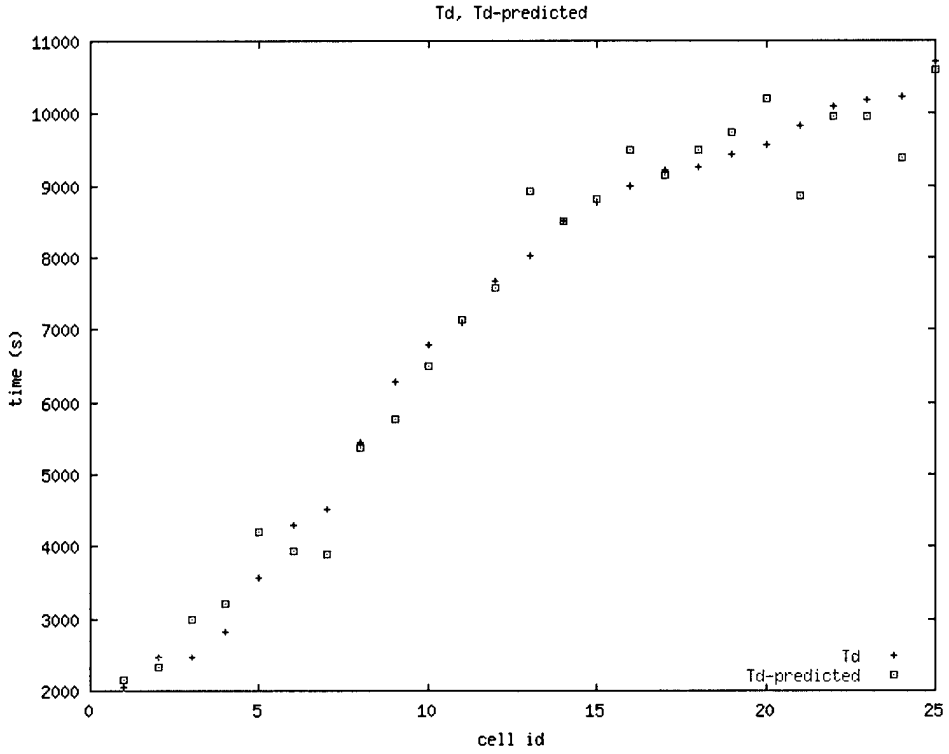

Figure 9-5 Prediction model for Lead Acid Cells with v_0-only as a predictor.

Figure 9-6 is the v_0-only model's proportional error plot.

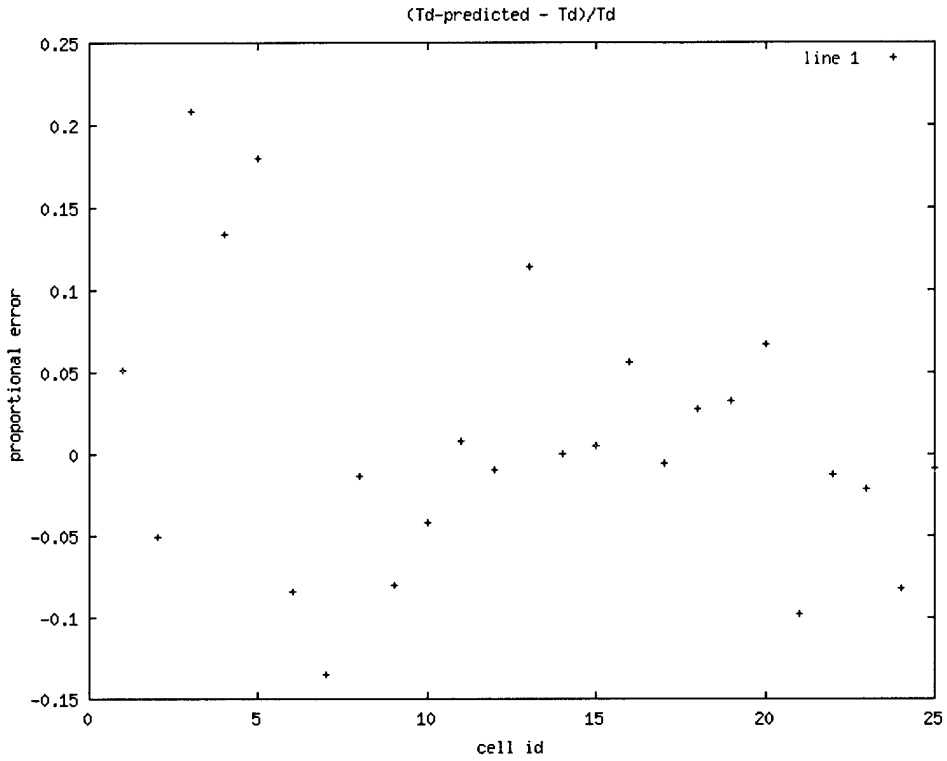

Figure 9-6 The v_0-only prediction model proportional errors for Lead Acid Cells.

To improve the model, the outlier was removed and one cross term or interaction term (a term involving the product of two or more predictors) was added. The model then becomes

$$T_d = F(\, v_0, a_0, a_1, b_2, b_3, a_4, b_4, a_5, b_5, a_1 \cdot b_1 \,) \qquad [16]$$

Figure 9-7 shows the predicted values vs. their residuals with the outlier removed and the interaction term added.

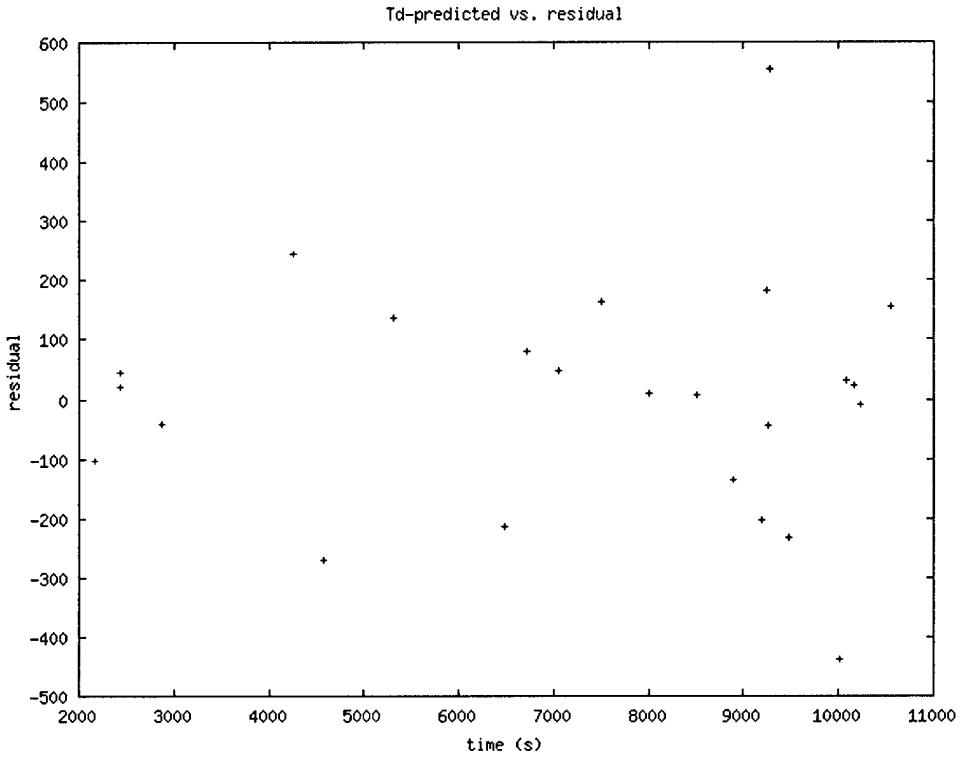

Figure 9-7 A residual plot of the MLR predicted values vs. their residuals for Lead Acid Cells

Data is shown with the outlier removed and the interaction term added.

Figure 9-8 shows the overplot of the predicted time to discharge with its true value with the outlier removed and the interaction term added.

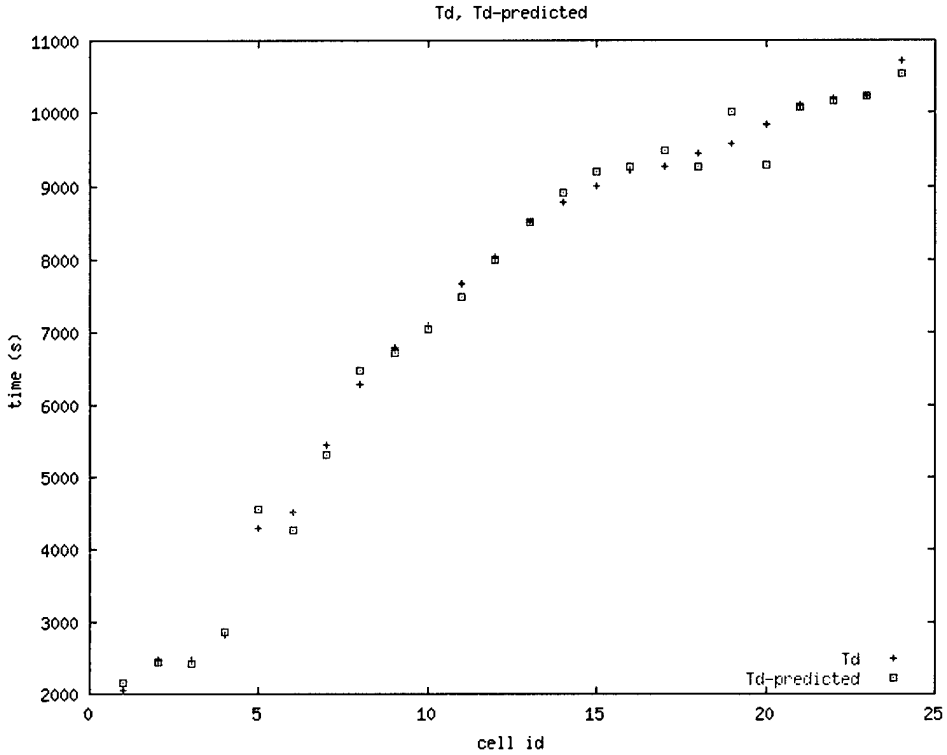

Figure 9-8 Over plot of the MLR predicted time to discharge and its true value for Lead Acid Cells

Data is shown with the outlier removed and the interaction term added.

This model showed only slight improvement over the original version, and no further improvements were attempted.

With ten predictor variables and only 24 samples, the ratio is below a rule of thumb for sample sizes, which states "three to five samples per variable, and a minimum of ten samples for one variable".

9.1.2 Artificial Neural Network - Lead Acid Cells (ref. appendix C)

The 25 samples from the pulse tests of the lead acid cells that had survived normality testing were divided into a training set of 14 and a test set of 11. The 14 training input cells and their discharge times are shown in Table 9-2.

ID	Td	ID	Td
1003	10226	1020	8998
1005	10104	1023	8518
1008	9248	1024	9569
1010	5443	1029	2454
1011	10704	1030	2826
1013	2055	1031	4296
1014	7660	1035	6795

Table 9-2 Lead Acid Cells training set for ADELINE

For the first training run, the 14 inputs were put through the affine combiner and Widrow's learing rule sequentially in increasing discharge time order. Next, six inputs were randomly chosen in the sequence, and they were sequentially combined. This process was repeated four times. For this initial run, the learning rate was set to 0.001, the weights matrix was initialized to zero, the bias vector was initialized to one, and the program allowed only 1000 iterations for each call to the Widrow/Hoff subroutine.

At this point, the data were tested. The results from the pure linear transfer function using the weights and biases from the first training run are shown in Table 9-3.

ID	Td	T Predicted	Residual	Relative Error
1028	2474	3161.094	-687.094	0.278
1033	3562	4216.824	-654.824	0.184
1032	4508	3975.961	532.039	-0.118
1036	6269	5694.918	574.082	-0.092
1037	7096	6906.442	189.558	-0.027
1009	8012	8589.441	-577.441	0.072
1016	8762	8776.741	-14.741	0.002
1021	9211	8547.444	663.556	-0.072
1017	9429	9276.214	152.786	-0.016
1002	9832	9229.860	602.140	-0.061

1018	10187	9375.362	811.638	-0.080

Table 9-3 ADALINE results for Lead Acid Cells after the first training run.

In an attempt to improve on the results of the initial training run, the process was repeated. The weight matrix was again initialized to zero, the bias vector was again initialized to one, and they were trained using a set with 30 iterations of 30 random selections. The results from the pure linear transfer function using the weights and biases from the second training run are shown in Table 9-4

ID	Td	T Predicted	Residual	Relative Error
1028	2474	3014.019	-540.019	0.218
1033	3562	4320.678	-758.678	0.213
1032	4508	3990.033	517.967	-0.115
1036	6269	6066.041	202.959	-0.032
1037	7096	7568.726	-472.726	0.067
1009	8012	9587.307	-1575.307	0.197
1016	8762	9864.524	-1102.524	0.126
1021	9211	9710.900	-499.900	0.054
1017	9429	10606.141	-1177.141	0.125
1002	9832	10596.720	-764.720	0.078
1018	10187	10642.752	-455.752	0.045

Table 9-4 ADALINE results for Lead Acid Cells after the second training run.

In an attempt to improve on the results of the second training run, the process was repeated. This time the weights matrix and bias vector were not reinitialized, and the learning rate was set to 0.0001. Once again, a set with 30 iterations of 30 random selections was used. The results from the pure linear transfer function using the weights and biases from the third training run are shown in Table 9-5

ID	Td	T Predicted	Residual	Relative Error
1028	2474	2977.498	-503.498	0.204
1033	3562	4102.683	-540.683	0.152
1032	4508	3844.821	663.179	-0.147
1036	6269	5675.033	593.967	-0.095
1037	7096	6966.370	129.630	-0.018
1009	8012	8757.801	-745.801	0.093
1016	8762	8959.028	-197.028	0.022
1021	9211	8719.265	491.735	-0.053
1017	9429	9495.731	-66.731	0.007

1002	9832	9448.025	383.975	-0.039
1018	10187	9598.340	588.660	-0.058

Table 9-5 ADALINE results for Lead Acid Cells after the third training run.

This was only a slight improvement over the second training run, and no further training on the ADALINE was attempted. The results from this last iteration are plotted in the graphs on the following pages.

Figure 9-9 shows the residual plot of the prediction vs. the error value for the results of the third training run. This graph shows a maximum residual of about 11 minutes, while the largest discharge time is about two hours and 40 minutes. The residual plot show that the model is satisfactory, but the sample size is marginal.

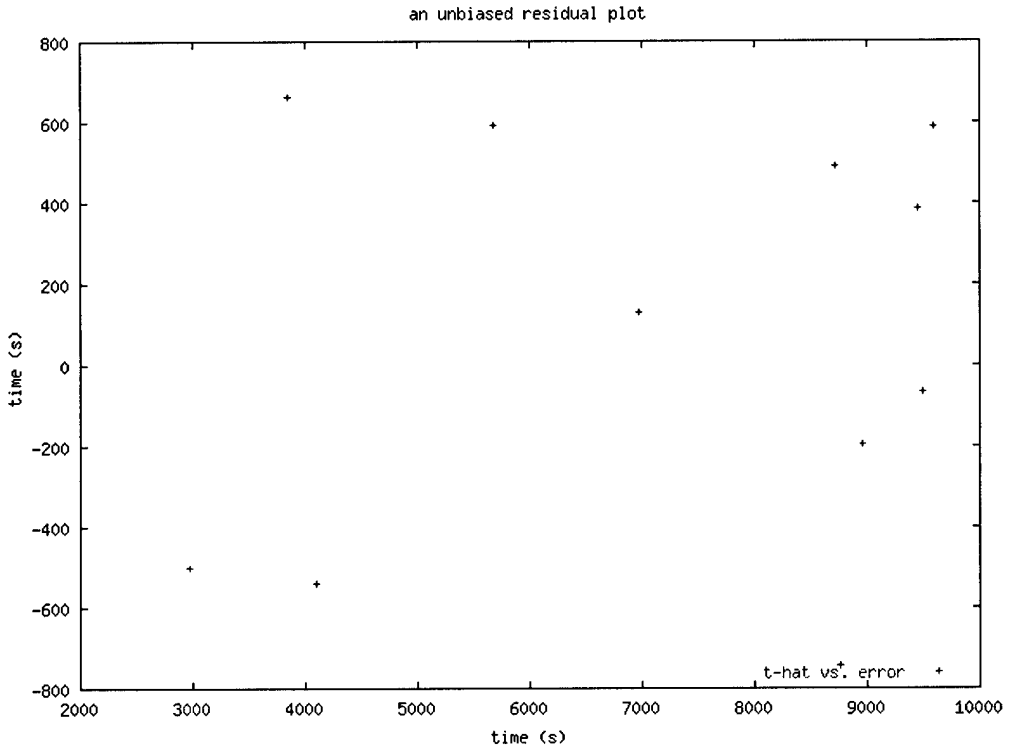

Figure 9-9 A residual plot of the predicted values vs. their residuals for Lead Acid Cells from the ADALINE third iteration

The next figure shows the concurrent plot of the estimated time with its actual time for the last iteration of the ADALINE. This shows a trend of underestimating the higher discharge times and overestimating the lower discharge times. More training, especially with a larger training set, may have clamped down both ends of this graph.

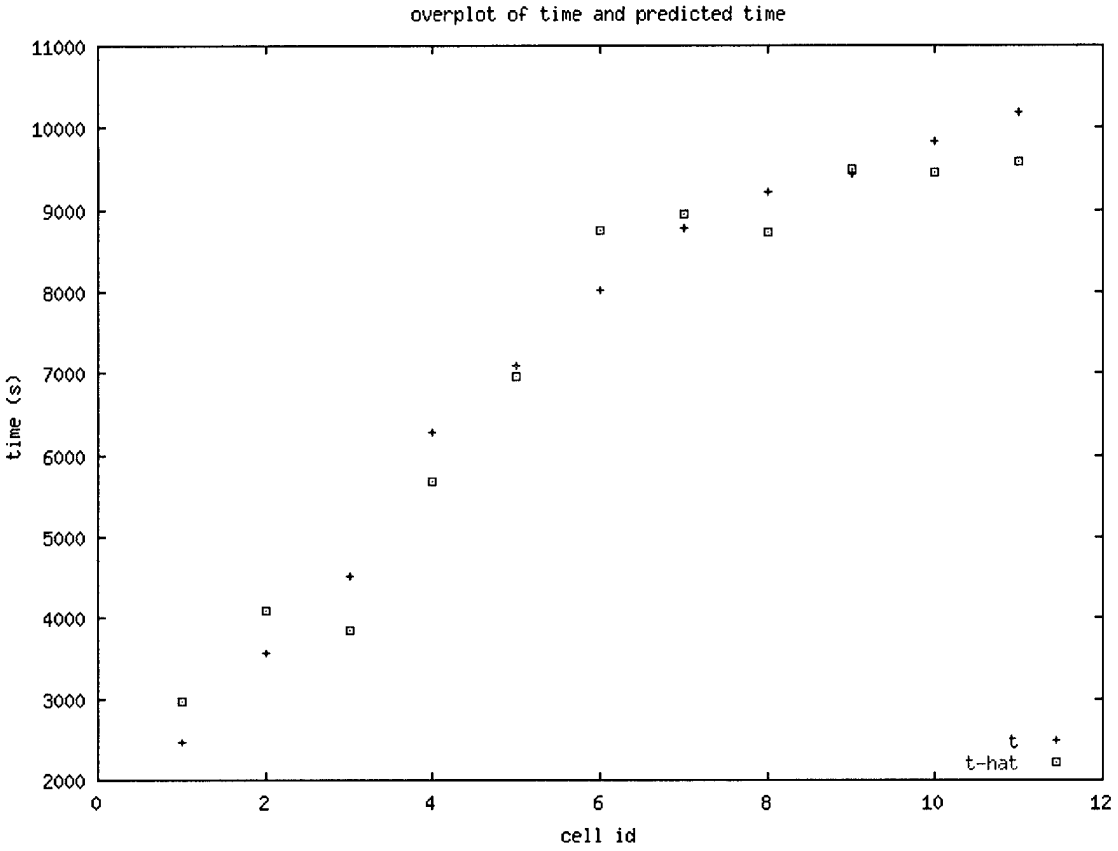

Figure 9-10 Over plot of the predicted time to discharge and its true value for Lead Acid Cells from the ADALINE third iteration.

Figure 9-11 shows a proportional error or relative error plot for the ADALINE third iteration. The data shows a maximum absolute error of 20%.

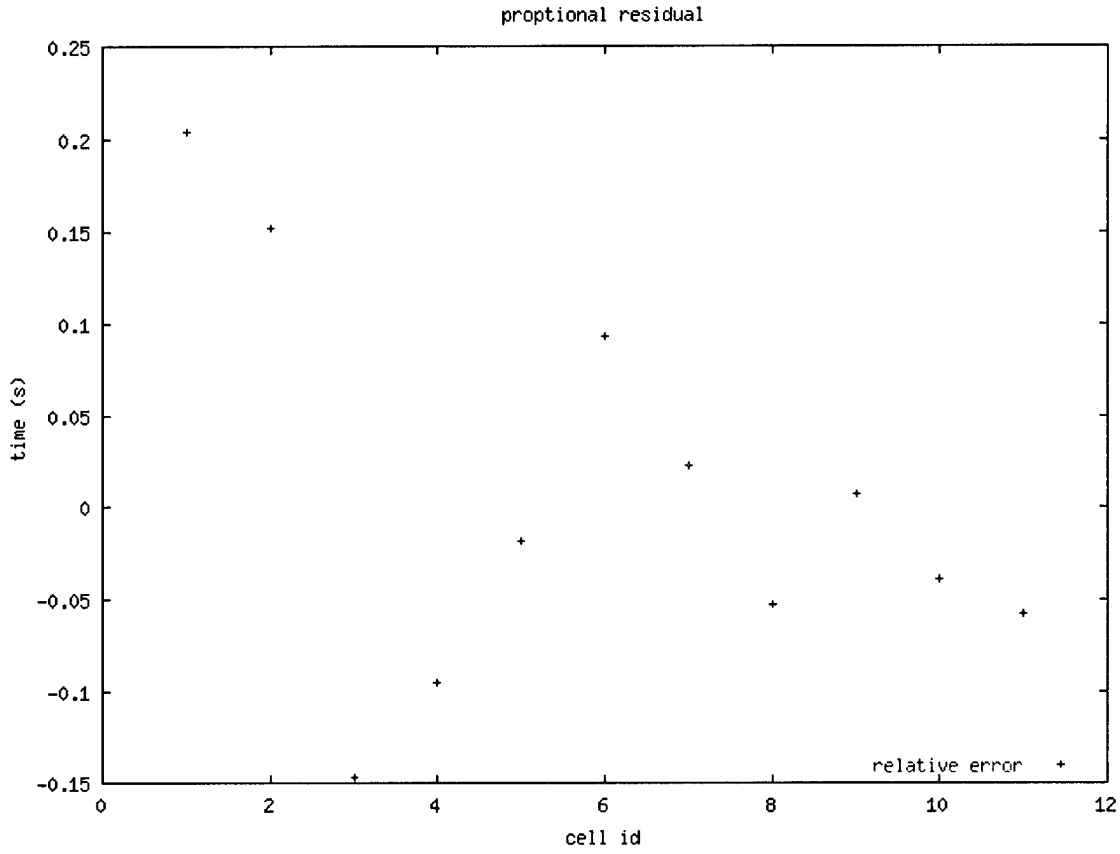

Figure 9-11 Proportional or relative error plot for Lead Acid Cells from the ADALINE third iteration.

9.2 Lead Acid Batteries

An unbiased Hawker battery set with sample size of eight was created, and the data were modeled with the SEM used for the lead acid cells. The results were reasonable, but the sample size was much too small for the twelve predictor variables. A new set with six independent variables was created using the TableCurve 3D program. The curve fit chosen for the voltage response is described as follows:

$$v(t) = a_0 + a_1 e^t + a_2 sqrt(t) log(t) + a_3 log^2(t) + a_4 sqrt(t) + a_5 log(t) \quad [17]$$

The MLR approach was not attempted with these new parameters due to time constraints.

9.3 Lithium Sulfur Dioxide Cells

The same SEM used for the lead acid cells was applied to the Lithium cell data, but it did not work well. An attempt was made to screen out data with high standard deviation within the columns (a practice common in data cleaning), but the model produced was not statistically significant.

Dr. Podlaha had determined through her analysis that the pulse response of the Lithium chemistry is not necessarily exponential, but might be better modeled by potential functions that are linear with the square root of time. This was confirmed by the failure of the MLR. The correlation coefficients indicated that only the intensities were highly correlated with T_d. No further work was done on these cells.

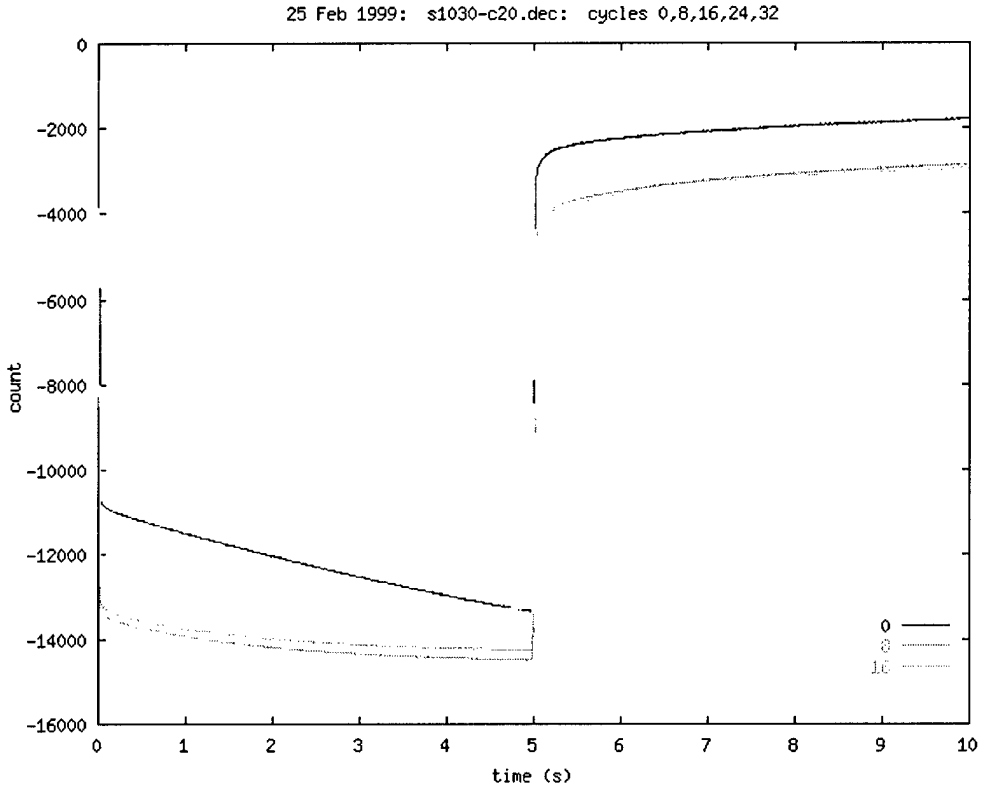

Figure 9-12 Example of Saft cell discharge and charge plot for a pulse test.

9.4 Lithium Sulfur Dioxide Batteries

9.4.1 Multiple Linear Regression – lithium sulfur dioxide batteries

The analysis of the Lithium Sulfur Dioxide cells had shown that the SEM was a poor choice for this chemistry. For this dataset, TableCurve 3D was used to fit the pulse curves, and the equation chosen for the pulse curve is described as follows:

$$v(t) = a_0 + a_1(t)log(t) + a_2 log^2(t) + a_3 log(t) + a_4/sqrt(t) + a_5 log(t)/t + a_6/t \qquad [18]$$

This was reasonable since Dr. Poldlaha had determined that the processes of Lithium batteries were better modeled with functions that are linear with the square root of time.

Figure 9-13 shows the residual plot vs. the voltage estimate from equation [18] over one discharge cycle, which clearly shows a trend in the data, indicating that more terms were necessary in equation [18].

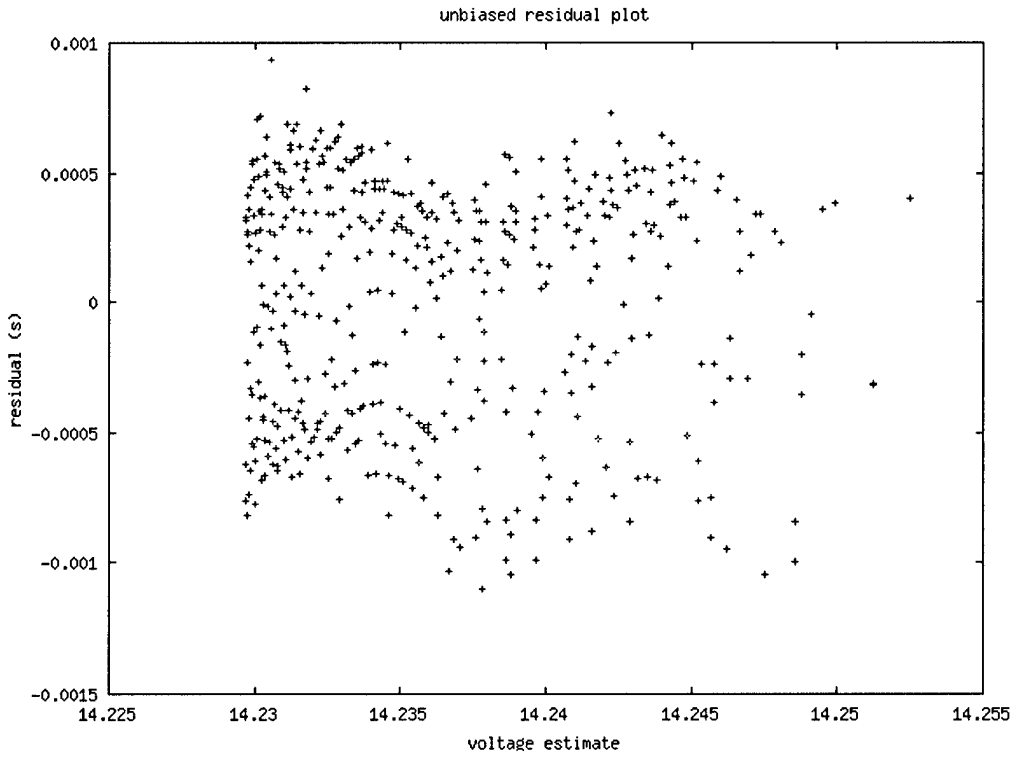

Figure 9-13 Residual plot of the voltage estimate for Lithium batteries from equation [18].

Figure 9-14 shows the overplot of the estimated and actual voltages for the same cycle, which shows the estimated voltage line inscribed right down the middle of the noisy data.

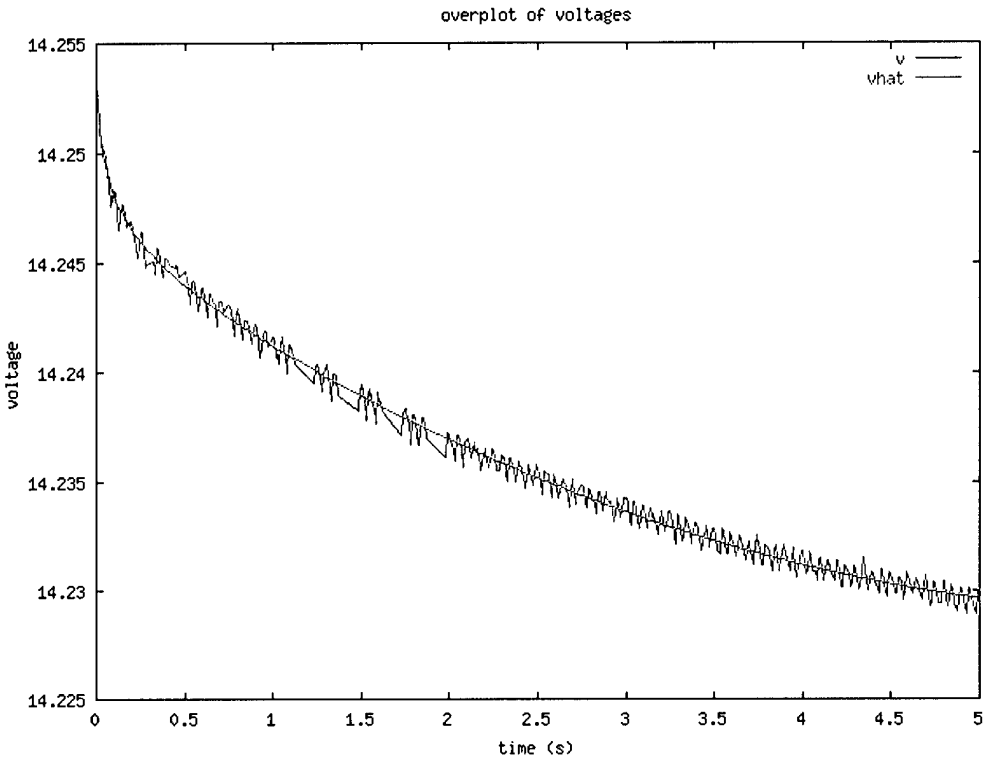

Figure 9-14 Overplot of the voltage estimate and actual voltage for Lithium batteries

Figure 9-15 shows the residual plot vs. time for the same cycle, which shows that the variability in the deviations from the curve fit are very small.

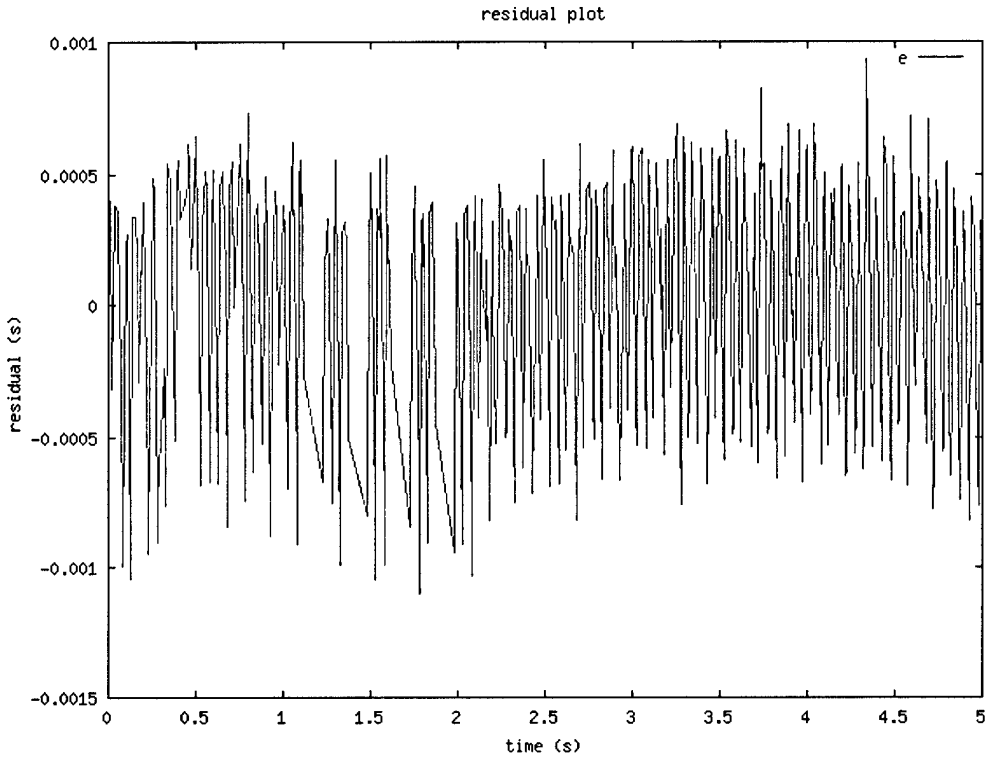

Figure 9-15 Residual plot of the voltage estimate vs. time for Lithium batteries

From these plots, it is obvious that more terms need to be added to the curve fit equation.

After the curve fitting was accomplished, the parameters for equation [18] were solved for each pulse curve. The Chi-square test for goodness of fit was accomplished, which showed that the first cycle in each test was an outlier. Therefore, the first cycle in each test was discarded, and the parameters for the 31 remaining pulse curves were averaged for each battery. Tests for normality decreased the number of batteries in the set from 13 to 11. These data were then gathered into a set, which is shown in Table 9-6. There are nine columns for each of the eleven rows. Each row represents the result of the curve fitting for one of the batteries tested, including a_0-a_6 and the dependent variable T_d.

id	a0	a1	a2	a3	a4	a5	a6	td
3	14.2355	0.000207	-0.00232	-0.00239	0.007152	-2.6E-05	-0.00028	14401
4	14.14584	0.000217	-0.00217	-0.00239	0.007309	-2.8E-05	-0.0003	11988
5	14.22722	2.26E-05	-0.00209	-0.00243	0.007094	-2.6E-05	-0.00028	8512
6	14.12658	0.000478	-0.00274	-0.00257	0.008432	-2.9E-05	-0.00031	3088

12	14.14612	0.000459	-0.00286	-0.00291	0.009116	-2.5E-05	-0.00028	17196
13	14.23293	0.000177	-0.00224	-0.00247	0.007428	-3E-05	-0.00032	15318
14	14.23841	0.000148	-0.00236	-0.00239	0.007367	-2.7E-05	-0.00029	13862
15	14.23036	-1.9E-05	-0.00192	-0.00219	0.006543	-2.4E-05	-0.00026	11864
16	14.20404	0.000153	-0.00214	-0.00231	0.006757	-2.6E-05	-0.00027	10393
17	14.19317	0.000112	-0.00211	-0.00231	0.006624	-2.4E-05	-0.00026	6363
18	14.20895	-1.8E-05	-0.00178	-0.00218	0.006161	-2.3E-05	-0.00024	8708

Table 9-6 Curve Fitting Data for Lithium Sulfur Dioxide Batteries

With such a small sample set, an "all-possible regressions" approach was used. All possible regressions on the 11 samples were performed. For each regression, one sample was left out, and the other ten were used to create the prediction coefficients. The odd-man-out was then tested. Using this method, the 11 samples were reduced to nine, and the final model for the Lithium Sulfur Dioxide batteries was developed.

$$Td = F(a_0, 1/a_3, 1/a_4, 1/a_5, 1/a_6) \quad [19]$$

Predictors a_0 and a_1 were eliminated from the regression model by an automatic stepwise procedure. The MLR produced the following prediction equation:

$$T_d = -3837.6751 + 250.1715*a_0 - 3.4620/a_3 + 4.0952/a_4 - 0.3328/a_5 + 4.0426/b_5 \quad [20]$$

Figure 9-16 is residual plot of the fitted data. With such a small sample size, it is nearly impossible to find any trend, but these data do not appear to show signs of abnormality.

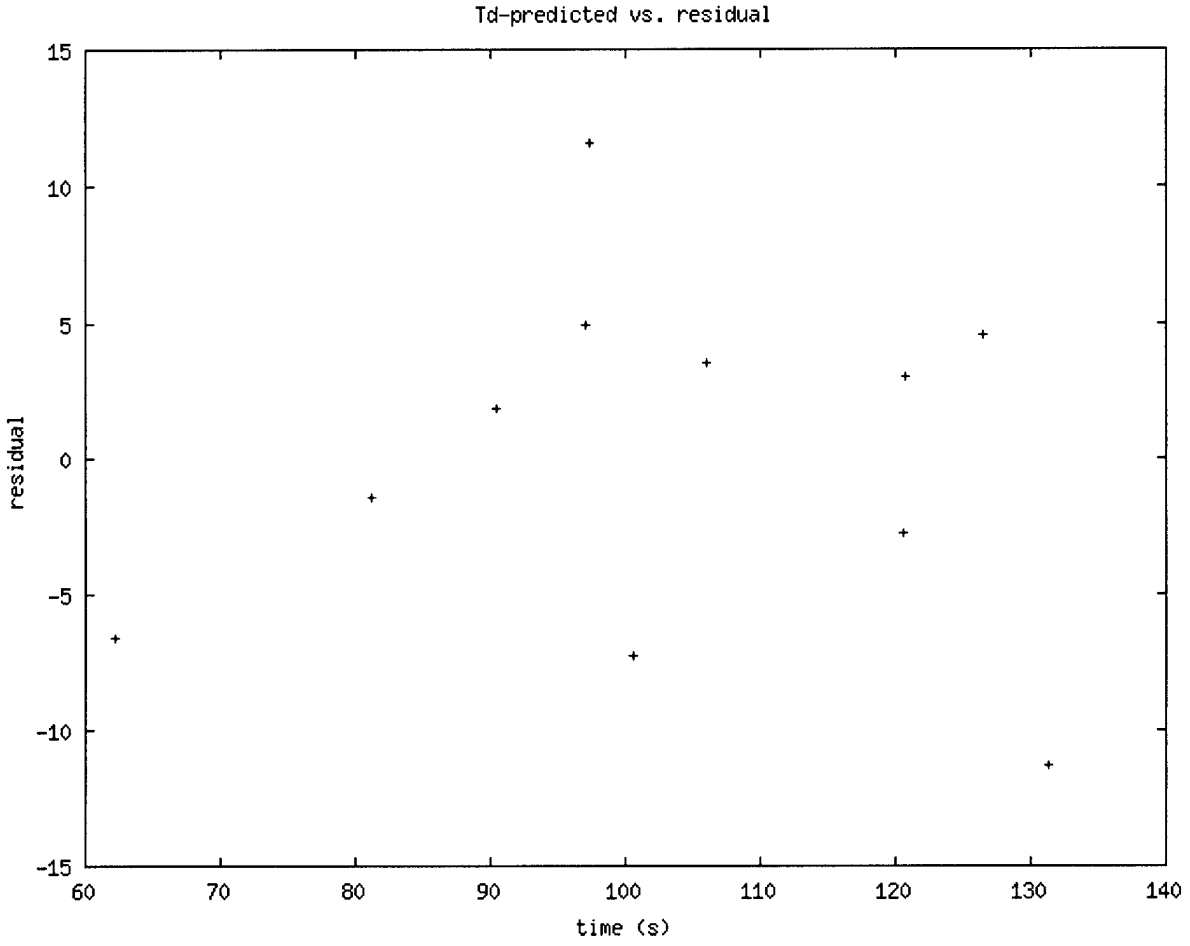

Figure 9-16 A residual plot of the MLR predicted values vs. their residuals for Lithium batteries.

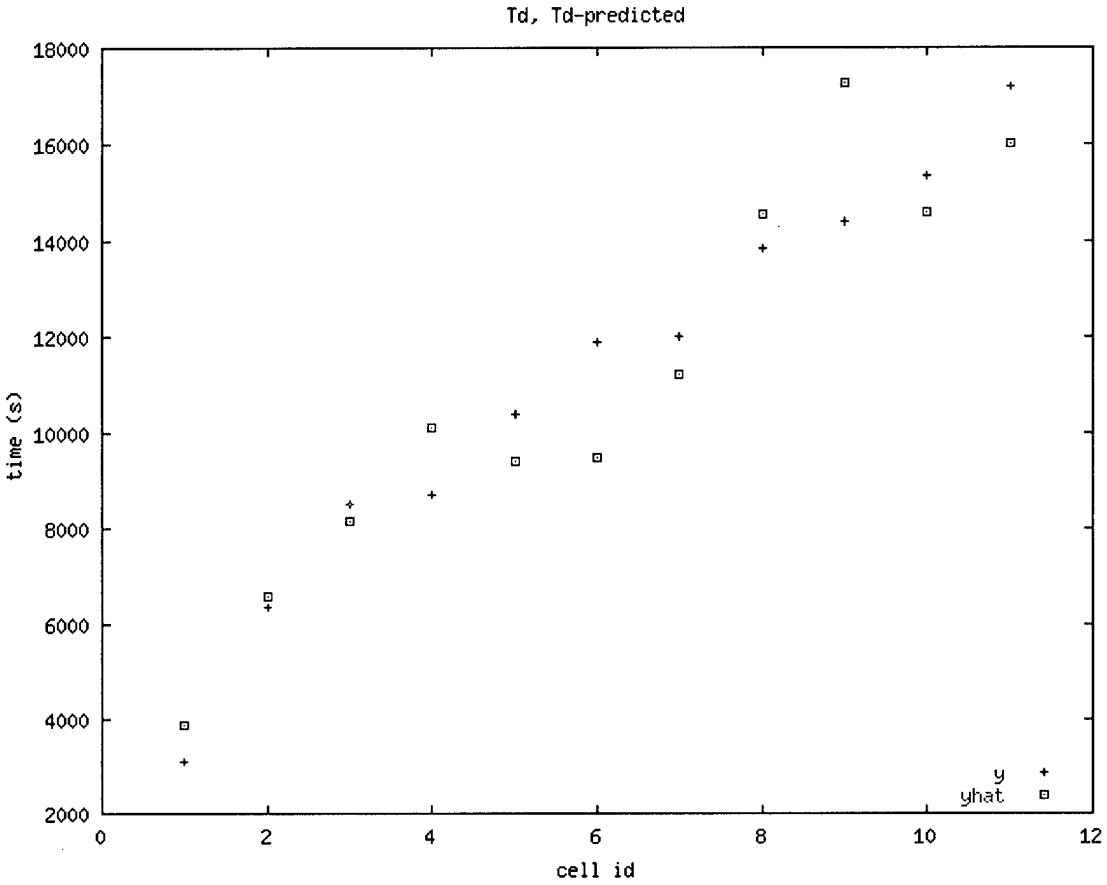

Figure 9-17 Over plot of the MLR predicted time to discharge and its true value for Lithium batteries.

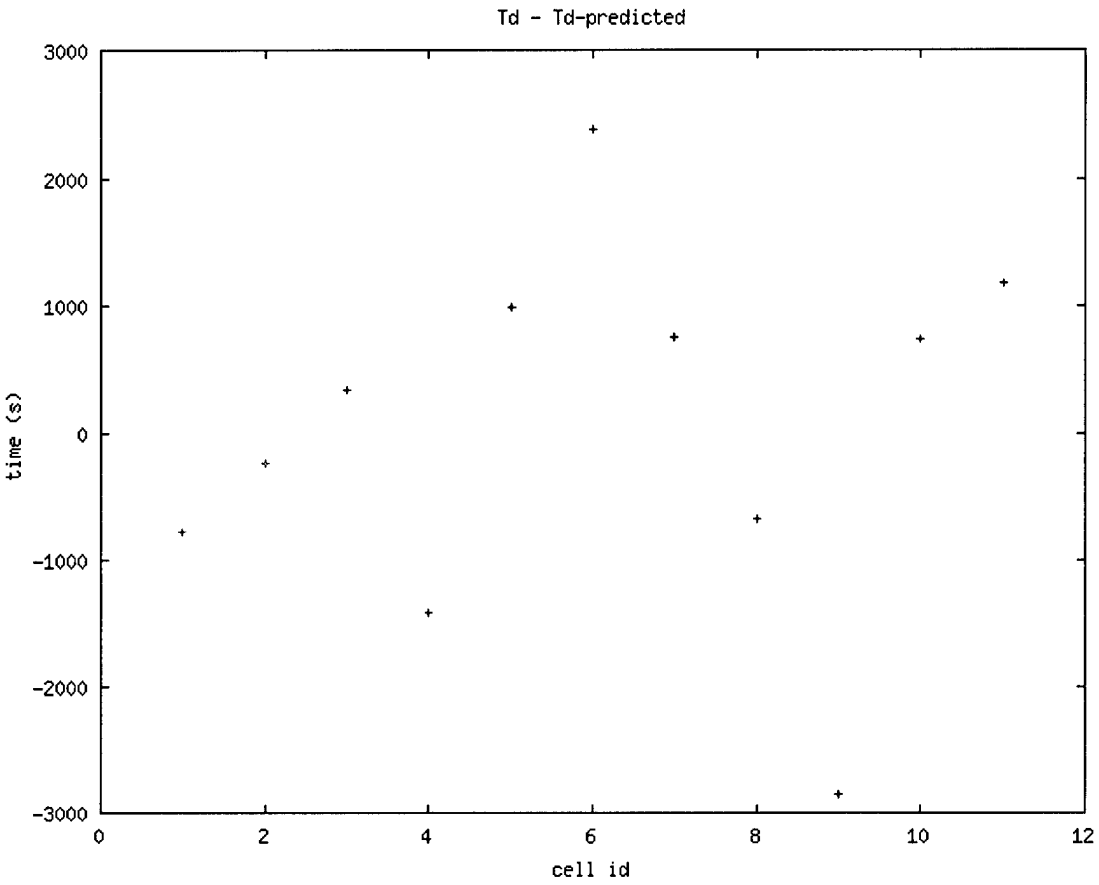

Figure 9-18 Proportional or relative error plot for Lithium batteries using MLR.

Because of the extremely small sample size, the results of the MLR are still inconclusive.

9.4.2 Artificial Neural Network – lithium sulfur dioxide batteries

The 13 data sets from the pulse tests of the Lithium Sulfur Dioxide Batteries were divided into a training set of eight and a test set of five. The eight training input batteries and their discharge times are shown in Table 9-7.

ID	Td
6	3088
17	6363
5	8512
16	10393
15	11864
14	13862
3	14401
12	17196

Table 9-7 Lithium Sulfur Dioxide battery training set for ADELINE

A set with 30 iterations of 30 random selections was used. The learning rate was set to 0.0001, the weights matrix was initialized to zero, the bias vector was initialized to one, and the program allowed only 1000 iterations for each call to the Widrow/Hoff subroutine.

At this point, the data were tested. Four of the batteries in the test set were tested once, while the last battery (ID #20) was tested eight times. The results for the first four batteries from the pure linear transfer function using the weights and biases from this training set are shown in Table 9-8.

ID	Td	T Predicted	Residual	Relative Error
7	8470	6795.954	1674.046	-0.198
19	8500	10223.682	-1723.682	0.203
4	11988	7638.281	4349.719	-0.363
13	15318	12474.143	2843.857	-0.186

Table 9-8 ADALINE results for the first four Lithium Sulfur Dioxide batteries

The relative error for these batteries was high because the sample size used for training is small. Also, these batteries had been excluded from the MLR model earlier because the data were non-normal. Since most of the data from the batteries in the test set were suspect, special attention was

paid to the one good battery in the test set. Battery ID #20 was tested eight times, and the results of each test are shown in Table 9-9.

ID	Td	T Predicted	Residual	Relative Error	Rest Time
20	15605	14877.590	727.410	-0.047	53580
20	15605	10784.647	4820.353	-0.309	24600
20	15605	14199.314	1405.686	-0.090	89580
20	15605	14406.510	1198.490	-0.077	77940
20	15605	14521.537	1083.463	-0.069	92460
20	15605	11803.686	3801.314	-0.244	1200
20	15605	10283.367	5321.633	-0.341	1320
20	15605	15994.671	-389.671	0.025	77940

Table 9-9 ADALINE results for the Lithium Sulfur Dioxide battery ID #20

Notice that the model works well when the battery is given one day of rest before the next test, but that the relative error is high when little or no rest is given. This may be related to diffusion phenomena, and it highlights the need for keeping all variables constant during the pulse testing. See Section 8.1.6 for a detailed discussion of the diffusion effects.

Figure 9-19 shows the residual plot of the prediction vs. the time of rest before testing. This graph shows that the model predicts the state of charge well (within +/- 10%) when the battery is allowed to rest for approximately one day prior to testing. The limited sample size prevented more verification of this model, but the initial results are very promising.

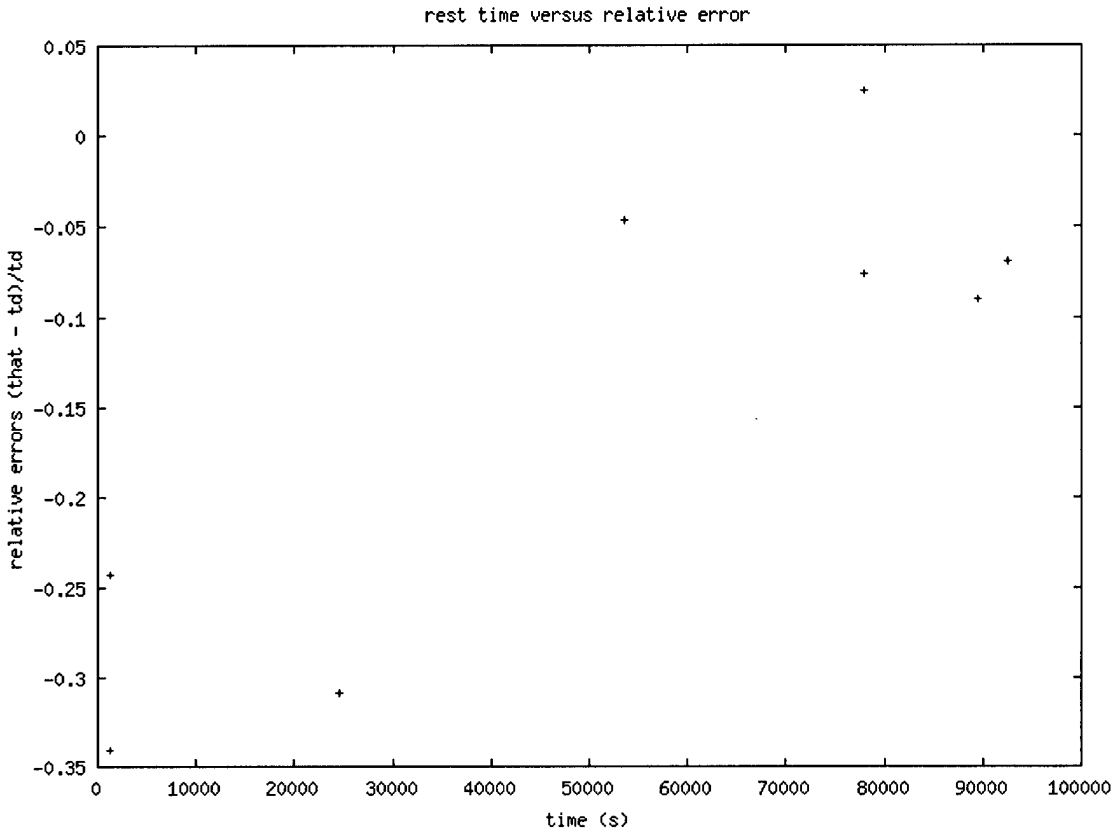

Figure 9-19 A residual plot of the ADALINE predicted values vs. time of rest for Lithium #20.

9.5 Nickel Cadmium Batteries

9.5.1 Multiple Linear Regression – Nickel Cadmium batteries

The same procedure was used on the Nickel Cadmium (NiCd) batteries as on the Lithium Sulfur Dioxide batteries. For this dataset, TableCurve 3D was used to fit the curve of the line, and the pulse curve is described as follows:

$$v(t) = a_0 + a_1 t + a_2(t)\log(t) + a_3 sqrt(t)\log(t) + a_4 \log(t) \qquad [20]$$

For each cell, the parameters for equation [20] were solved for each pulse curve. The Chi-square test for goodness of fit showed that each cycle in each test was reasonable. The parameters for the 32 pulse curves were averaged for each battery. These data were then gathered into a set of seven different batteries, which is shown in Table 9-10. There are seven columns for each of the seven rows. Each row represents the result of the curve fitting for one of the batteries tested, including a_0-a_4 and the dependent variable T_d.

id	a0	a1	a2	a3	a4	Td
1	3.844043	-0.01057	0.001711	0.004146	0.000432	8272
3	4.03127	-0.01165	0.001997	0.00468	0.00053	8513
4	3.993697	-0.00991	0.00157	0.003912	0.000447	8350
5	3.961117	-0.00933	0.001396	0.003603	0.000408	8496
6	3.912826	-0.01056	0.001693	0.004156	0.000455	6312
7	3.937128	-0.01251	0.002218	0.005068	0.000561	4275
8	3.995611	-0.01035	0.001673	0.004106	0.000462	7034

Table 9-10 Curve Fitting Data for Nickel Cadmium Batteries

The MLR equation is then,

$$sqrt(Td) = F(a_0, 1/a_1, 1/a_2, 1/a_3, 1/a_4) \qquad [21]$$

And the reduced model produced by the MLR is described by the following equation:

$$T_d = -715.621 + 65.601*a_0 + 23.076/a_1 - 3.896/a_2 + 22.678/a_3 - 0.196/b_4 \qquad [22]$$

Figure 9-20 is the residual plot of the fitted data. With such a small sample size, it is impossible to find any trend.

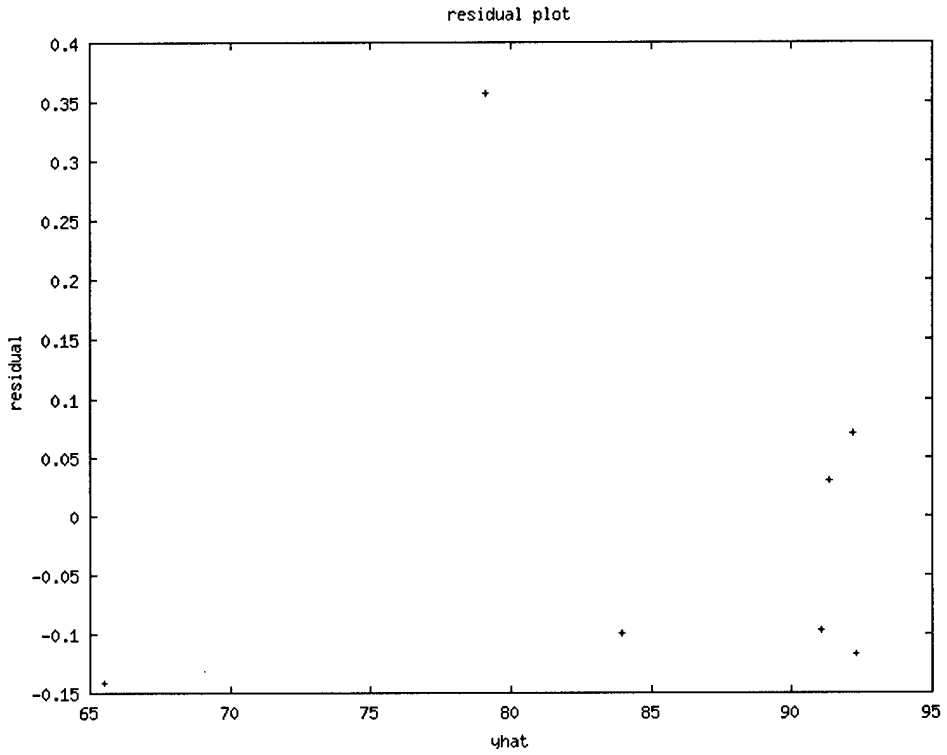

Figure 9-20 A residual plot of the MLR predicted values vs. their residuals for NiCd batteries.

Figure 9-21 shows the overplot of the estimated time with its real time.

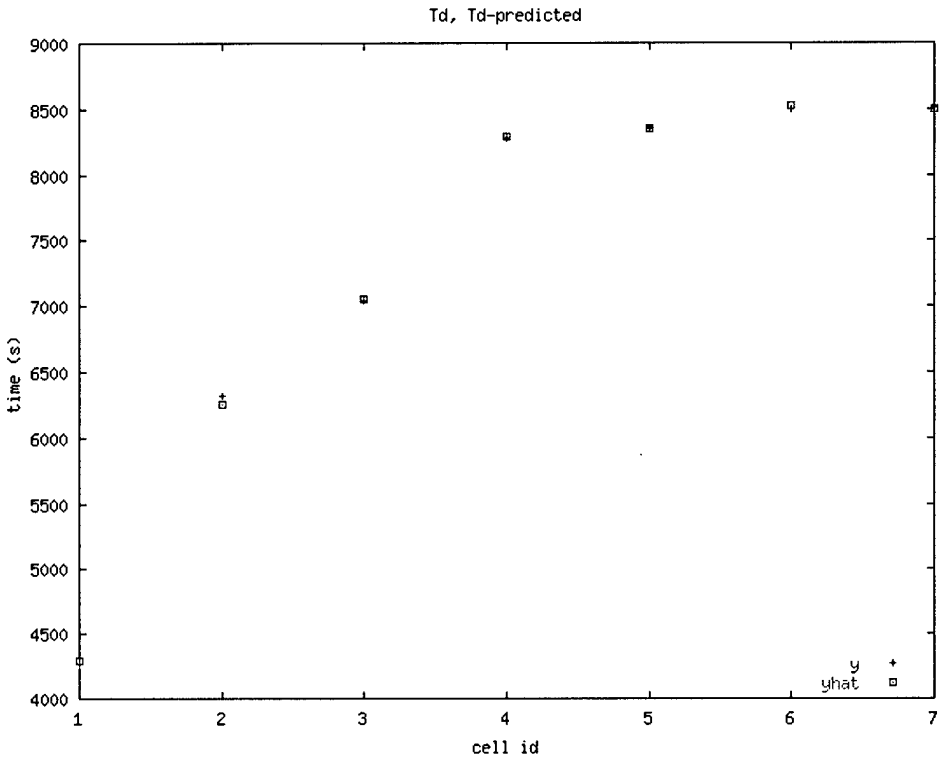

Figure 9-21 Over plot of the MLR predicted time to discharge and its true value for NiCd batteries.

Figure 9-22 shows a proportional error or relative error plot.

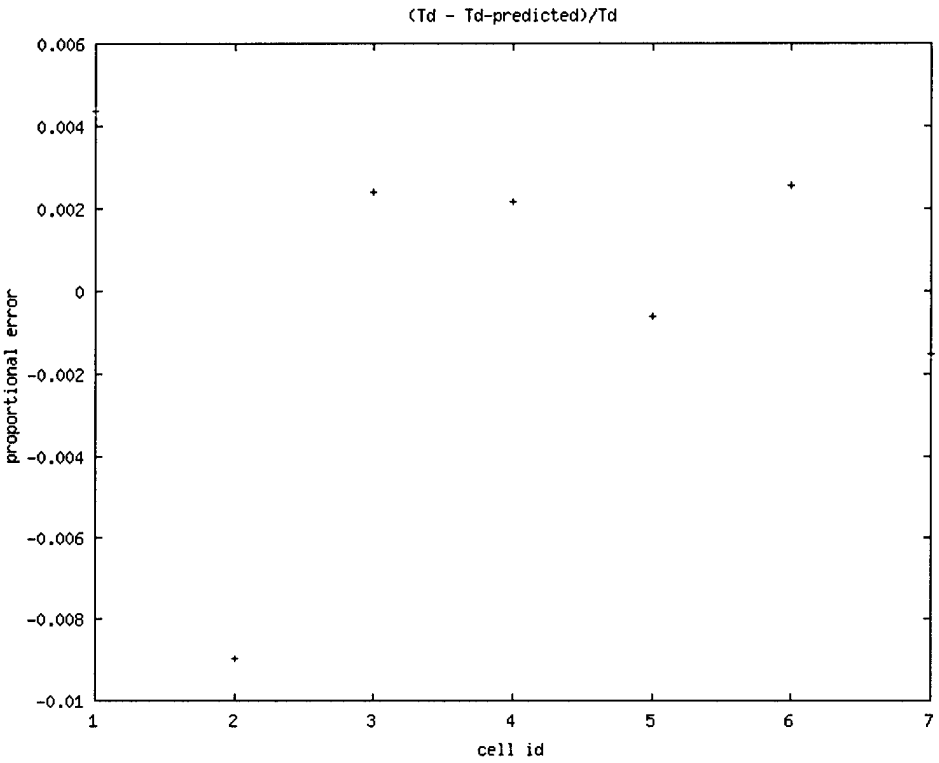

Figure 9-22 Proportional or relative error plot for NiCad batteries.

Because of the extremely small sample size (seven samples with five predictors), the results of the MLR are still inconclusive.

9.5.2 Artificial Neural Network - Nickel Cadmium batteries

The seven data sets from the pulse tests of the Lithium Sulfur Dioxide Batteries were divided into a training set of six and a test set of one. The single testing battery was chosen because there were three other batteries in the training set with similar discharge times. The six training input batteries and their discharge times are shown in Table 9-11.

ID	Td
1	8272
3	8513
5	8496
6	6312
7	4275
8	7034

Table 9-11 NiCd battery training set for ADELINE

A set with 30 iterations of 30 random selections was used. The learning rate was set to 0.0001, the weights matrix was initialized to zero, the bias vector was initialized to one, and the program allowed only 1000 iterations for each call to the Widrow/Hoff subroutine.

At this point, the data were tested. The last battery (ID #4) was tested once, and the results from the pure linear transfer function using the weights and biases from this training set are shown in Table 9-12.

ID	Td	T Predicted	Residual	Relative Error
4	8350	8480.229	-130.229	0.0156

Table 9-12 ADALINE results for the NiCad battery ID #4

Again, the small sample size is a problem, but the relative error on the single battery tested is very low. Since the battery chosen had three training samples at nearly the same state of charge, the model worked well. If enough training samples with varying states of charge were applied to the ADELINE, this model would likely work equally well over the entire range of discharge times.

10. CONCLUSIONS

The data and analysis completed in this project represent a giant step forward in the creation of an Automated Battery Charger/Analyzer. Efforts to determine better methods for charging batteries with complex waveforms and to develop battery models using frequency domain analysis were not successful. However, the results of this project show that the state of charge for a battery can be determined through non-invasive pulse testing for both primary and secondary batteries.

The electro-chemical analysis helped to determine the processes that dominate the voltage response for particular battery chemistries. These results were used to verify that the curve-fitted equations for a battery set were well chosen and to verify that a battery's voltage response was as expected.

The use of MLR for modeling the state of charge vs. voltage response worked well considering the marginal sample sizes for each of the battery types. The MLR model is hard to employ because it requires clean data and it is unable to extrapolate with any accuracy. The MLR model's need for clean data aggravated the problem of having a small sample size by requiring that non-normal samples be thrown out. This required extensive data cleaning, but the procedures developed for normalizing the data may help to identify batteries with a poor state of health. All in all, the MLR method for battery modeling is the second best choice.

The use of the ADALINE ANN proved much easier to employ, and its results were comparable. Again, the results from the ANN modeling were hampered by the limited number of samples, which limited the training of the ADALINE and also allowed for very little verification. The results from the ANN showed that the batteries could be modeled with data taken at a much slower sample rate than previously thought (100 Hz vs. 50,000 Hz) and with much less work. The use of ANNs for modeling the state of charge for a battery is the simplest, best choice of the alternatives studied, and research into different types of ANNs for this type of modeling should be pursued.

The results of the battery pulse testing and data analysis conducted as the major part of this project indicate that it is feasible to develop unique "state of charge" prediction algorithms for various primary and secondary battery chemistries using ANN analysis. Furthermore, the use of the MLR techniques can be used with the same data to characterize voltage response curves and provide a non-quantitative indication of battery "state of health". The simplicity of the ANN procedures indicate that reliable, portable and stationary battery analysis equipment can be developed without the need for extremely powerful processors or complex DSP processes.

11. APPENDIX A

11.1 Consultants

The following consultants were used in the performance of this effort.

11.1.1 Badiollah (Badie) R. Asrabadi

Department of Mathematics, Nicholls State University
Tel. (504) 448-4433, Fax (504) 448 -4927
e-mail math-bra@nich-nsunet.nich.edu
Home Page: http://www.nich.edu/~badie

EDUCATION: Ph.D. in Statistics, Kansas State University, 1974.

EXPERIENCE AT NSU

August 1984 to present: Distinguished Service Professor at Nicholls State University.
August 1980 to August 1984: Associate Professor at Nicholls State University.

AWARDS AND RECOGNITIONS

Distinguished Service Professor Award, August 1985
Outstanding Faculty Mentor Award, Jan. 1995
Certificate of Recognition for Assistance in Freshman Advising, Jan. 1998

SOFTWARE DEVELOPMENT

Comprehensive graphic software package for teaching dynamical systems, chaos and fractals, and numerous mathematical and statistical software tailored to perform special mathematical and statistical computations.

SCIENTIFIC PACKAGES

Proficient in using and teaching packages like SAS, SPSS, LISREL, MINITAB, NCSS, MATHCAD, MATHEMATICA, MATLAB, MAPLE, etc.
Fluent in C, Pascal, and FORTRAN.

CONSULTING AND EXPERIMENTAL EXPERIENCES

Complete Statistical Analysis in the area of Parenting Children with Disabilities: Stress Moderation Through Parental Self-Efficacy, Parenting Satisfaction, Coping, and Social Support Affecting Family Functioning and Depression
Complete Statistical Analysis in the area of Abducted and Murdered Children: Behavioral Based Analysis of Victims, Offenders, and Remains Disposal Methodologies.
Applications of statistics and applied mathematics in the areas of psychology, business, education, biology, chemistry, economics, law, and health sciences.
Statistical Consultant to NSU, Student Evaluation
Official Statistical Consultant to LDNR, Thibodaux Office.
Statistical Consultant to Neptune Science, INC. Slidell, LA

RECENT PUBLICATIONS (refereed articles)

"A Biased Estimate of Proportion," International Journal of Mathematical Education in Science and Technology, 1998, Vol. 29, No. 2. 225-232.
"An Acculturative Stress Scale for International Students," A Book of Resources, 1998, Volume 23, edited by Carlos Zalequett and Richard wood, published by Scarecros Press/UPA. (co-author D. S. Sandhu -- University of Kentucky).

"Expected Value of Perfect Information," 1999, accepted for presentation at the Southwest decision science Institute March 10 - 13, 1999;

"A Multidimensional Statistical Model to Assess School Technology," 1999, accepted for presentation at the Southwest Decision Science Institute March 10 - 13, 1999 --co-author Raymond Folse;

RESEARCH IN PROGRESS

"A Discrete -Time Survival Analysis to Study College Dropouts," (under review);

FUNDED GRANT PROPOSAL

Co-director of LaSIP "Reforming the Teaching of secondary Mathematics Through Technology, Experimentation, and Statistics, 1999-2000. ($149,156.00).

SERVICES ON PROFESSIONAL COMMITTEES

Member of a Ph.D. dissertation committee at Louisiana State University, Medical School;
Referee for Metrika;
Referee for IJMEST.

SERVICE AT THE UNIVERSITY LEVEL

Elected member of the Graduate Council;
Elected member of the University Promotion and Tenure Appeals Committee;
Statistical Analysis of the test-retest data from ETS students' evaluation of the faculty at NSU;
Member of Professor Emeritus Selection Committee;
Member of committee to propose M.S. in Biological Sciences;
Chairperson for Post-tenure Review Committee;
Member of the Search Committee for Dean of the College of Arts and Sciences;
Chair of Graduate Faculty Committee for Department of Mathematics.

PROFESSIONAL MEMBERSHIPS: The American Statistical Association

11.1.2 Elizabeth J. Podlaha

Clarence M. Eidt Professional Development Professor, Assistant Professor Louisiana State University
Tel. (225) 388-3056
E-mail: podlaha@che.lsu.edu
EDUCATION: Ph.D., Columbia University, 1992.

Dr. Podlaha's research targets the area of Electrochemical Engineering. Electrochemical processes are important for the fabrication of micromachines, microelectronics and protective coatings, as well as for the operation of batteries and corrosion. The research aim is concerned with the understanding and characterization of electrochemical processes for the development of new materials, processes and applications.

Current research interests are devoted towards the understanding of alloy codeposition and composite plating. Electrodeposition offers a cost effective means of producing not only single element coatings, but alloy and composite materials, with the advantage of tailoring the deposit chemical composition and microstructure by the appropriate choice of operating conditions. Experimental studies are complemented with theoretical, numerical simulation of electrochemical systems. Experiments are conducted under well defined mass transport and current distribution conditions in order to test model predictions.

Development of a model to describe alloy plating is essential to control the electroplating process and in the development of new alloys. Particularly interesting are those alloys, which undergo interactive behavior during the codeposition process. One example is the induced codeposition of Mo that cannot be electroplated as a single metal, but can be plated as an alloy with iron-group elements. Other research topics concern the electrodeposition into deep, high aspect ratio holes. This interest is motivated by the fabrication of new microsystems via the LIGA process. As a material is plated inside a recess, the geometry of the electrode changes and imparts a dynamic change on the current distribution and mass transport of reacting species. The influence of these changes on the alloy composition and deposition rate is considered. Also, unique multilayered structures having a modulated composition in the nano-range exhibit unusual magnetic and mechanical properties. These materials can be readily prepared by electrodeposition. The relationship between the deposition parameters and the material structure are considered. During electrodeposition, solid particles added to the plating bath can be incorporated into the deposit for improved mechanical and tribological properties. The influence of the plating process on the particle deposition rate is another research direction, with a view towards the synthesis of nano-composites.

Recent Publications

- E.J. Podlaha and D. Landolt, "Pulse-Reverse Deposition of Nanocomposite Coatings," *Journal of the Electrochemical Society*, **144**, L200 (1997).
- E.J. Podlaha and D. Landolt, "Induced Codeposition: III. Molybdenum Alloys with Nickel, Cobalt and Iron," *Journal of the Electrochemical Society*, **144**,1672 (1997).
- E.J. Podlaha, A. Bogli, Ch. Bonhote and D. Landolt, "Development of an Inverted Rotating Shaft-Disc Electrode (IRSDE)," *Journal of Applied Electrochemistry*, **27**, 85 (1997).
- E.J. Podlaha and D. Landolt, "Induced Codeposition: II. A Mathematical Model Describing the Electrodeposition of Ni-Mo Alloys," *Journal of the Electrochemical Society*, **143**, 893 (1996).

- E.J. Podlaha and D. Landolt, "Induced Codeposition: I. An Experimental Investigation of Ni-Mo Alloys," *Journal of the Electrochemical Society*, **143**, 885 (1996).
- E.J. Podlaha and J.M. Fenton, "Characterization of a Flow-by RVC Electrode Reactor for the Removal of Heavy Metals from Dilute Solutions," *Journal of Applied Electrochemistry*, **25**, 299-306 (1995).
- E.J. Podlaha and H.Y. Cheh, "Modeling of Cylindrical Alkaline Cells, VII. A Wound Cell Model," *Journal of the Electrochemical Society*, **141**, 1751 (1994).
- E.J. Podlaha, Ch. Bonhote and D. Landolt, "A Mathematical Model and Experimental Study of the Electrodeposition of Ni-Cu Alloys from Complexing Electrolytes," *Electrochimica Acta*, **39**, 2649 (1994).
- E.J. Podlaha and H.Y. Cheh, "Modeling of Cylindrical Alkaline Cells, VI. Variable Discharge Conditions," *Journal of the Electrochemical Society*, **141**, 28 (1994).
- E.J. Podlaha and H.Y. Cheh, "Modeling of Cylindrical Alkaline Cells, V. High Discharge Rates," *Journal of the Electrochemical Society*, **141**, 15 (1994).
- E.J. Podlaha, M. Matlosz and D. Landolt, "Electrodeposition of High Mo Content Ni-Mo Alloys under Forced Convection," *Journal of the Electrochemical Society*, **140**, L147 (1993).

11.1.3 Kenneth William Holladay

BIRTHDATE: October 20, 1950: Columbus, Ohio

PERSONAL: Married with four children.

EDUCATION:

The Ohio State University, SSTP Mathematics Program, 1966-1968, Summers Massachusetts Institute of Technology, B.S. 1972, Mathematics
Massachusetts Institute of Technology, Ph. D. 1975, Applied Mathematics
Thesis Advisor: Professor Gian-Carlo Rota
Field: Combinatorics
Thesis Title: Some Aspects of the Cell Growth Problem

PROFESSIONAL EXPERIENCE:

1969, 1970	Counselor, SSTP Mathematics Program, The Ohio State University (summers)
1975 - 1977	Bateman Research Instructor, California Institute of Technology
1977 - 1982	Assistant Professor, University of Miami
1982 -1985	Assistant Professor, University of New Orleans
1985 - Present	Associate Professor, University of New Orleans

AWARDS:

Sponsored Merit Scholarship from Battelle Memorial Institute, Columbus Laboratories for 1968-1972 undergraduate studies.
NSF Fellowship for 1972-1975 graduate studies.
UNO Graduate Research Council Award, 1983-1984,
project title: "2-irreducibles on 2-isohedral Tilings"

PROFESSIONAL AND HONORARY SOCIETIES:

American Mathematical Society
Mathematical Association of America
Society for Industrial and Applied Mathematics
American Association for the Advancement of Science Sigma Xi

CONSULTING WORK:

American Performance Monitoring Systems of Bay St Louis, Mississippi, June 20 - December 20, 1985. Duties included C programming, software design and systems testing for an onboard ship fuel monitoring system.

Lockheed Engineering and Management Services Company (LEMSCO) at NSTL, August I 1, 1986 to July 23, 1992. LEMSCO was the scientific and engineering support contractor to the Earth Resources Laboratory (ERL) of NASA,. Duties include serving as a consulting applied mathematician, software design and testing, database engineering, and scientific computing consultant. Late in 1988 LEMSCO changed its name to

Lockheed Engineering and Science Company (LESC), ERL changed its name to Science and Technology Laboratory (STL) and NSTL changed its name to the Stennis Space Center (SSC). At the end of July 1992, the LESC contract expired and this branch of Lockheed was disbanded.

Subcontractor to LEMSCO. Deliverables were software and documentation for a database system for preparing and running presentations involving images (especially remote sensing images.) The project required system integration of hardware including a microcomputer, an advanced graphics subsystem and a write-once-read-many (WORM) optical storage disk.

Sverdrup Technology, Inc at Stennis Space Center, July 24, 1992 to August 1994. Sverdrup is the engineering support contractor to the entire Stennis Space Center. The tasks performed by LESC mentioned above were carried over to the Sverdrup contract.

Lockheed Martin Engineering & Science Company, December 1994. Sverdrup's engineering support contract was taken over by LMESC. Continued the same tasks.

PRESENTATIONS AT PROFESSIONAL MEETINGS:

1. "The Four Color Theorem," Southern California MAA sectional meeting,March 12, 1977. "Permutations of a Multiset," Goldcoast Florida MAA minisectional meeting, November 18, 1977. "On 3-irreducible Animals," (see publication #2) 10th S.E. Conference, Boca Raton, April 2-6, 1979.
2. "Recognizing the 17 Periodic Plane Symmetry Groups," Goldcoast Florida MAA minisectional meeting, November 21, 1980.
3. "Growth Rules for a Class of Polygonal Animals," (see publication #5) 12th S.E. Conference, Baton Rouge, March 2-5, 1981.
4. "On Some Classes of Context-Free Array Grammars," (see publication #7) 13th S.E. Conference, Boca Raton, February 15-18, 1982.
5. "Some Families of Context-Free 2-Irreducibles," (see publication #8) 14th S.E. Conference, Boca Raton, February 14-17, 1983.
6. "Homomorphism Polynomials for Chemical Graphs," (see publication #10) 3rd SIAM Conference on Discrete Math, Clemson, May 14-16, 1986.
7. "Digital Geometry, Linear Minimization and Filtering Algorithms," One week lecture series Summer Visiting Scientist I Engineer Program Earth Resources Laboratory of NASA at NSTL, June 2-6, 1986.
8. "Modeling Capabilities of ELAS," ELAS User's Conference, ERL-NSTL-NASA, October 16-17, 1986.
9. "Filtering and Filtering Techniques," ELAS User's Conference, ERL-NSTL-NASA, November 19-20, 1987.
10. "Applications of Computational Linear Algebra to Remote Sensing Image Processing," Short Course for Louisiana-Mississippi MAA sectional meeting, Northwestern State U., Natchitoches, February 26-27, 1988.
11. "Application of the Active Electromagnetic Induction Profiler in Coastal Environments, American Water Resources Association, La. Sec. Fall Symposium, Baton Rouge, La., Oct.27, 1993.
12. "Utility of Airborne Electromagnetic Profiler Data for Geomorphological Characterization of Shallow Coastal Environments: Case Study - The Cape Lookout, NC Area,"
13. Second Thematic Conf. on Remote Sensing for Marine and Coastal Environments, New Orleans, La., 31 Jan.- 2 Feb. 1994 (see publication #N4)
14. "AEM (Airborne Electromagnetic Profiler) American Water Resources Association, La. Sec. Fall Symposium, Gonzales, La., Oct. 11, 1995,
15. "An Equivalence Relation on Animals," 27th S.E. Conference, Baton Rouge, La Feb. 19 - 23, 1996.

16. "Airborne Electromagnetic Profiler Data from Barataria Basin" 12th Annual Louisiana Remote Sensing and GIS Workshop, Lafayette, La. April 16 - 18, 1996

POSTERS AT PROFESSIONAL MEETINGS

1. "Utility of Airborne Electromagnetic Profiler Data for Geomorphological Characterization of Shallow Coastal Environments: Case Study - The Cape Lookout, NC Area," Second Thematic Conf. on Remote Sensing for Marine and Coastal Environments, New Orleans, La., 31 Jan.- 2 Feb. 1994 (see publication #N4)
2. "Study the Spatial Variability of Organic Soil Layer Thickness Within Barataria Bay Marshes, Louisiana," W.H. Hudnall, L.C. Dharmasri, K.W. Holladay, R. Pelletier, 4" Thematic Conf. Remote Sensing for Marine and Coastal Environments, Orlando, Florida, March 17 - 19, 1997. (see publication #N6)
3. "Detection of a Freshwater Lens Off the Louisiana Coast Using AEM," K.W. Holladay,
4. C.J. Bergeron, J.W. loup, G.E. loup, L.J. Rouse, 4" Thematic Conf. Remote Sensing for Marine and Coastal Environments, Orlando, Florida, March 17 - 19, 1997.

OTHER PROFESSIONAL ACTIVITIES:

1. Visitor, University of North Carolina, Chapel Hill, summer 1974.
2. Participant, Institute for Higher Combinatorics, a NATO Advanced Study Institute, Berlin, Germany, September 1-10, 1976.
3. Supervised (with Prof. M. Wachs) a Combinatorics Seminar at the University of Miami, 1977-1981.
4. Reviewer for Math Reviews 1984 - 1986.
5. Chairman of sessions of contributed papers at the I Oth, 12th, I 3th and 14th S.E. Conferences on Combinatorics, Graph Theory and Computing.
6. "Data Smoothing and Filtering," instructional lecture in the Jackson State University / Earth Resources Laboratory Seminar Series, January 26, 1987.
7. "Fermat's Last Theorem," expository lecture for the UNO Delta Epsilon Math Club, April 26, 1988.
8. Member of the planning committee for a proposed Ph. D. program at UNO in Engineering and Applied Physics, 1988 - 1995.
9. UNO Representative to LaSpace, the Louisiana Space Grant Consortium, 1990 - Present.
10. Participant in Interactive Mathematics Text Program (IMTP) Summer workshop University of Houston, Downtown, July 19 - 24 1993.
11. Member of Search Committee for the first occupant of the Freeport McMoran Endowed Chair in Environment Modelling, 1993 - 1994.
12. Math department representative to Program Committee of Ph. D. program in Engineering and Applied Physics, 1995 - Present. College of Sciences representative to the admissions committee.
13. Participant in 4t' National NASA Space Grant I EPSCOR Conference, Williamsburg Virginia, May 20 - 22, 1996.
14. Participant in HiRes 97, a conference on geophysical remote sensing using electromagnetic techniques, Tucson, Arizona, Jan 6 -8, 1997.
15. "The Use of Airborne Electromagnetic Profile Data in a North Carolina Barrier Island Environment," R.E. Pelletier Travis, K.W. Holladay, E.C. Mozley, Ocean Technology at Stennis Space Center Conference, April 23-24, 1997, SSC Ms.
16. "Fermat's Last Theorem," expository lecture for the UNO Delta Epsilon Math Club, May 1, 1997.

GRANT APPLICATIONS:

1983 Coordinator of a group of about 10 mathematics department members that submitted an equipment grant proposal to the NSF for a minicomputer and graphics workstation for the department's use. The proposal was not funded.

1985 Principal investigator with D.M. Berman of Math and R.L. Flurry of Chemistry on a proposal to study the properties of molecules using a graph invariant, the
hornomorphism polynomial, of the structure graph of the molecule. This proposal was submitted to the state program Louisiana Stimulus for Excellence in Research (LASER) for possible inclusion in the state's proposal under the NSF's Experimental Program to Stimulate Competitive Research (EPSCoR). Our proposal was rated 7th out of 12 from UNO and was not included.

1988 Member of a committee (G. loup of physics chairman) that submitted a planning grant proposal "UNO Science and Technology Research Center Planning Grant Proposal" to the NSF. The proposal was not funded.

1989 Principal investigator for an equipment grant proposal to the state of Louisiana's Educational Enhancement Fund ("Title 8g grants"). The grant requested money for approximately 40 personal computers and workstations to be used in a computer classroom, a laboratory, and in the offices of the professorial faculty of the Math department. Awarded $220,000.

1991 Co-Investigator of a Director's Discretionary Fund grant at the Stennis Space Center with R.E. Pelletier -Travis of NASA STL as the Principal Investigator. Title: "Technique Development for Processing Low-Frequency Data in an Image Processing System." Awarded $ 1 5,000.

1992 Principal Investigator for the first Louisiana Aerospace Forum of the Louisiana Space Grant Consortium (LaSpace.) This appeared as a grant of up to $5850 from LSU Baton Rouge, who is the fiscal agent for LaSpace. This was the first annual meeting of Louisiana's Space Grant Consortium with UNO as host.

1994 Principal Investigator for the Global Change Group of the Louisiana submission to NASA's EPSCOR program. Project title: "Carbon Cycling and Hydrology in a Shallow Coastal Estuary." The group involves 12 scientists from five universities and 4 scientists from the Stennis Space Center in a three year project to study the Barataria Basin of Louisiana using a variety of remote sensing techniques. Awarded $983,200. In 1997 the project was extended for two more years with another $655,466.

PUBLICATIONS - REFEREED:

1. "A Partition Theory of Planar Animals," Studies in APRI. Math., Vol. 63 (1980) pp. 169-183.
2. "On 3-irreducible Animals," Proc. 10" S.E. Conf. on Comb., Gr. Th. and Computing, Boca Raton, Congressus Numeratium, Vol. 24 (1979) pp. 511-521.
3. "A Partition Theory for Trees," Comb. lnf. & System Sciences, Vol. 7, No. 1 (1982) pp. I- 16. mR 85g:05059a
4. "Structure and Growth of 3-irreducible Graphs," Comb. lnf. & System Sciences, Vol. 7, No. I (I 982) pp. 17-37. mR 85g:05059b
5. "Growth Rules for a Class of Polygonal Animals," Proc. 12t' S.E. Conf on Comb., Gr. Th. and Computing, Baton Rouge, Congressus Numeratium, Vol. 33 (1981) pp. 109-128.
6. "2-Isohedral Triangulations," Geometriae Dedicata Vol. 15 (1983) pp. 155-170. mR 85f 52036
7. "On Some Classes of Context-Free Array Grammars," Proc. 13" S.E. Conf on Comb., Gr. Th. and Computing, Boca Raton, Congressus Numeratium, Vol. 36 (1982) pp. 325-332. mR 85b:68027.

8. "Some Families of Context-Free 2-irreducibles," Proc. 14". S.E. Conf. on Comb., Gr. Th. and Computing, Boca Raton, Congressus Numeratium,, Vol. 40 (1983) pp. 43-56. mR 85g:68038
9. "Estimating the Size of Context-Free Tiling Languages," Can. -1. Math., Vol. XXXIX, No. 6 (1987) pp. 1413-1433.
10. D.M. Berman and K.W. Holladay, "Homomorphism Polynomials of Chemical Graphs, "J. Math.Chemistry", Vol. I (I 987) pp. 405-414. mR 88k:92109
11. A.K.M. Sarwar and K.W. Holladay, "Modified Gelfand-Levitan Inverse Scattering Technique in Exploration Seismology: A Suggestion for a Fast Approximate Algorithm," Exp. Abst . 57, SEG Meeting, New Orleans (1987) pp. 444-446.
12. D. Rickman, M.C. Ochoa, K.W. Holladay, and O.K. Huh, "Georeferencing Airborne Imagery Over New Deltas in Louisiana," Photogrammetric Eng. Remote Sensing, Vol. 55, No. 8, August 1989, pp. 1161-1165.
13. A.K.M. Sarwar and K.W. Holladay, "An Efficient Algorithm for Impedance Reconstruction by the Modified Gelfand-Levitan Inverse Method," Theo!:y and Practice of Geophysical Data Inversion, Proc. Bth Int'i Math.Sem.on Model Optimization in Exploration Geophysics, Berlin, 1990, pp 179-190.
14. K.W. Holladay and D. Rickman, "A New Approach for Recognizing a Spectral-Spatial Class," Remote Sensing Science For The Nineties, Vol 11, IGARSS '90, College Park MD, May 20-24, 1990, pp 1645-1648.
15. H.G. Downing, G.A. Carter, KW. Holladay, and W.G. Cibula, "The Radiative-Equivalent WaterThickness of Leaves," Remote Sens. Environ., 46, 1993, pp 103-107.
16. R.E. Pelletier and K.W. Holladay, "Mapping Sediment and Water Properties in a Shallow Coastal Environment with Airborne Electromagnetic Profile Data: Case Study the Cape Lookout, NC. Area," Marine Technology Society journal, Vol 28, No. 2 pp. 57 - 67.

PUBLICATIONS - NOT REFEREED:

N1. D. Rickman, M.C. Ochoa and K.W. Holladay, "Multitemporal CAMS over Coastal Louisiana: A Problem in Automated Georeferencing," Remote Sensing for Resource lnvento!:X Planning, and Monitorin , Proc. 2nd Forest Service Remote Sensing Applications Conference, Slidell, La and NSTL, Miss., April 11-15, 1988, pp. 258-267.

N2. D. Rickman, M.C. Ochoa, K.W. Holladay, and O.K. Huh, "Georeferencing Airborne Imagery of New Land in Louisiana," Proc. 6th Annual Workshop on Remote Sensinz and GIS for Coastal Management in Louisiana, LSU Baton Rouge, La, April 17-19, 1990, pp 27-28.

N3. K.W. Holladay and D. Rickman, "A Superior Edge Preserving Filter With a Systemic Analysis," NASA Technical Memorandum 431 1, August 1991, pp I - 38.

N4. R.E. Pelletier and K.W. Holladay, "Utility of Airborne Electromagnetic Profiler Data for Geomorphological Characterization of Shallow Coastal Environments: Case Study - The Cape Lookout, NC Area," Proc. of the Second Thematic Conf. on Remote Sensing for Marine and Coastal Environments, New Orleans, La., Jan. 31 - Feb. 2, 1994

N5. R.L. Miller, M. Giardino, B.A. McKee, J.F. Cruise, G. Booth, R. Rovansek, D. Muirhead, W. Cibula, K.W. Holladay, R.E. Pelletier, W. Hudnall, C. Bergeron, J. loup, G. loup, G. Love, "Processes and Fate of Sediments and Carbon in Barataria, Bay, La.", Proc. 3rd Thematic Conf. Remote Sensing for Marine and Coastal Environments, Vol. 1, Sept. 18 - 20, 1995, Seattle, Washington, pp. 1-233 - 1-244.

N6. W.H. Hudnall, L.C. Dharmasri, K.W. Holladay, R. Pelletier, "Study the Spatial Variability of Organic Soil Layer Thickness Within Barataria Bay Marshes, Louisiana," Proc. 4th Intl. Conf. on Remote Sensing for Marine and Coastal Environments, Orlando, Fl., March 17-19, 1997, pp. 11-588 - 11-597.

12. APPENDIX B

12.1 Summary of statistical Analysis of Secondary Battery Data

The following criteria were used to establish a relationship between the response variable TD and the 12 predictor variables v0, a0, a1,b1,a2,b2,a3,b3,a4,b4,a5,b5.

1. Multivariate test of normality, graphical analysis of the first two Principal Components, and Andrew's graphs all revealed that observation 21 (ID# 10152) seems to be an oulier and it was eliminated from further analyses. (see the attachment file secdataout1.lst).
2. The hypothesis of equality of variances is not rejected (p-value of 0.70). Relevant statistics are given below.
3. The Durbin-Watson test of no serial correlation is not rejected. Relevant statistics are given below.
4. Statistical methods of finding a relatively reliable and adequate model (BACKWARD, MINR, and PC) all indicated that the best linear model consists of 9 predictor variables: v0, a0, a1, b2, b3, a4, b4, a5, and b5. Selection of this model is based on the following characteristics:
   a. Mallows' CP a measure of adequacy of the model is 7.266 indicating that this model adequately represents the data.
   b. R-square value is 0.99, indicating that 99% of the total variation in the data (response variable) is captured by the model. It should be pointed out that sample size is moderate and small to moderate sample sizes tends to inflate R-square.
   c. The overall significant test of the model has an F value of 186.00 with an associated p-value of 0.0001 indicating that the model as whole is highly significant.
   d. The individual tests for the coefficients of the parameters in the model all are strongly significant. The largest p-value is 0.0404 corresponding to a0. (see the table given later in this document).
   e. Only one observation [(observation 10 (ID # 24033)] has an absolute studentized residual of higher than 2. This same observation has relatively large values of COOK's distance and Rstudent None of these values are alarmingly large but they suggest that the values associated with this observation should be reviewed carefully.
   f. Only one observation [observation 24(ID # 10182)] has relatively large value (the diagonal element of the hat matrix) that indicates this observation is an influential observation. That is, it has pulled the model toward itself more than any other observation. This characteristic is also supported by a large covariance ratio of 18.6, (very large number). The values associated with this observation should be reviewed carefully.
   g. All DFBETA's are within limits. Relevant statistics are given below.

12.2 Recommendations:

Review the measurements taken for observations 10, and 24 if all values seem to be accurate and there is no reason to doubt any of the values the following model seems to represent the data well and should be used to predict TD. Of course the values of the predictors to be used for this model should be within the range of the numbers used for this analysis.

TD=-81710.49717 +53188.825269 V0 + 3.684333 A0 +6.607846 A1 + 0.752397 B2-5.317693 B3-11.0156002 A4 -33.744215 B4-28.908321 A5 -37.027972 B5.

The following is a partial list of the output extracted from SAS.

```
Test of First and Second Moment Specification
              DF:   28   Chisq Value:      23.6477   Prob>Chisq:   0.7000

Durbin-Watson D              2.603
(For Number of Obs.)            25
1st Order Autocorrelation  -0.358

                              R-square = 0.99116573  C(p) =  7.26680698

                    DF         Sum of Squares      Mean Square          F   Prob>F

     Regression      9        194466048.98774  21607338.776416     186.99   0.0001
     Error          15        1733277.2522596  115551.81681731
     Total          24        196199326.24000

                    Parameter        Standard          Type II
     Variable        Estimate           Error  Sum of Squares          F   Prob>F

     INTERCEP  -81710.49717137   9203.65954547  9107756.1389581      78.82   0.0001
     V0         53188.82526902   3092.00235987  34193057.925823     295.91   0.0001
     A0             3.68433301      1.64260927  581334.36068084       5.03   0.0404
     A1             6.60784629      1.87221902  1439406.0950897      12.46   0.0030
     B2             0.75239717      0.15082925  2875411.1019132      24.88   0.0002
     B3            -5.31769289      1.29148831  1959035.5762765      16.95   0.0009
     A4           -11.01560022      3.30886388  1280664.3134774      11.08   0.0046
     B4           -33.74421460      8.61946786  1770983.5121631      15.33   0.0014
     A5           -28.90832130      8.34186563  1387701.7754060      12.01   0.0035
     B5           -37.02797181     11.82226302  1133536.1954110       9.81   0.0069
Secondary data on batteries OBS 8, 13 and 21 removed                    519
                    Case 21 excluded       11:43 Tuesday, August 10, 1999
          Dep Var   Predict   Std Err  Lower95%  Upper95%  Lower95%  Upper95%
    Obs      TD       Value   Predict      Mean      Mean   Predict   Predict  Residual
      1    2474.0    2354.2   202.394    1922.8    2785.6    1511.0    3197.5     119.8
      2    2454.0    2277.8   261.468    1720.5    2835.1    1363.7    3191.9     176.2
      3    4296.0    4508.4   172.315    4141.2    4875.7    3696.1    5320.8    -212.4
      4    4508.0    4119.4   172.064    3752.6    4486.1    3307.3    4931.5     388.6
      5    6795.0    6563.5   222.053    6090.2    7036.8    5698.1    7429.0     231.5
      6    6269.0    6331.5   180.093    5947.6    6715.3    5511.5    7151.4   -62.4578
      7    7096.0    7013.3   116.685    6764.5    7262.0    6247.2    7779.3    82.7485
      8    2826.0    2724.1   169.875    2362.1    3086.2    1914.2    3534.1     101.9
      9    3562.0    4131.1   195.366    3714.7    4547.5    3295.4    4966.8    -569.1
     10    9832.0    9366.7   199.706    8941.1    9792.4    8526.4   10207.0     465.3
     11   10226.0   10129.4   222.863    9654.4   10604.5    9263.1   10995.8    96.5573
     12   10104.0    9952.2   264.535    9388.3   10516.0    9034.1   10870.3     151.8
     13    9248.0    9602.8   206.409    9162.8   10042.7    8755.1   10450.4    -354.8
     14    8012.0    8237.3   260.243    7682.6    8792.0    7324.8    9149.8    -225.3
     15    5443.0    5604.8   202.161    5173.9    6035.7    4761.8    6447.7    -161.8
     16   10704.0   10365.4   267.579    9795.0   10935.7    9443.3   11287.4     338.6
     17    2055.0    2234.4   199.795    1808.6    2660.3    1394.0    3074.9    -179.4
     18    7660.0    7310.0   207.275    6868.2    7751.8    6461.4    8158.6     350.0
     19    8762.0    9037.6   206.486    8597.5    9477.8    8189.9    9885.4    -275.6
     20    9429.0    9362.5   213.752    8906.9    9818.1    8506.6   10218.4    66.5003
     21   10187.0   10185.2   321.285    9500.4   10870.0    9188.2   11182.1     1.8335
     22    8998.0    9173.2   149.541    8854.4    9491.9    8381.6    9964.7    -175.2
```

23	9211.0	9367.7	255.289	8823.6	9911.8	8461.6	10273.8	-156.7
24	8518.0	8288.0	221.954	7815.0	8761.1	7422.7	9153.4	230.0
25	9569.0	9997.5	175.933	9622.5	10372.5	9181.7	10813.4	-428.5

Obs	Std Err Residual	Student Residual	Cook's -2-1-0 1 2	Hat Diag D	Cov Rstudent	H	Ratio
1	273.109	0.439		0.011	0.4265	0.3545	2.7145
2	217.224	0.811	*	0.095	0.8014	0.5916	3.1173
3	293.018	-0.725	*	0.018	-0.7130	0.2570	1.8780
4	293.165	1.326	**	0.061	1.3629	0.2562	0.7711
5	257.380	0.899	*	0.060	0.8932	0.4267	1.9978
6	288.302	-0.217		0.002	-0.2096	0.2807	2.6860
7	319.275	0.259		0.001	0.2510	0.1178	2.1607
8	294.439	0.346		0.004	0.3356	0.2497	2.4526
9	278.180	-2.046	****	0.206	-2.3277	0.3303	0.1130
10	275.081	1.691	***	0.151	1.8165	0.3451	0.3668
11	256.679	0.376		0.011	0.3652	0.4298	3.1803
12	213.479	0.711	*	0.078	0.6989	0.6056	3.5871
13	270.087	-1.314	**	0.101	-1.3489	0.3687	0.9305
14	218.690	-1.030	**	0.150	-1.0323	0.5861	2.3128
15	273.282	-0.592	*	0.019	-0.5786	0.3537	2.4353
16	209.650	1.615	***	0.425	1.7169	0.6196	0.7755
17	275.016	-0.652	*	0.022	-0.6394	0.3455	2.2839
18	269.423	1.299	**	0.100	1.3321	0.3718	0.9621
19	270.029	-1.021	**	0.061	-1.0223	0.3690	1.5378
20	264.314	0.252		0.004	0.2436	0.3954	3.1608
21	111.031	0.017		0.000	0.0160	0.8933	18.6827
22	305.269	-0.574	*	0.008	-0.5605	0.1935	1.9800
23	224.453	-0.698	*	0.063	-0.6857	0.5640	3.2863
24	257.465	0.893	*	0.059	0.8868	0.4263	2.0120
25	290.860	-1.473	**	0.079	-1.5391	0.2679	0.5704

Obs	INTERCEP Dffits	V0 Dfbetas	A0 Dfbetas	A1 Dfbetas	B2 Dfbetas	B3 Dfbetas	A4 Dfbetas	Dfbetas
1	0.3160	-0.1071	-0.0129	-0.0881	-0.1417	-0.1763	0.2200	0.2074
2	0.9647	0.6277	-0.6041	0.1196	0.2866	0.0022	-0.2676	-0.5361
3	-0.4193	-0.1904	0.1583	-0.1858	-0.2172	-0.2931	0.2033	0.0874
4	0.7999	0.0374	0.0797	-0.0522	0.0215	0.1640	-0.0560	0.1895
5	0.7706	-0.0430	0.1413	-0.4226	-0.2834	-0.0345	-0.1124	0.0555
6	-0.1309	-0.0510	-0.0125	-0.0728	-0.0860	-0.0792	0.0822	0.0580
7	0.0917	-0.0237	0.0112	-0.0478	-0.0470	-0.0190	0.0143	0.0158
8	0.1936	-0.0138	-0.0287	-0.0262	-0.0358	-0.0796	0.0655	0.0781
9	-1.6348	0.0762	0.3358	-0.6455	-0.2139	-0.0206	-0.1037	-0.3066
10	1.3187	0.7840	-0.5798	0.6209	0.8203	0.5247	-0.4903	-0.6531
11	0.3170	0.0410	0.0152	0.1628	0.1507	0.1613	-0.0598	-0.0284
12	0.8661	-0.1267	0.3346	0.2983	0.1521	-0.0601	-0.0410	-0.2415
13	-1.0309	-0.0314	-0.0698	0.1412	-0.0851	-0.2740	0.1360	-0.0246
14	-1.2285	0.3981	-0.6821	-0.0947	-0.0334	0.4067	-0.0989	-0.2289
15	-0.4281	0.0327	-0.0389	0.0146	0.0572	-0.0611	0.0014	0.0469
16	2.1913	-0.2805	-0.0576	0.4561	0.3178	0.2135	0.0335	0.2258
17	-0.4645	-0.1252	0.2369	0.0744	0.0762	0.0207	-0.0677	0.0484
18	1.0249	-0.5812	0.6180	0.0154	-0.3028	-0.2805	0.2765	0.2228
19	-0.7818	-0.0515	-0.1205	0.4401	0.1992	-0.0849	0.1018	0.0858
20	0.1970	-0.0700	0.0439	-0.1164	-0.1152	-0.1079	0.1156	0.0788
21	0.0462	-0.0037	0.0020	-0.0071	-0.0018	0.0098	-0.0035	0.0058
22	-0.2746	0.0972	-0.0289	0.0319	0.0908	0.1550	-0.1527	-0.0816
23	-0.7799	-0.3753	0.2631	-0.0341	-0.1917	-0.1313	0.4479	0.4852
24	0.7645	-0.1439	-0.1693	-0.1542	-0.2668	-0.1562	0.1572	0.1506
25	-0.9309	0.2092	-0.1132	-0.1006	0.0832	0.3725	-0.3940	-0.1238

Obs	B4 Dfbetas	A5 Dfbetas	B5 Dfbetas
1	0.1491	0.1348	0.0331
2	-0.2115	-0.1369	0.0563
3	0.1450	0.1116	0.1325
4	-0.2802	-0.2916	-0.2502
5	-0.1327	-0.1788	0.2455
6	0.0875	0.0733	0.0712
7	0.0218	0.0033	0.0573
8	0.0472	0.0528	0.0405
9	-0.7354	-0.9483	-0.0309
10	-0.5474	-0.4784	-0.7618

11	-0.0972	-0.0823	-0.2571
12	0.0030	0.1426	-0.2456
13	0.3506	0.4748	-0.1740
14	0.0445	-0.0599	-0.1551
15	-0.0154	0.0423	-0.0083
16	0.4819	0.3837	0.7995
17	-0.0541	-0.0205	0.0084
18	0.3721	0.2558	0.1677
19	0.3709	0.5365	-0.0854
20	0.0359	-0.0031	-0.0076
21	-0.0034	0.0066	0.0019
22	-0.1461	-0.1218	0.0068
23	0.1430	0.0628	-0.2523
24	0.4888	0.4702	0.3811
25	-0.2991	-0.2449	0.3087

13. APPENDIX C

13.1 Project Report for Electrical Engineering 6583, Neural Networks

Prepared for Edit J. Kaminsky Bourgeois, University of New Orleans by David H. Fabre, Neptune Sciences, Inc.

13.1.1 Background

A battery is made up of many cells. For example, a car battery usually has many individual cells (that occasionally may need water) and a large flashlight I own requires 6 D cells to operate. The definition of a secondary cell or battery implies that the unit can be recharged. A primary unit, on the other hand, cannot be recharged.

The particular cell set that will be discussed here is a Hawker 12.5 amp hour 2 volt J-cell. This is a secondary cell (i.e., it is rechargeable) and its chemistry is lead acid.

The U.S. Navy uses an enormous amount of batteries. One of the goals of the Universal Battery Charger/Analyzer Project that I have been involved with this year was to produce methods to help Naval personnel use them more efficiently. To that end, Neptune Sciences, Inc. has constructed a system that will test and analyze cells or batteries in order to more efficiently make use of them. Besides hardware and software written to test the batteries, we have constructed several sets of data for analyzing their state of charge.

State of charge in the discussion that follows will be defined as the amount of discharge time remaining in a cell. Other assumptions for our set creation were that the cell or battery was charged with a certain protocol (constant current or constant voltage or a combination). There are other assumptions involved with these data that are not pertinent to this class project that will not be discussed.

As part of the results of the Battery Project, a Multiple Linear Regression (MLR, a good reference is Draper and Smith) approach was performed on a set of nearly 30 cells. The cells were preconditioned at a uniform random time spacing to the approximate maximum discharge time of about 3 hours with a certain charging protocol. These data, after being checked for normality, became a sample of size 25. Several cells were eliminated for human and other reasons. In applying the MLR model, a check of the statistics of the input data against the test set is required.

As a reference to the images in the Results section that follow, 2 plots will be shown now. Figure 13-1 is an over plot of the predicted discharge time and the actual discharge time from our sample set of 25 cells. Figure 2 show a kind of proportional error or relative error from the predicted time and the actual discharge time. In Figure 13-2 note that if a cell's discharge time was underestimated it is represented as a negative proportion. On the other hand if a cell's discharge time was overestimated, the value is a positive proportion.

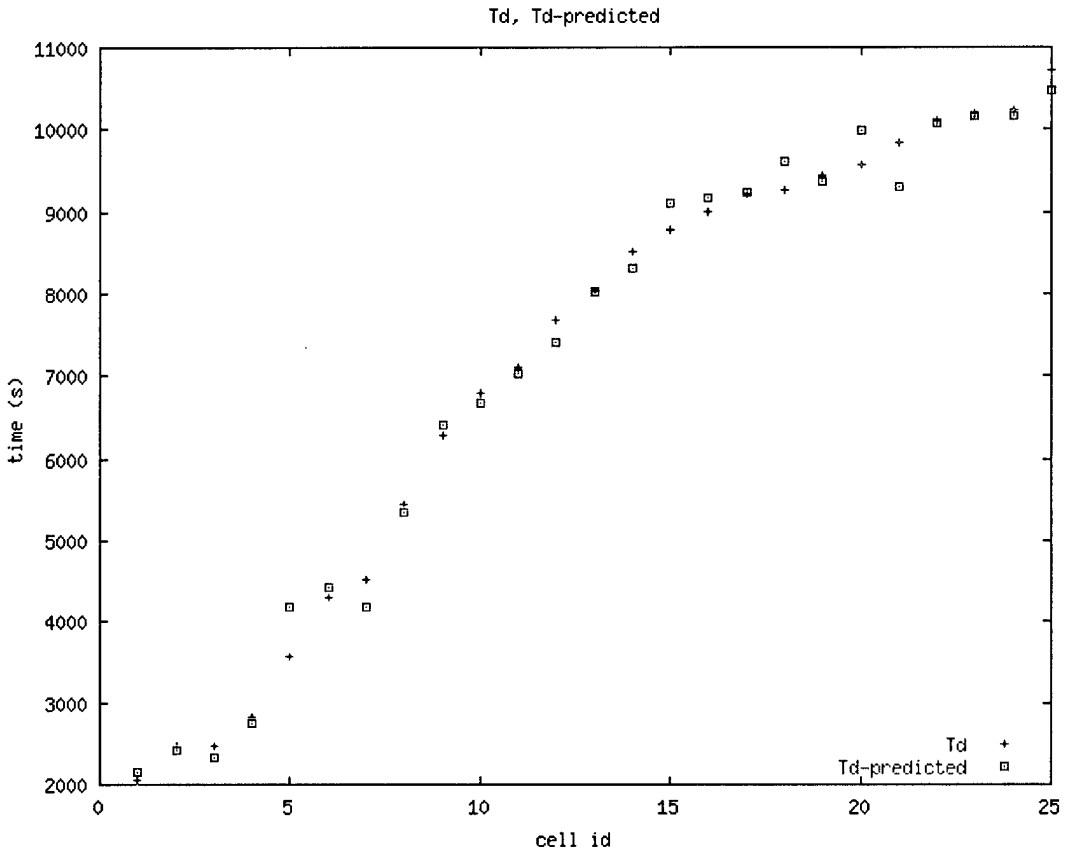

Figure 13-1. Over plot of results from the MLR time to discharge prediction model.

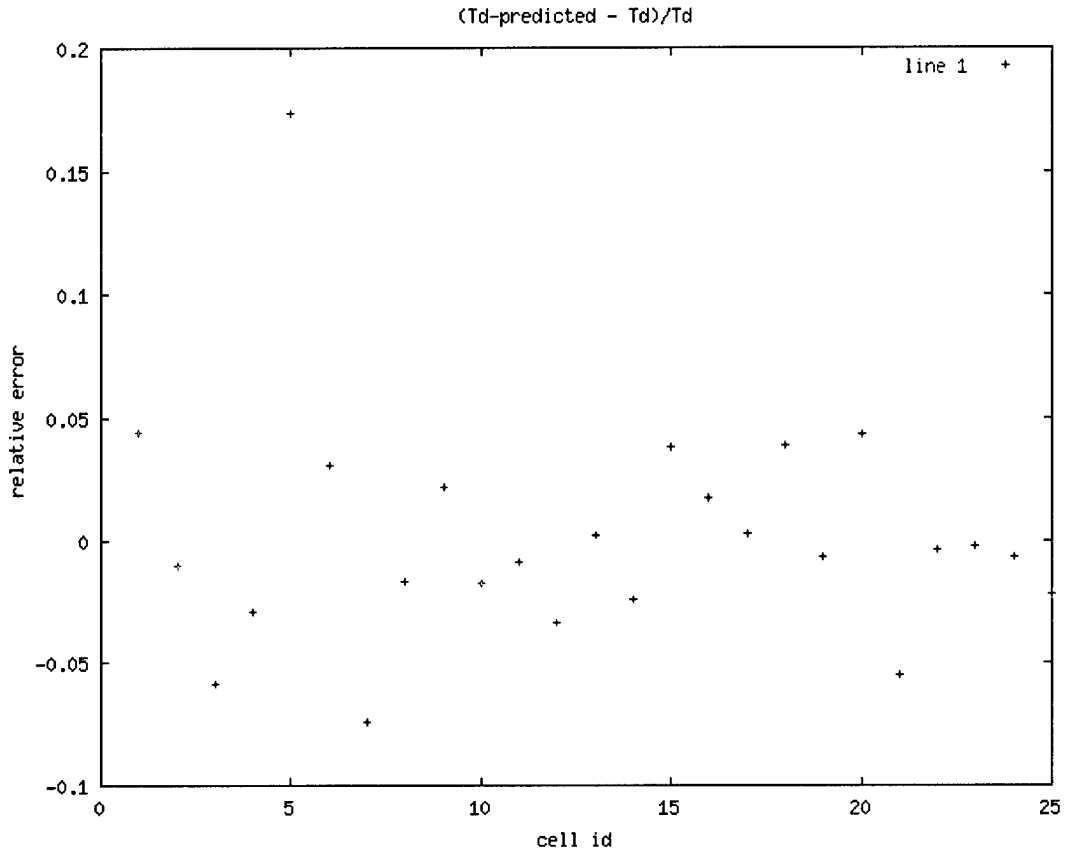

Figure 13-2. Relative errors from the MLR prediction model.

Several other cell samples were created for confirmation of the MLR model but they were not used in the Artificial Neural Network (ANN) approach detailed below.

13.1.2 Method

The ANN selected for this application is the ADALINE (ADAptive LINear Element). Hagan, et.al. describe an ADALINE Network as a having the same basic structure as the Perceptron (one of the first neural networks), only differing in the choice of transfer functions. ADALINE uses a pure linear transfer function whereas a Perceptron uses the hard limiter as its transfer function. The mathematical definitions for $a = f(n)$ where f is *hardlim* or *purelin*, respectively are

$a = hardlim(n) = 0, if\ n < 0$
$a = hardlim(n) = 1, if\ n >= 0$

$a = purelin(n) = n$

where $n = w*p + b$, w is the matrix of weights, p is the input vector, and b is the bias vector.
ADALINE is an ANN that uses performance learning. It applies the Least Mean Squared (LMS) learning law to adjust the weights and biases in a supervised notion till some criteria is met. LMS is

also known as the Widrow learning law, the Widrow/Hoff learning law, and the delta rule. It can be stated as

$$w(k+1) = w(k) + 2*alpha*e*p$$

where k represents the iteration number, $e = t - a$, t is the target value in the supervised training sense, and $0 < alpha < 1$ is the learning rate. The learning rate can be calculated analytically but is usually "tweaked".

Hecht-Nielsen describes the ADALINE's output as determining the hyperplane that is perpendicular to the weights that a particular input vector lies on. He also states that ADALINE is sometimes called a linear combiner or an affine combiner.
The ADALINE has a restriction similar to the perception in that it can only solve linearly separable problems. In layman's terms, according to a colleague of mine (Patrick McDowell) "ADALINE's like smooth data". This probably is not the best choice for this application. It was simple enough to understand and use, however.

13.2 The Data Set

The set of 25 samples was split into 2 sets. For training 14 samples were used and the remaining 11 were used for testing. Nearly every other sample was chosen for the testing set. Extras were left for training around the end points of the discharge times. Each sample file represents data from a pulse test. A pulse test is a series of discharge and then charge cycles at relatively low rates. The sampling rate of data collection was 50 kHz. The cycle duration is 10 seconds (5 seconds discharge and 5 seconds charge). The data are stored in the file as 16 bit short integers. A total of 32 pulses per sample are stored. That creates files that are about 32 MB each.

For input to the ANN these data were sub-sampled down to 100 Hz. Also note that the only the discharge parts of the pulse curves are used in the analyses. Figure 13-3 shows an over plot of all 32 discharge cycles for the cell with serial number H1033.

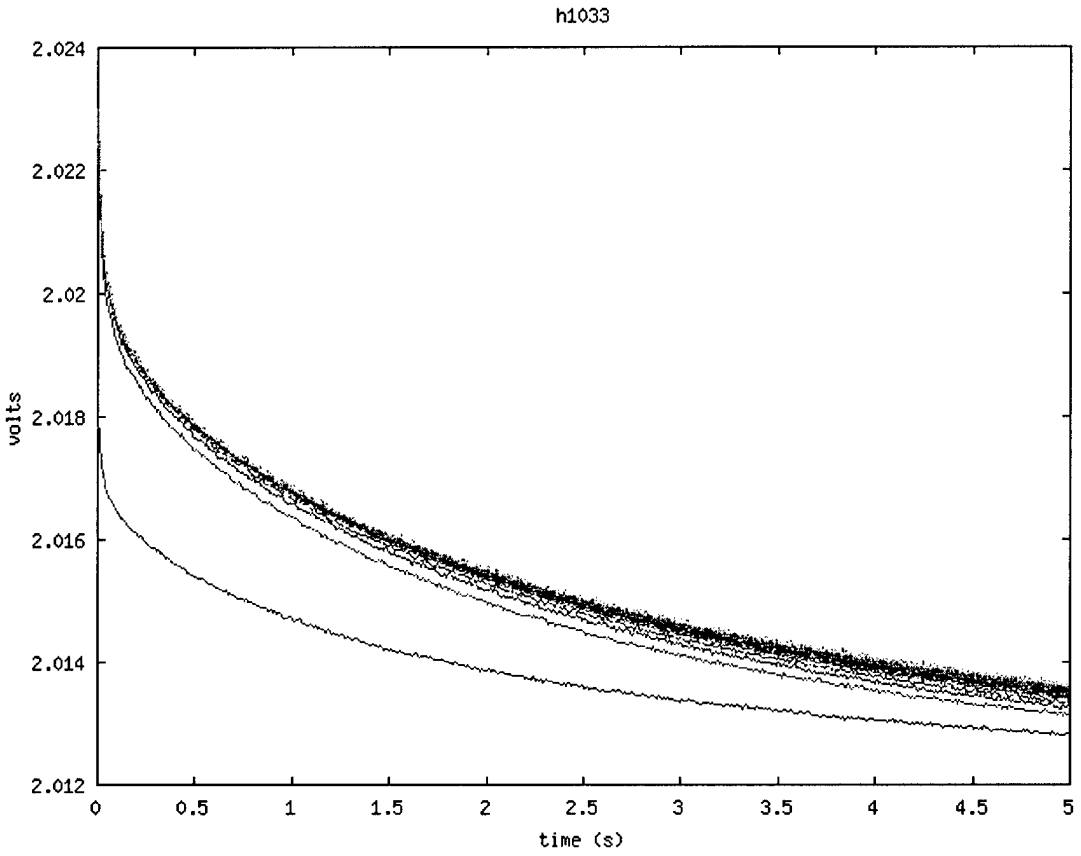

Figure 13-3. Over plot of Hawker cell H1033's discharge pulse curves sub-sampled to 100 Hz.

The ANN has voltage as input. The input vectors p are of length 500. The weight matrix w has 32 rows and 500 columns corresponding to the 32 cycles and input vector length. The bias vector b is of length 32. Thus passing an input through the ADALINE is synonymous with performing a large dot product with a bias added. In summary, the processing element is

$$a[32, 1] = purelin(w[32, 500]*p[500,1] + b[32,1])$$

Before being input to the processing element above, the data were scaled so that both the voltages and the times fell within the exclusive interval (0, 1). This was done by determining a large enough value for the time to be $tmax=10800$. Each voltage was scaled between the values $vmax=2.14$ and $vmin=1.98$.

Upon testing our network the answer is taken to be the average of the a vector times $tmax$.

13.3 Training

Training was performed in a quite simplistic fashion. The weights were initialized to zero and the bias was initialized to one. Then the 14 inputs were put through the affine combiner and Widrow's learning rule sequentially (in increasing discharge time order) and then 6 were randomly chosen in the sequence. Then they were sequentially combined, etc. This was done 4 times. At this point the data were tested. And the results from using the weights and biases with the pure linear transfer function on the test set of 11 cells are as follows:

test.out.6and4

1028	2474.00000	3161.09398	-687.09398	0.27773
1033	3562.00000	4216.82382	-654.82382	0.18384
1032	4508.00000	3975.96112	532.03888	-0.11802
1036	6269.00000	5694.91802	574.08198	-0.09158
1037	7096.00000	6906.44232	189.55769	-0.02671
1009	8012.00000	8589.44141	-577.44141	0.07207
1016	8762.00000	8776.74073	-14.74073	0.00168
1021	9211.00000	8547.44446	663.55554	-0.07204
1017	9429.00000	9276.21410	152.78590	-0.01620
1002	9832.00000	9229.86030	602.13970	-0.06124
1018	10187.00000	9375.36197	811.63803	-0.07967

(Note that the learning rate above was initially set to 0.001. Also another parameter was "tweeked" in the process, the epsilon stopping criteria in the Widrow/Hoff subroutine. Further to avoid infinitely looping I allowed a maximum number of iterations of 1000 to occur on any one call to the Widrow/Hoff routine.) What is clumsily listed above by column is the battery's identification number, the actual discharge time, the ANN's prediction of discharge time, the residual, and a relative error. Thinking that this was not enough mixing up (randomizing)I tried to run a set with 30 iterations of 30 random selections. So starting over again with $w=0$ and $b=1$ we got

test.out.30and30

1028	2474.0000	3014.0192	-540.0192	0.2183
1033	3562.0000	4320.6780	-758.6780	0.2130
1032	4508.0000	3990.0326	517.9674	-0.1149
1036	6269.0000	6066.0410	202.9590	-0.0324
1037	7096.0000	7568.7255	-472.7255	0.0666
1009	8012.0000	9587.3068	-1575.3068	0.1966
1016	8762.0000	9864.5244	-1102.5244	0.1258
1021	9211.0000	9710.9002	-499.9002	0.0543
1017	9429.0000	10606.1410	-1177.1410	0.1248
1002	9832.0000	10596.7198	-764.7198	0.0778
1018	10187.0000	10642.7524	-455.7524	0.0447

Attempting to improve upon the set of 30 and 30 I then decreased the learning rate to 0.0001 without reinitializing. The results improved slightly as listed below

test.out.3030improve

1028	2474.00000	2977.49844	-503.49844	0.20352
1033	3562.00000	4102.68338	-540.68338	0.15179

1032	4508.00000	3844.82062	663.17938	-0.14711
1036	6269.00000	5675.03309	593.96691	-0.09475
1037	7096.00000	6966.36958	129.63042	-0.01827
1009	8012.00000	8757.80136	-745.80136	0.09309
1016	8762.00000	8959.02844	-197.02844	0.02249
1021	9211.00000	8719.26468	491.73532	-0.05339
1017	9429.00000	9495.73101	-66.73101	0.00708
1002	9832.00000	9448.02468	383.97532	-0.03905
1018	10187.00000	9598.33964	588.66036	-0.05779

This process could have continued, but these results seemed good enough.

13.4 Results

The results are presented in the form of figures. Figure 13-4 shows a classic residual plot (see Draper and Smith). It's an unbiased plot of the prediction versus the error value. Desired is a uniform band about the zero error axes. This figure does not contradict that pattern so we may say the data are well modeled.

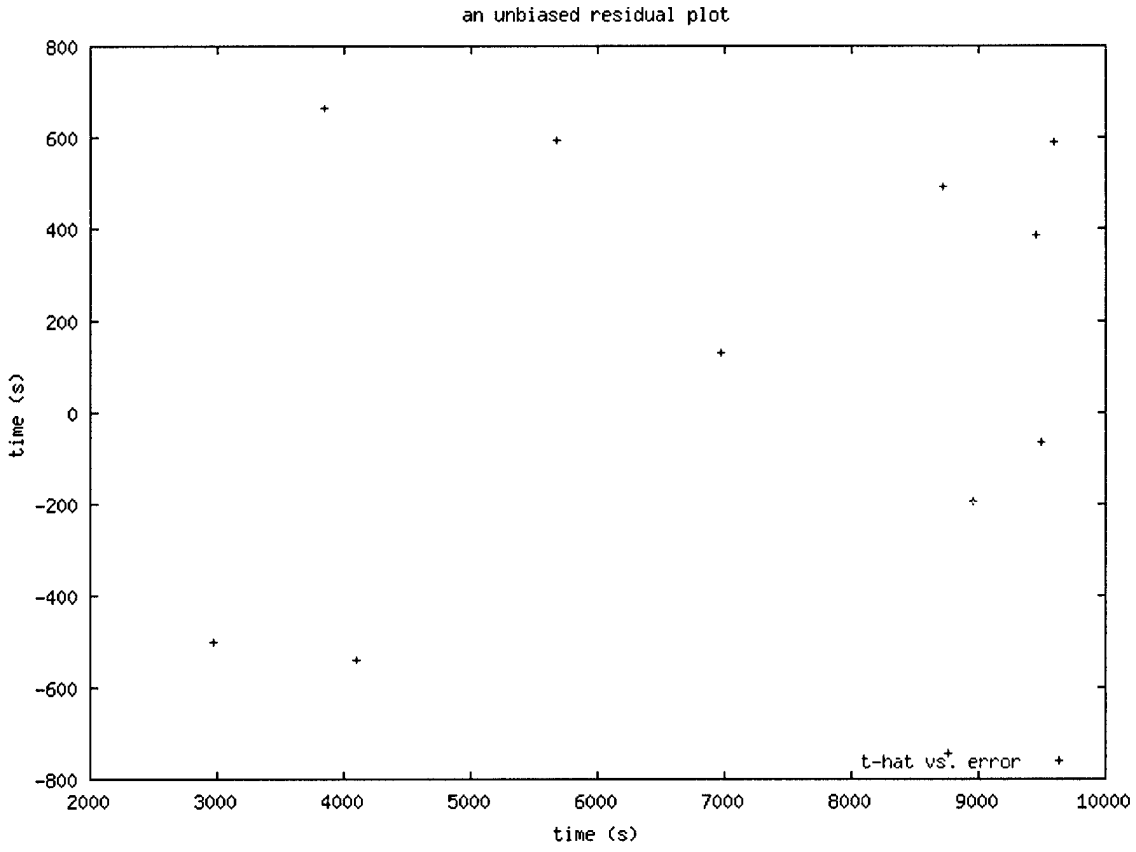

Figure 13-4. Residual plot for the "improved" version of the 30 epoch with 30 random iterations training run.

Figure 13-5 corresponds to figure 13-1. Its an over plot of both the real times and the predicted times. Note in this figure the higher times seem to be underestimated and the lower times seem to be overestimated. We probably could have trained more and clamped down on the end. This trend can actually be seen in the 3 tables above.

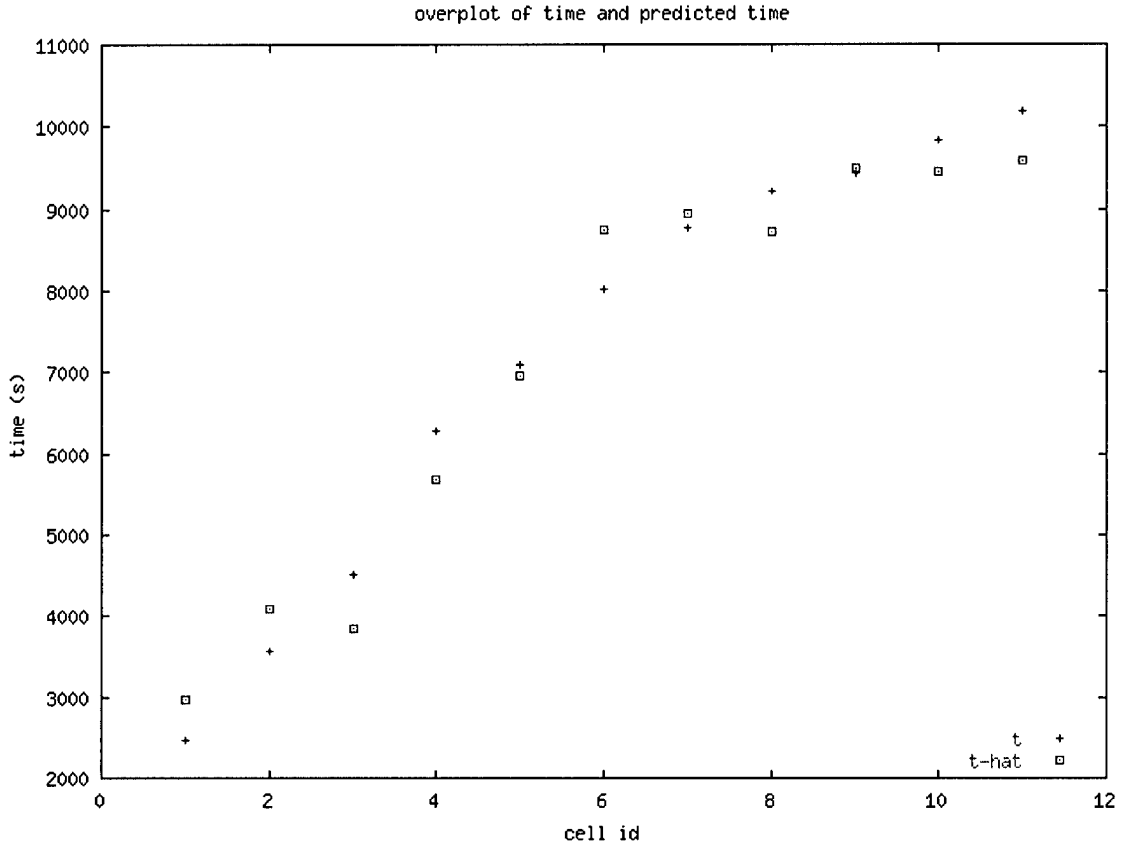

Figure 13- 5. Training set (of 11 samples) over plot of predicted and actual discharge times.

The Figure 13-6 shows the residuals. Notice that a nominal residual of about 13 minutes is the maximum time. This is not bad considering the maximum discharge time is about 3 hours.

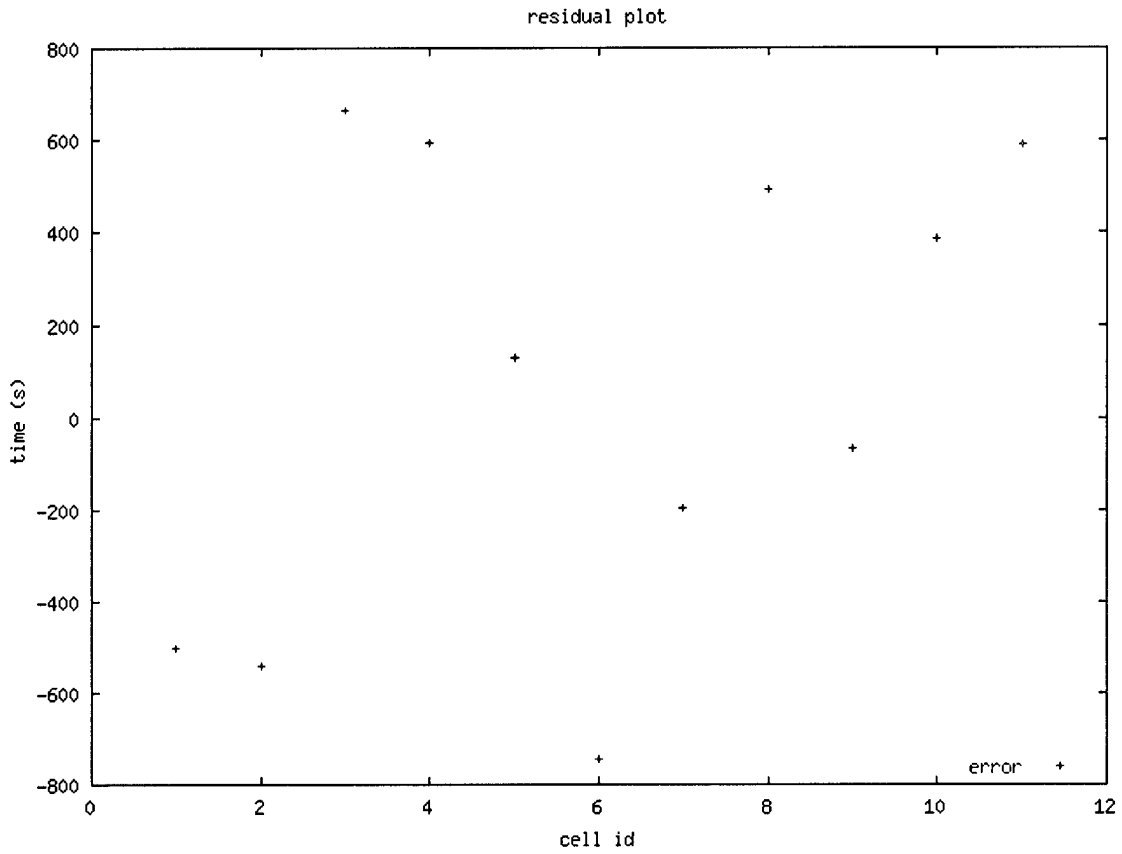

Figure 13-6. Residual plot showing the absolute error.

Lastly, figure 13-7 shows the relative or proportional error plot. It can be compared to Figure 14-2 from the MLR approach.

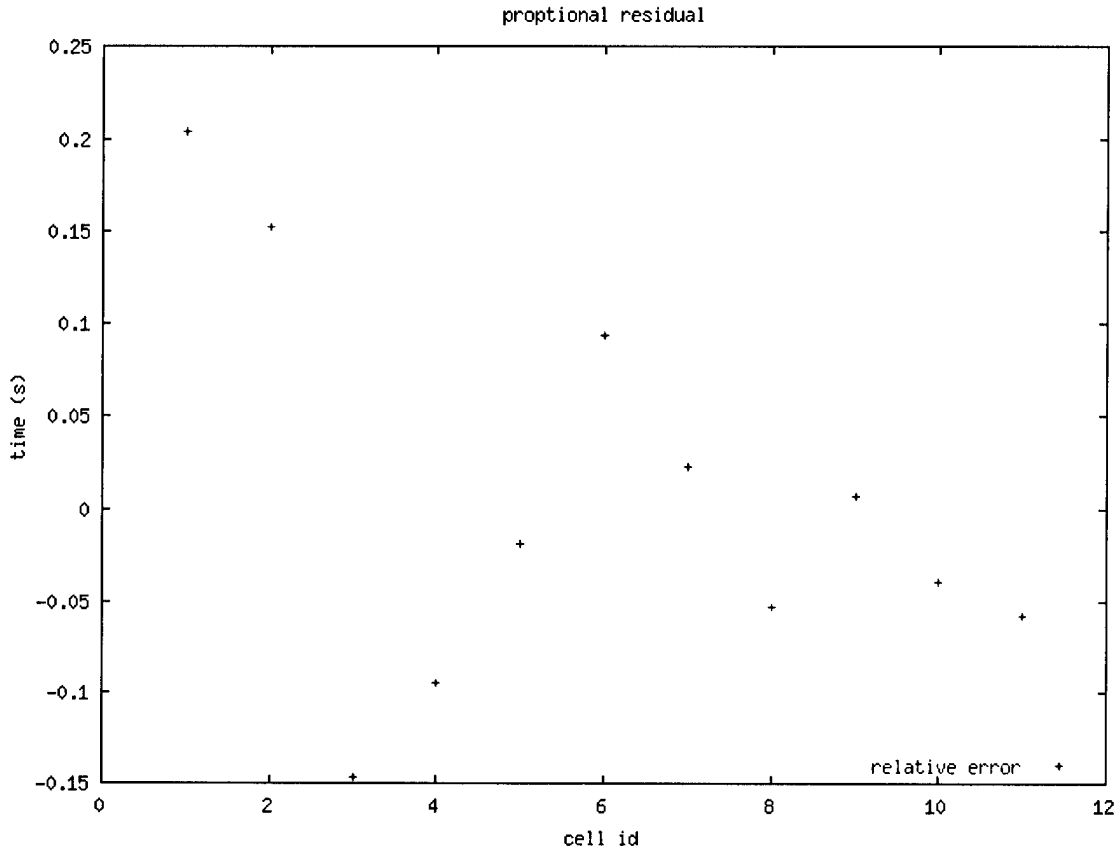

Figure 14-7. Proportional error plot showing approximately a maximum absolute error of 20%.

13.5 Conclusions/Insights

Conclusions that can be made are that the data are well behaved, as expected. Like the MLR this ADALINE is a method applied to help us discover n-dimensional relationships in the data. These results are acceptable. The fact that I began with a clean data set (which is not generally the practice in ANN applications) probably led to this acceptable result. In the end, if a method can be applied to help a sailor more efficiently use batteries, then we have accomplished the task. And I believe that it can be done with either method. This sample size is at best moderate. Future work should consider this.

13.6 Acknowledgments

I would like to thank Julio Melhado, lead Electronics Engineer at Neptune Sciences, Inc. for this project, for getting me involved. I would also like to thank Patrick McDowell of Planning Systems, Inc. for his helpful discussions on the data preparation, presentation, and training methodologies. Thanks also to Badiollah Asrabadi of Nicholls State University for cleaning up the initial set of cells. Many thanks to the project's sponsors at the Naval Surface Warfare Center in Crane, Indiana, for allowing me to use of data set for my class project.

14. APPENDIX D

14.1 - GNU Octave Source code for ADALINE

```
%runem.m
%     purpose:  to initialize and train the weight and bias vectors.
%
alpha = 0.001;
epochs = 6;
w = zeros(32, 500);
b = ones(32, 1);
save wb.out w b
for i=1:4
     %dhf rand("seed", i);
     train( alpha, epochs )
endfor
last
% train.m
%     purpose:  to sequentialize and to then randomize
%          the training set.
function train( alpha, epochs )
tdmax = 10800;  %maximum of 3 hours (in seconds)
vmax = 2.14;   %maximum voltage from plots
vmin = 1.98;
vrng = vmax - vmin;
load train.td
id = train(:,1);
t = train(:,2);
nsamp = max( size(train) );
toti = 0;
clear train;
load -force wb.out
%dhf alpha = 0.001;    %determined from 1/max(eig(R)) for 1 input
for j = 1:nsamp
     prefix = id(j,1);
     filename = "";
     mydata = zeros(32, 500);
     for i = 1:32
          filename = sprintf("project/h%d_%d.sub", prefix, i);
          [handle, errmsg] = fopen(filename, "r");
          [data, count] = fscanf(handle, "%f %f", [2, Inf]);
          mydata(i,:) = ( data(2,:) - vmin )/vrng;
          fclose(handle);
     endfor
     td = zeros(32, 1) .+ t(j,1)/tdmax;     %divide by 3 hours
     for i = 1:32
          p = mydata(i,:)';
```

```
            [a, e, w, b, iter] = widhof(w, b, p, td, alpha);
            toti = toti + iter;
        endfor
        clear mydata;
    endfor
    fprintf(stdout, "0 %d\n", toti);
    % do epochs in random order
    for k = 1:epochs
        iran = floor(1 + rand*nsamp);
        prefix = id(iran,1);
        filename = "";
        mydata = zeros(32, 500);
        for i = 1:32
            filename = sprintf("project/h%d_%d.sub", prefix, i);
            [handle, errmsg] = fopen(filename, "r");
            [data, count] = fscanf(handle, "%f %f", [2, Inf]);
            mydata(i,:) = ( data(2,:) - vmin )/vrng;
            fclose(handle);
        endfor
        td = zeros(32, 1) .+ t(iran,1)/tdmax;   %divide by 3 hours
        for i =  1:32
            p = mydata(i,:)';
            [a, e, w, b, iter] = widhof(w, b, p, td, alpha);
    %b
    %fflush(stdout);
    %kbhit();
            toti = toti + iter;
        endfor
        clear mydata;
        fprintf(stdout, "%d %d\n", iran, toti);
        fflush(stdout);
        toti = 0;
    endfor
    save wb.out w b
    %improve.m
    %   purpose:  to train the weights and biases more with smaller
    %             and smaller learning rates.
    %
    alpha = 0.001;
    %alpha = 0.0001;
    %alpha = 0.00001;
    epochs = 6;
    load -force wb.out
    %w = zeros(32, 500);
    %b = ones(32, 1);
    for i=1:4
        %dhf rand("seed", i);
        train( alpha, epochs )
    endfor
```

```
function [a, e, w, b, i] = widhof(win, bin, p, t, alpha)
% widhof.m
%     purpose: create weights of an adaline
%              with the widrow-hoff (LMS) learning rule.
%     author: dave fabre
%     function [a, e, w, b, i] = widhof(win, bin, p, t, alpha)
%
maxiter = 1000;
myeps = 1.0e-5;
[mp, np] = size(p);
[mw, nw] = size(win);
[mt, nt] = size(t);
if ( mp ~= nw )
    return;
end
%too bad matlab is missing the do-while construct
a = purelin(win*p + bin);
e = t - a;
w = win + 2*alpha*e*p';
b = bin + 2*alpha*e;
wold = ones(size(w));
bold = ones(size(b));
smallw = zeros(size(w)) + myeps;
smallb = zeros(size(b)) + myeps;
i = 0;
while ( i < maxiter && abs(w - wold) > smallw && abs(b - bold) > smallb )
    wold = w;
    bold = b;
    a = purelin(w*p + b);
    e = t - a;
    w = w + 2*alpha*e*p';
    b = b + 2*alpha*e;
    i = i + 1;
end
%if ( i >= maxiter )
%     fprintf(stdout, "widhof:  maxiter reached\n");
%     fflush(stdout);
%end
```

15. REFERENCES

[i]J. S. Newman and C. W. Tobias, "Theoretical Analysis of Current Distribution in Porous Electrodes," Journal of the Electrochemical Society, 109 (12) 1183-1191 (1999).

[ii]V. Srinivasan and J. Weidner, "Mathematical Model of Electrochemical Capacitors," Journal of the Electrochemical Society, 146 (5) 1650-1658 (1999).

[iii]H. Cheh, "Electrochemistry of Gold by Pulsed Current," Journal of the Electrochemical Society, 118 (4) 551-553 (1971).

[iv]J. S. Newman and W. Tiedemann, "Porous-Electrode Theory with Battery Applications," AIChE Journal, 21 (1) 25-41 (1975).

[v]M. Verbrugge and B. Koch, "Electrochemistry of Intercalation Materials, Charge-Transfer Reaction and Intercalate Diffusion in Porous Electrodes" Journal of the Electrochemical Society, 146 (3) 833-839 (1999).

N. Ibl, "Some Theoretical Aspects of Pulse Electrolysis," Surface Technology, 10, 81 (1980).

D.D. MacDonald, "Transient Techniques in Electrochemistry," Plenum Press, NY 1977.

Bard and L. Faulkner, "Electrochemical Methods , Fundamentals and Applications," John Wiley & Sons, 1980.

J. Newman, Electrochemical Systems, Prentice Hall, NJ 1973

D. Landolt, "Traité des Matériaux 12. Corrosion et Chimie de Surfaces des Métaux," Alden Press, Oxford, 1993.

Giordano, Frank R., M.D. Weir, A First Course in Mathematical Modeling, Brooks/Cole Publishing Co., Monterey, CA, 1983.

N.R. Draper, H. Smith, Applied Regression Analysis, 2nd Edition, John Wiley & Sons, Inc. 1981.

David G. Kleinbaum, Lawrence L. Kupper, Applied Regression Analysis and Other Multivariable Methods, Duxbury Press, Boston, MA, 1985.

William H. Press, B.P. Flannery, S.A. Teukolsky, W.T. Vetterling, Numerical Recipes in C, The Art of Scientific Computing, Cambridge University Press, 1988.

Brian W. Kernighan, D.M.Ritchie, The C Programming Language, 2nd Edition (ANSI C), Prentice-Hall, 1988.

Jandel Scientific, Inc., TableCurve 3D v1.0 Users's Manual, Software Copyright 1993 AISN Software.

Nell Dale, D. Orshalick, Introduction to PASCAL and Structured Design, D. C. Heath and Co., 1983.

Martin T. Hagan, H.B. Demuth, M. Beale, Neural Network Design, PWS Publishing Co., 1996.

Robert Hecht-Nielsen, Neurocomputing, Addison-Wesley Publishing Co., 1990.